The Impact of Host-Microbe Interactions on *Nasonia* Evolution

By

Edward Jake van Opstal

Dissertation

Submitted to the Faculty of the

Graduate School of Vanderbilt University

in partial fulfillment of the requirements

for the degree of

DOCTOR OF PHILOSOPHY

in

Biological Sciences

October 31, 2018

Nashville, Tennessee

Approved:

Julian F. Hillyer, Ph.D.

Maulik R. Patel, Ph.D.

John A. Capra, Ph.D.

Timothy L. Cover, M.D.

Seth R. Bordenstein, Ph.D.

DEDICATION

To

My incredibly patient and loving wife, Laura van Opstal, and my supportive family who have been with me every step of the way and probably know what I do.

ACKNOWLEDGEMENTS

I started at Vanderbilt expecting to become a better scientist and researcher, but the people at Vanderbilt went above and beyond to also make me a better communicator and leader. I must thank the entire BRET office for all the time and effort they put into enriching my time here including Dr. Roger Chalkley, Dr. Kathy Gould, Dr. Ashley Brady, Dr. Kim Petrie, Kate Stuart, and Angela Zito for the numerous enrichment programs they have put on over the past five years. I would also like to thank the members of my thesis committee for all their support and helpful advice: Dr. Julián Hillyer (chair), Dr. Tony Capra, Dr. Maulik Patel, and Dr. Tim Cover.

I must thank my thesis advisor, Dr. Seth Bordenstein, for his constant guidance and support and for always pushing me out of my comfort zone, which was vital for my growth as a scientist and as a professional. I feel much more prepared for my future because of him. I have also been extremely fortunate to have an amazing group of lab colleagues who made everyday a fun, scientific adventure. Thank you to Sarah Bordenstein for being the unwavering pillar that keeps the lab together through success and hardship, and to my fellow (former and current) lab mates and friends: Dr. Robert Brucker, Dr. Jason Metcalf, Dr. Lisa Funkhouser-Jones, Dr. Daniel LePage, Dr. Kevin Kohl, Dr. Aram Mikaelyan, Dr. Brittany Leigh, Andrew Brooks, Jessie Perlmutter, Dylan Shropshire, and Emily Layton. A special thanks to Andrew Brooks who played many roles to keep me going including: chair back brother, cheerleader, and accountabili-buddy. Thank you also to my amazing undergraduate mentee Ananya Sharma for all her hard work on the projects presented in this thesis; she will become a great medical doctor.

Finally, I would like to thank my family for all their love and support. To my parents and in-laws, thank you for being the best listeners and cheerleaders, particularly when I needed both. To all my siblings, you have inspired me greatly in chasing my career goals after seeing you achieve yours. Lastly, to my wife, Laura, absolutely none of this would have been possible without you beside me. You were my compass when I lost my perspective, and I lost it lot.

My work has been generously supported by Vanderbilt University, the Gisela Mosig Travel Fund, and the National Science Foundation.

TABLE OF CONTENTS

Page

LIST OF TABLES

LIST OF FIGURES

LIST OF ABBREVIATIONS

BLAST	Basic Local Alignment Search Tool
cDNA	complementary DNA
CI	Cytoplasmic incompatibility
DNA	Deoxyribonucleic acid
dsRNA	double-stranded RNA
FISH	Fluorescent in situ hybridization
FDR	False discovery rate
Gb	Gigabases
GFP	Green fluorescent protein
GSCN	Germ-line stem cell niche
kb	Kilobases
Mb	Megabases
MWU	Mann-Whitney U
MYA	Million years ago
NCBI	National Center for Biotechnology Information
NMDS	Non-metric multidimensional scaling
NRM	*Nasonia* rearing media
ns	Not significant
PBS	Phosphate-buffered saline
PBST	Phosphate-buffered saline with Triton X-100
PCR	Polymerase chain reaction
PGRP	Peptidoglycan recognition receptor protein
RNA	Ribonucleic acid
RNAi	RNA interference
RT-qPCR	Reverse transcription quantitative PCR
SSCN	Somatic stem cell niche
QC	Quality control
qPCR	Quantitative PCR
QTL	Quantitative trait loci

CHAPTER I. INTRODUCTION*

Defining symbiosis in host-microbe interactions

Bacterial symbionts are widely recognized as important drivers of insect physiology, development, behavior, reproduction, nutrition, and evolution (Buchner 1965; Moran 2007; Douglas 2010, 2015). Historically, symbiosis research focused primarily on binary interactions between insect hosts and particular symbionts, whether they are harmful or helpful (Duron et al. 2008; Moran et al. 2008; Moya et al. 2008; Werren et al. 2008). The advent of new DNA sequencing technologies over the last ten years resulted in what has recently been termed 'the microbiome revolution' (Blaser 2014), providing an unprecedented wealth of information on insect microbiotas from various species. Biologists now recognize that symbioses are shaped by complex multipartite interactions, not only between the host and its associated microbes, but also between different members of the microbial community and the environment. This understanding has led to the view of hosts as complex ecosystems (McFall-Ngai et al. 2013; Sicard et al. 2014), and to the recognition that a more holistic approach is needed to understand the role of the microbiota in major facets of host biology (Gilbert et al. 2012). In insects, specific endosymbionts and the entire microbiota can modulate numerous host phenotypes spanning development (Shin et al. 2011), nutrition (Chandler et al. 2011; He et al. 2013; Wong et al. 2014), immunity (Chu and Mazmanian 2013), vector competence and susceptibility to pathogen infection (Dong et al. 2009; Koch and Schmid-Hempel 2012), among others. The microbiota can also mediate reproductive isolation and thus the mechanisms that drive speciation (Brucker and Bordenstein 2012c, 2013; Shropshire and Bordenstein 2016), underscoring the need to understand host-microbe dynamics over evolutionary timescales.

The recognition of the significance and complexity of host-microbe interactions has led to the revival of old terms and the establishment of new ones to describe host-microbe assemblages. As such, the term "holobiont", originally coined by Margulis (1991), is now frequently used to refer to a host together with its entire microbial consortium, while the "hologenome" encompasses the genomes of all members of the holobiont (Rosenberg et al. 2007; Zilber-Rosenberg and Rosenberg 2008). These terms provide structural definitions that can be universally applied to any

*This chapter was modified from the publication in *Frontiers in Microbiology* (2016) 7:1478 with Dylan Shropshire, Seth Bordenstein, Greg Hurst, and Robert Brucker as co-authors. Jessica Dittmer was first author.

host-microbiota assemblage. Moreover, they are pluralistic in that they encompass constant or inconstant, intracellular or extracellular, horizontally or vertically transmitted, harmful or helpful microbial symbionts (Rosenberg et al. 2007; Bordenstein and Theis 2015; Theis et al. 2016). This perception of a holobiont therefore embraces both competition and cooperation between a host and its associated microbes. This is particularly obvious in the case of symbionts like *Wolbachia*, which override host reproduction to increase their own transmission (Duron et al. 2008; Werren et al. 2008). More generally, the microbial partners present in a host organism contribute to the "extended phenotype" of this particular host-symbiont assemblage, i.e., the holobiont. However, many aspects regarding holobionts need to be elucidated. For instance, one may ask whether phenotypic variation in traits, caused by different holobiont assemblies, could drive a multigenerational response to selection, as originally proposed as part of the hologenome concept of evolution (Rosenberg et al. 2007; Zilber-Rosenberg and Rosenberg 2008). Moreover, if there is a response to selection, does it occur at the host, microbe, or microbial community level? While the broad utility of the hologenome concept remains debated (Bordenstein and Theis 2015; Moran and Sloan 2015; Douglas and Werren 2016; Theis et al. 2016), it is clear that the microbiome represents an important component of insect biology as well as a source of phenotypic and evolutionary novelty.

With tools available to investigate the diversity and complexity of host-microbe associations, the next challenge will be to disentangle the holobiont in a functional context to understand (i) how different microbes, alone or in synergy, contribute to host phenotype and fitness; (ii) the role of the host, the symbionts, and the environment in establishing and regulating symbiont populations with each generation (**CHAPTER II**); (iii) the role of the microbiota in evolutionary processes such as speciation (**CHAPTER III**); and (iv) the resilience and adaptability of the host towards a particular microbiota community over time (**CHAPTER V**).

Nasonia as a model organism

The parasitoid wasp genus *Nasonia* (also referred to as "jewel wasp") is a species complex comprised of four interfertile species: *N. vitripennis*, *N. longicornis*, *N. giraulti*, and *N. oneida* (Figure I-1A) (Darling and Werren 1990; Raychoudhury et al. 2010a). The older species *N. vitripennis* is estimated to have diverged from the three younger species 1 million years ago (mya). The other species were discovered only in the last 26 years and have diverged 0.4 mya in the case

of *N. longicornis* and *N. giraulti* and 0.3 mya in the case of *N. giraulti* and *N. oneida* (Werren and Loehlin 2009; Werren et al. 2010). While *N. vitripennis* is cosmopolitan (Figure I-1B), the three younger species have only been observed in North America, where they show species-specific distributions: *N. longicornis* is restricted to the west, *N. giraulti* to the northeast and the most recently discovered species *N. oneida* has so far only been observed in New York state (Figure I-1C) (Darling and Werren 1990; Raychoudhury et al. 2010a). All species are parasitoids of fly pupae (Werren and Loehlin 2009; Desjardins et al. 2010). Adult *Nasonia* females lay their eggs within the fly puparium (Figure I-1D) and inject a venom that prevents the fly from mounting an immune response against the intruders (Danneels et al., 2014). A single fly pupa may be parasitized by multiple females of the same or different species (superparasitism and multiparasitism, respectively) (Darling and Werren 1990). Under laboratory conditions (constant temperature of 25°C), *Nasonia* has a short generation time of only 14 days: Larvae emerge 24-36 hours after egg laying and undergo four larval instars (during which they feed on the fly host), followed by pupation after 7-8 days and emergence from the fly as adults (Figure I-1D).

Nasonia is a well-established model for insect development (Rosenberg et al. 2014), behavior (Bertossa et al. 2013), sex determination (Beukeboom and van de Zande 2010; Verhulst et al. 2010), evolutionary genetics (Desjardins et al. 2010, 2013; Loehlin et al. 2010), immunity (Tian et al. 2010; Brucker et al. 2012a; Sackton et al. 2013), speciation (Breeuwer and Werren 1995; Ellison et al. 2008; Buellesbach et al. 2013; Gibson et al. 2013) and symbiosis with the reproductive parasites *Wolbachia* (Breeuwer and Werren 1990; Bordenstein et al. 2001; Raychoudhury et al. 2009). In addition, *Nasonia* is emerging as a model for insect-gut microbiota symbioses across recent evolutionary time periods and speciation events (Brucker and Bordenstein 2012c, 2013). Major reasons for this versatility are its ease of rearing in the laboratory, the ability to establish interspecies hybrids after curing of *Wolbachia*, and the advantages of haplodiploid sex determination, wherein males and females develop from unfertilized (haploid) and fertilized (diploid) eggs, respectively (Figure I-1D). Haplodiploidy is particularly useful for quantitative genetics as all recessive alleles are expressed in the male haploid state (Werren and Loehlin 2009).

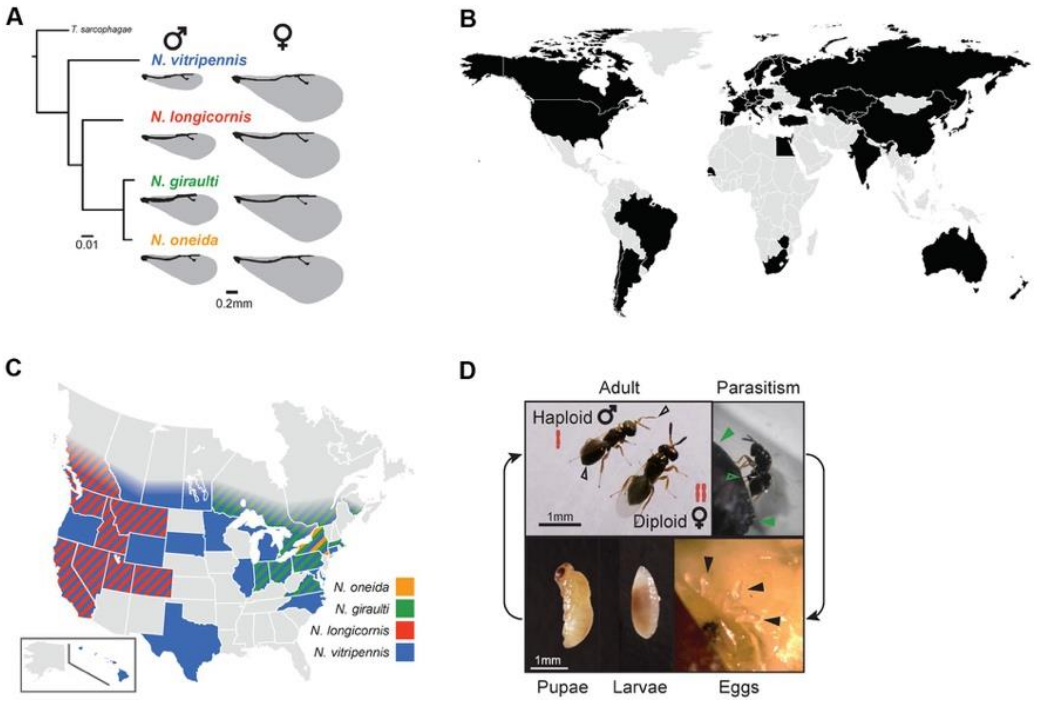

Figure I-1. *Nasonia* phylogeny, geographical biodiversity, and life cycle. (A) Phylogenetic relationships within the *Nasonia* species complex based on the CO1 gene. The parasitoid wasp *Trichomalopsis sarcophagae* was used as outgroup. The scale bar indicates substitutions per site. Note the morphological differences in wing size between species and genders (drawing based on Loehlin et al. 2010). (B) Countries in which *Nasonia* has been observed, based on published records of *N. vitripennis* [Universal *Chalcidoidea* Database (Noyes 2016) and (Raychoudhury et al. 2009, 2010b; Paolucci et al. 2013)]. The gray color indicates countries for which no observations are documented, in most cases due to missing sampling information. For all countries except the US, records state that the observed species was *Nasonia vitripennis* – however, many of these observations were made before the discovery of the three younger species in the US. Therefore, this global map shows observations of *Nasonia* without distinguishing between species. (C) Observations of all four *Nasonia* species in the US and Canada, based on published information (Darling and Werren 1990; Raychoudhury et al. 2009, 2010a,b). (D) *Nasonia* life cycle from oviposition to adulthood. Sex-specific differences in ploidy are indicated for adult males and females. Additional sexual dimorphisms include smaller wing size, less pigmented antennae and rounded abdomen in males (open black arrows). Parasitism is representing by a female wasp ovipositing into a fly pupa (closed green arrows: Fly pupa; open green arrows: Ovipositor of the wasp). Embryos are approximately 100 μm by 500 μm in size (closed black arrows). The *Nasonia* larva and pupa were photographed outside of their fly host. Photo credit: Matthew C. Johnson © 2016

Perhaps the most recognizable aspect of *Nasonia* biology is the body of literature on speciation. Several types of hybrid maladies have been studied in *Nasonia*, including cytonuclear, cytoplasmic and microbiota-nuclear incompatibilities (Figure I-2). Specifically, cytonuclear incompatibilities exist between mitochondrial and nuclear genes presumably involved in the oxidative phosphorylation pathway, leading to reduced energy production and hybrid fitness (Ellison et al. 2008; Niehuis et al. 2008; Koevoets et al. 2012; Gibson et al. 2013). On the other hand, cytoplasmic and microbiota-nuclear incompatibilities result from the influence of bacterial

endosymbionts (e.g., *Wolbachia*) or the extracellular microbiota on reproductive fitness, either by affecting offspring viability at the embryonic stage or by altering the immune response of developing larvae, respectively (Bordenstein et al. 2001; Brucker and Bordenstein 2013). These incompatibilities influence *Nasonia* reproductive isolation in an additive fashion, since removal of one incompatibility does not necessarily remove the others (Brucker and Bordenstein 2013).

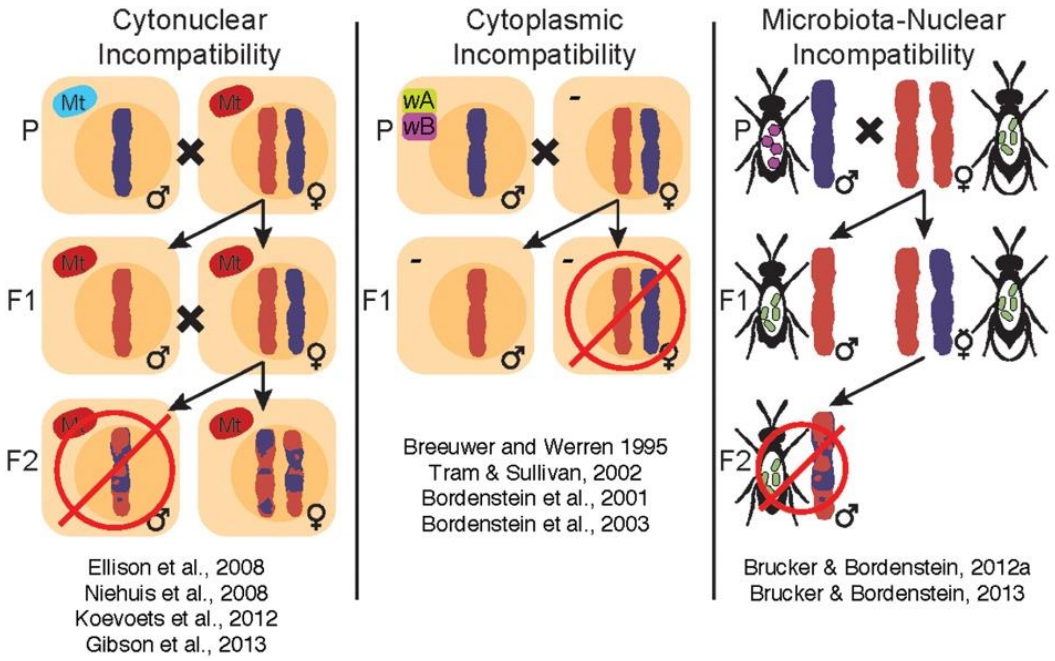

Figure I-2. Hybrid incompatibilities within the *Nasonia* clade. There are three published sources of hybrid incompatibilities: cytonuclear, cytoplasmic, and microbiota-nuclear incompatibilities. Cytonuclear incompatibilities, or negative interactions between mitochondria and the nuclear genome, are associated with lethality in F2 males from younger interspecific crosses (*N. giraulti* and *N. longicornis*) and near complete lethality in older interspecific crosses (*N. vitripennis* and *N. giraulti* or *N. longicornis*). Hybrid lethality has some plasticity due to environmental factors (Koevoets et al. 2012), but clear cytonuclear incompatibilities that complicate development and gene regulation (Ellison et al. 2008; Niehuis et al., 2008; Koevoets et al. 2012; Gibson et al. 2013) have been genetically mapped across the *Nasonia* genomes. Cytoplasmic incompatibilities are a consequence of infection with different *Wolbachia* strains (*w*A and *w*B), which causes post-fertilization chromatin defects that result in inviable fertilized eggs (Bordenstein et al. 2001, 2003; Tram and Sullivan 2002). Finally, microbiota-nuclear incompatibilities result from negative interactions between the microbiota and host genome and lead to hybrid lethality, altered microbial communities and innate immune regulation (Brucker and Bordenstein 2013). The collective influences of these incompatibilities on *Nasonia* make it a powerful model for evolutionary and symbiotic studies of speciation and reproductive isolation. How these incompatibilities have evolved relative to each other is an important avenue for future research.

The growing interest in *Nasonia* has also resulted in a wealth of available resources, many of which are advantageous for the study of host-microbe interactions: Annotated genomes are available for all species except *N. oneida* (Werren et al. 2010), together with an extensive genetic

toolbox (reviewed in Werren and Loehlin 2009; Lynch 2015), transcriptome and methylome for *N. vitripennis* (Sackton et al. 2013; Wang et al. 2013; Beeler et al. 2014), a well-characterized complex innate immune system (Tian et al. 2010; Brucker et al. 2012a; Sackton et al. 2013), and a procedure for host genetic manipulation via RNAi (Lynch and Desplan 2006; Werren et al. 2009). The most promising technique for the purpose of this review is the recently developed *in vitro* rearing technique, allowing the successful rearing of *Nasonia* from embryos to adults outside of its fly host (Brucker and Bordenstein 2012b; Shropshire et al. 2016), thereby providing the means to establish axenic and gnotobiotic lineages (**CHAPTER IV**).

Wolbachia, an influential partner over evolutionary time-scales

Wolbachia are widespread obligate intracellular Alphaproteobacteria, estimated to infect 40-65% of insect species (Hilgenboecker et al. 2008; Werren et al. 2008; Zug and Hammerstein 2012). While being primarily maternally transmitted, horizontal transfers have frequently occurred over evolutionary time-scales (O'Neill et al. 1992; Rousset et al. 1992; Werren et al. 1995). To date, *Wolbachia* strains are divided into 16 clades, referred to as "supergroups" A-Q (Lo et al. 2007; Ramírez-Puebla et al. 2015).

The *Nasonia* species complex has been a major model system for *Wolbachia*-insect symbioses for more than 25 years (Breeuwer and Werren 1990). This young species complex has enabled scientists to reconstruct the history of *Wolbachia* acquisitions and transmission routes across the *Nasonia* clade (van Opijnen et al. 2005; Raychoudhury et al. 2009). Moreover, the ability to produce interspecies hybrids has been exploited to introgress the cytotype (including the *Wolbachia*) of a given species into the nuclear genotype of another, thereby providing insights into *Wolbachia*-host genotype interactions, different modes of CI and the role of *Wolbachia* in speciation (Breeuwer and Werren 1990, 1993b, Bordenstein and Werren 1998; Bordenstein et al. 2001, 2003; Chafee et al. 2011; Raychoudhury and Werren 2012).

The emerging picture of the *Nasonia*-*Wolbachia* association is as follows: The four *Nasonia* species together harbor 11 different *Wolbachia* strains from the A and B supergroups (Figure I-3A) (Raychoudhury et al. 2009), two major arthropod-*Wolbachia* clades that diverged about 60 million years ago (Werren et al. 1995). *N. vitripennis* carries two *Wolbachia* strains (one from each supergroup), while the three younger species are all triple infected: *N. giraulti* and *N. oneida* both harbor two supergroup A strains and one supergroup B strain, whereas *N. longicornis*

harbors one supergroup A strain and two supergroup B strains (Figure 3A) (Raychoudhury et al. 2009). Comparing the phylogenetic relationships between these *Wolbachia* strains with host phylogenies based on nuclear and mitochondrial genes revealed that several *Wolbachia* strains were most likely acquired independently via horizontal transfers from other insects, including *Drosophila spp.* (supergroup A strains of *N. giraulti* and *N. longicornis*), the parasitoid wasp *Muscidifurax uniraptor* (supergroup A strain of *N. vitripennis*) as well as the blowfly *Protocalliphora sialia* (supergroup B strain of *N. vitripennis*) (van Opijnen et al., 2005; Raychoudhury et al. 2009). The latter cases point towards an ecological interaction as the source of the *Wolbachia* transfers to *N. vitripennis*, since both *Nasonia* and *M. uniraptor* parasitize blowflies. Indeed, horizontal transfers between parasitoids and their fly hosts as well as between different parasitoid species infecting the same host are known to occur occasionally (Heath et al. 1999; Vavre et al. 1999; Huigens et al. 2004).

The supergroup B *Wolbachia* of *N. longicornis* and *N. giraulti* were acquired prior to the speciation of the two species and subsequently co-diverged with their hosts (Figure I-3A) (van Opijnen et al. 2005; Raychoudhury et al. 2009). Hence, the supergroup B strain from *N. giraulti* is nearly identical to one of the B strains from *N. longicornis* and the estimated divergence time of the two *Wolbachia* strains coincides with the divergence of their host species, i.e., about 0.4-0.5 mya (van Opijnen et al. 2005; Raychoudhury et al. 2009). In addition, the second B strain of *N. longicornis* is estimated to have diverged from the other B strains about 1.5 mya. Considering that this time point was long before the speciation of the two host species, it is likely that the common ancestor of *N. longicornis* and *N. giraulti* harbored two B strains, one of which was lost in *N. giraulti* after the speciation event (Raychoudhury et al. 2009). A similar co-divergence event between the A strains of *N. longicornis* and *N. giraulti* is possible, but the similarity of these strains with *Wolbachia* from several *Drosophila* species currently makes it impossible to rule out independent horizontal transfer events (Raychoudhury et al. 2009). The three *Wolbachia* strains in the recently discovered species *N. oneida* are identical (for 5 house-keeping genes and the *wsp* gene) to those of the closely related *N. giraulti* and have likely been acquired via hybridisation between the two species, resulting in a mitochondrial-*Wolbachia* sweep from *N. giraulti* to *N. oneida* (Figure I-3A) (Raychoudhury et al. 2009). Future phylogenomic comparisons based on the entire genomes of the different *Wolbachia* strains will be needed to obtain a higher resolution.

Nonetheless, these findings illustrate a high *Wolbachia* diversity in the *Nasonia* species complex, along with various patterns of *Wolbachia* transfers within a single insect genus.

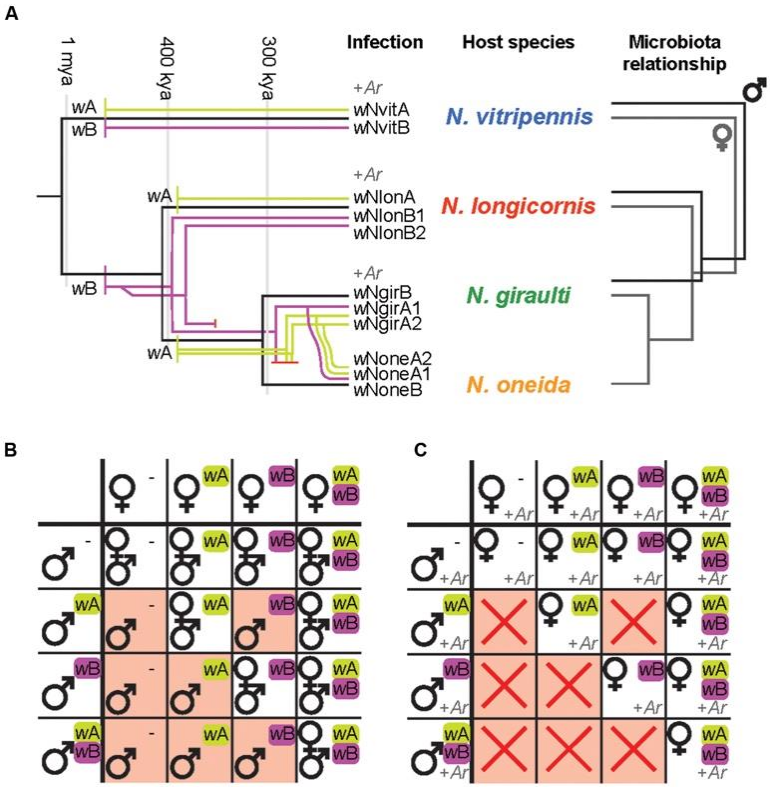

Figure I-3. *Nasonia* phylosymbiosis and reproductive phenotypes of their endosymbionts. (A) *Wolbachia-Nasonia* associations and phylosymbiosis (modified from Raychoudhury et al. 2009; Brucker and Bordenstein 2012b,c). *Wolbachia* acquisitions and subsequent divergence are overlaid on the *Nasonia* phylogeny. Strains from *Wolbachia* supergroup A are represented in green, strains from supergroup B in purple. *Arsenophonus* (+Ar) has been found to infect three species of *Nasonia*. The microbial community relationships parallel the host phylogeny, indicating species-specific microbiota assemblies that establish phylosymbiosis. This pattern has been observed in males for three species (Brucker and Bordenstein 2012a, 2013) as well as in females for all four species (R. M. Brucker and S. R. Bordenstein, personal communication). (B) Impact of *Wolbachia*-induced CI on offspring production. *Wolbachia* present in males induce a sperm modification that needs to be rescued by the same *Wolbachia* strain in the fertilized egg for normal offspring production. CI (red background) occurs if the female is uninfected (-) (unidirectional CI) or harbors a different *Wolbachia* strain (bidirectional CI) and results in male-only (or male-biased) broods due to loss of the paternal chromosomes. Note that although *Wolbachia* modify male sperm, the symbiont is only maternally transmitted. Offspring will therefore harbor the same *Wolbachia* strain(s) as their mothers. *w*A/*w*B indicate different *Wolbachia* strains. (C) Impact of Arsenophonus-induced male-killing on offspring production, in combination with *Wolbachia*-mediated CI. Male-killing results in all-female broods in the absence of CI (white background) and no offspring production in combination with CI (red crosses), since the males that are not affected by CI would be killed by male-killing.

One of the most prominent aspects of *Wolbachia* is undoubtedly its ability to manipulate host reproduction in various ways (Werren et al. 2008). All *Nasonia*-associated *Wolbachia* induce

cytoplasmic incompatibility (CI), a reproductive incompatibility consisting of two components: A symbiont-induced modification of the paternal chromosomes during spermatogenesis and a rescue factor by the same symbiont being present in the fertilized egg (Tram and Sullivan 2002; Serbus et al. 2008). If the female is uninfected (unidirectional CI) or harbors a different bacterial strain (bidirectional CI), the modification may not be rescued, resulting in CI (Figure I-3B). Consequently, infected females have a fitness advantage over uninfected females, since they can reproduce successfully with all available males, regardless of male infection status. Similarly, bidirectional CI results in a fitness benefit for multiply infected females since they are at lower risk to suffer from CI (Mouton et al. 2003, 2004). The fact that all *Nasonia* species generally harbor double or triple infections that are mutually incompatible reinforces bidirectional incompatibility between all species pairs, with the notable exception of *N. giraulti* and *N. oneida*, whose *Wolbachia* strains are identical (Breeuwer and Werren 1990; Breeuwer et al. 1992; Bordenstein and Werren 1998, 2007; Bordenstein et al. 2001, 2003; Raychoudhury et al. 2010a). In *Drosophila* melanogaster, two *w*Mel phage WO genes, *cifA* and *cifB*, were determined to cause the CI phenotype (Lepage et al. 2017), however the exact molecular mechanisms of CI are still under investigation. It is evident that the paternal chromosomes fail to condense correctly and may be lost during the first mitotic division, causing embryo mortality in diploid organisms (Tram and Sullivan 2002). In contrast, in haplodiploid insects such as *Nasonia*, CI can be manifested in different ways. The most extreme phenotypes are Male Development and Female Mortality (Vavre et al. 2000; Bordenstein et al. 2003; Vavre et al. 2009). In the first case, the paternal genome is completely lost, which restores haploidy in fertilized eggs and results in the conversion of female into male offspring. Hence, this type of CI is characterized by all-male broods (Figure I-3B) with little or no embryonic mortality compared to compatible crosses. In contrast, an incomplete loss of the paternal chromosomes would instead cause aneuploidy and a high mortality of fertilized eggs (i.e., female offspring), resulting in smaller broods with male-biased sex-ratios (Bordenstein et al. 2003).

It has been hypothesized that paternal chromosome loss was mediated by the intensity of *Wolbachia*-induced sperm modification, with less efficient modifications leading to only partial chromosome loss and aneuploidy in fertilized eggs (Vavre et al. 2009). While CI-induced mortality seems to be common in haplodiploid species, including the younger *Nasonia* species *N. longicornis* and *N. giraulti* (Bordenstein et al. 2003; Dedeine et al. 2004; Vavre et al. 2009), *N.*

vitripennis is an exception from the rule in that the Male Development type is the predominant CI phenotype in this species (Breeuwer and Werren 1990; Bordenstein et al. 2003). Interestingly, interspecies crosses and introgression experiments between *N. vitripennis* and *N. giraulti* revealed that this rare CI phenotype is determined by the *N. vitripennis* nuclear genotype rather than *Wolbachia*-related effects, since it is even observed in incompatible crosses between infected *N. giraulti* males and uninfected *N. vitripennis* females (Bordenstein et al. 2003). These results indicate that the host genotype may determine the fate of the paternal chromosomes in fertilized eggs, independent of *Wolbachia* (Bordenstein et al. 2003). On an evolutionary scale, the conversion of incompatible fertilized eggs into viable haploid males may represent a selective advantage for the more widely distributed *N. vitripennis*, in that it prevents embryo mortality as a consequence of incompatible matings with its microsympatric sister species (Bordenstein et al. 2003). Taken together, the above illustrates the preeminent role of *Nasonia* as a model to understand host-*Wolbachia* interactions, notably in terms of diverse acquisition routes, *Wolbachia*-host genotype interactions and modes of CI.

Maternal transmission of Wolbachia

As a primarily maternally-transmitted bacteria, *Wolbachia* infects the ovaries of their hosts by targeting the somatic stem cell niche (SSCN) and germline stem cell niche (GSCN) to gain access to the developing oocyte for successful propagation (Fast et al. 2011; Frydman et al. 2006; Serbus et al. 2008; Toomey et al. 2013). During early oogenesis of *Drosophila*, *Wolbachia* are distributed between the dividing germline stem cells (GSCs) so the resulting cyst of 16 interconnected germline cells have an even distribution. There are also high levels of *Wolbachia* in the SSCN that surround the germline cyst, which may act to secondarily transmit the *Wolbachia* into the germline (Serbus et al. 2008). During mid-to-late oogenesis, the developing oocyte is then loaded with *Wolbachia* from the surrounding nurse cells through cytoskeletal transport machinery and localized to the posterior pole before the end of oogenesis. This posterior localization of *Wolbachia* before embryogenesis promotes germline-based transmission in the subsequent embryos. While *Wolbachia* transmission mechanisms have not been well-studied in *Nasonia spp.*, in **CHAPTER II** I present microscopy of *Nasonia* germaria that show a similar *Wolbachia* localization pattern during oogenesis as previously described in *Drosophila*.

Regulation of Wolbachia transfer in hosts

To maintain stable host-microbe interactions in maternally-transmitted bacteria, the host regulation of symbiont transfer and titer is critical. Hosts must keep symbiont titers at a level that maintains a particular niche and conveys an adaptation to their host while preventing bacterial overproliferation. In one extreme case of overproliferation, *Wolbachia* strain *w*MelPop overproliferates in *Drosophila* reproductive and somatic tissues, including brain and nervous tissues, and is able to reduce the lifespan by half (Min and Benzer 1997). Importantly for *Wolbachia*, the titer that is transferred from mother to the developing offspring can ultimately influence *Wolbachia*'s ability to manipulate host reproduction. Therefore, the host undergoes selection over time that drives genetic changes to stably control this symbiont. Influence of the host genotype on *Wolbachia* titers has previously been observed in mosquitos, fruit flies, *Nasonia* wasps, and other insects (Emerson and Glaser 2017; Newton and Sheehan 2015; Funkhouser-Jones et al. 2018; Reumer BM et al. 2012). In natural populations of insects, co-evolution between *Wolbachia* and its hosts results in host regulatory mechanisms to stabilize *Wolbachia* titers. Experiments in which a *Wolbachia* strain is introduced into a host background that is naïve to that particular strain have shown that different *Wolbachia* titers are maintained in different hosts (Boyle et al. 1993; Kondo et al. 2005; Hughes and Rasgon 2013). For example, when *w*VitA from *N. vitripennis* is introgressed into an *N. giraulti* background, there is an 80-fold increase in *Wolbachia* titer with expanded tissue tropism (Chafee et al. 2011). The determination of specific *N. vitripennis* genetic factors that regulate *Wolbachia* titers during maternal transmission is explored in **CHAPTER II**.

Gaining in complexity: the *Nasonia* microbiota

Tremendous progress has been made regarding our understanding of the intricate relationships between diverse insects and their co-evolved primary symbionts, particularly regarding metabolic complementarity and metabolite exchange between different partners (McCutcheon et al. 2009; McCutcheon and Moran 2010; Wilson et al. 2010; Hansen and Moran 2011; McCutcheon and von Dohlen 2011; Husnik et al. 2013; Luan et al. 2015) and adaptations of the host immune system to recognize and regulate resident symbionts (Wang et al. 2009; Login et al. 2011; Futahashi et al. 2013; Kim et al. 2013; Shigenobu and Stern 2013; Masson et al. 2015). However, achieving the same level of insight into host-symbiont cross-talk for highly complex

insect microbiotas remains challenging. Many host-associated microbes may not be culturable and therefore impossible to manipulate outside of the host's body. Hence, we need a study system where the host (i) is easy to rear in the lab; (ii) is genetically tractable with resources available for genomic/transcriptomic or immunity-related investigations; and (iii) has a complex but well-characterized microbiota, and the microbiota can be relatively easily manipulated in the host organism, which can be an asset for testing the influence of the microbiome on host traits. Previous work demonstrates that *Nasonia* maintains a relatively high level of microbial diversity, microbiome functionality, and experimental tractability, even while kept under laboratory conditions.

Microbiota diversity

The bacterial diversity of *Nasonia* has been described in lab-reared larvae, pupae and adult males for the three *Nasonia* species *N. vitripennis*, *N. giraulti*, and *N. longicornis* (Figure I-3) (Brucker and Bordenstein 2012a, 2013). Microbial diversity in these strains ranged from 44 to 83 OTUs at a 97% identity cutoff and varies between host species and developmental stages (Figure I-4). Overall bacterial diversity in *Nasonia* is similar to other Hymenoptera, such as honey bees (*Apis mellifera*, 82-116 OTUs), bumblebees (*Bombus sp.*, 33-47 OTUs), and fungus farming ants (*Mycocepurus smithii*, an average of 52 OTUs) (Martinson et al., 2011; Cariveau et al. 2014; Corby-Harris et al. 2014; Kellner et al. 2015). Like most insects, the *Nasonia* microbiota is dominated by members of the Proteobacteria phylum. The average *Nasonia* microbiota in adult males is composed of 74.4% Proteobacteria, 15.7% Actinobacteria, and 9.5% Firmicutes (Figure I-4) (Brucker and Bordenstein 2013). Interestingly, at the bacterial genus level, there are three major taxa (Gammaproteobacteria) that account for up to 75% of the male microbiota: *Providencia*, *Proteus*, and *Morganella* (Figure I-4). Alone, *Providencia spp.* compose 59, 68, and 41% of the microbiota in *N. vitripennis*, *N. giraulti*, and *N. longicornis*, respectively. Comparatively, *Nasonia* is a more tractable laboratory model for controlled experiments and is consistently comprised of 4-5 OTUs that make up the majority of all bacterial sequences.

The two genera *Providencia* and *Proteus* are often the most dominant OTUs observed in the three-wasp species throughout their development. These same two OTUs are frequently found in the fly host as well, which could represent a natural reservoir of the bacteria for *Nasonia*. Notably, *Nasonia* undergoes bacterial community successions throughout its development: The

microbial community remains relatively simple when the developing larvae are feeding on the likewise relatively simple microbiota of the fly pupa. Then, microbiota composition shifts during pupation, a time when the wasp is no longer feeding, and again before emergence as adult wasps (Figure I-4). As such, *Providencia* and *Proteus* represent 95-100% of the microbiota in larvae (Brucker and Bordenstein 2012a, 2013). Although the microbiota of pupae is less diverse than the microbiota of adults, both tend to exhibit a reduction in the dominance of Proteobacteria (Brucker and Bordenstein 2012a, 2013).

While little is known about the specific functional roles of the microbiota in *Nasonia*, several of the major bacterial genera have been previously studied in other insect models. For instance, *Proteus* has been shown to control the gut microenvironment in blowflies from overgrowth by other bacteria (Erdmann et al. 1984). This colonization resistance could be important for *Nasonia*, which feed on a decaying pupal fly host. Another major taxon, *Providencia*, has been implicated in two symbiotic roles: (i) Providing vitamin B to the blood-feeding leech *Haementeria officinalis* (Manzano-Marin et al. 2015) and (ii) acting as a natural control against the insect pathogen *Paenibacillus* in the Japanese honeybee *Apis cerana japonica* (Yoshiyama and Kimura 2009).

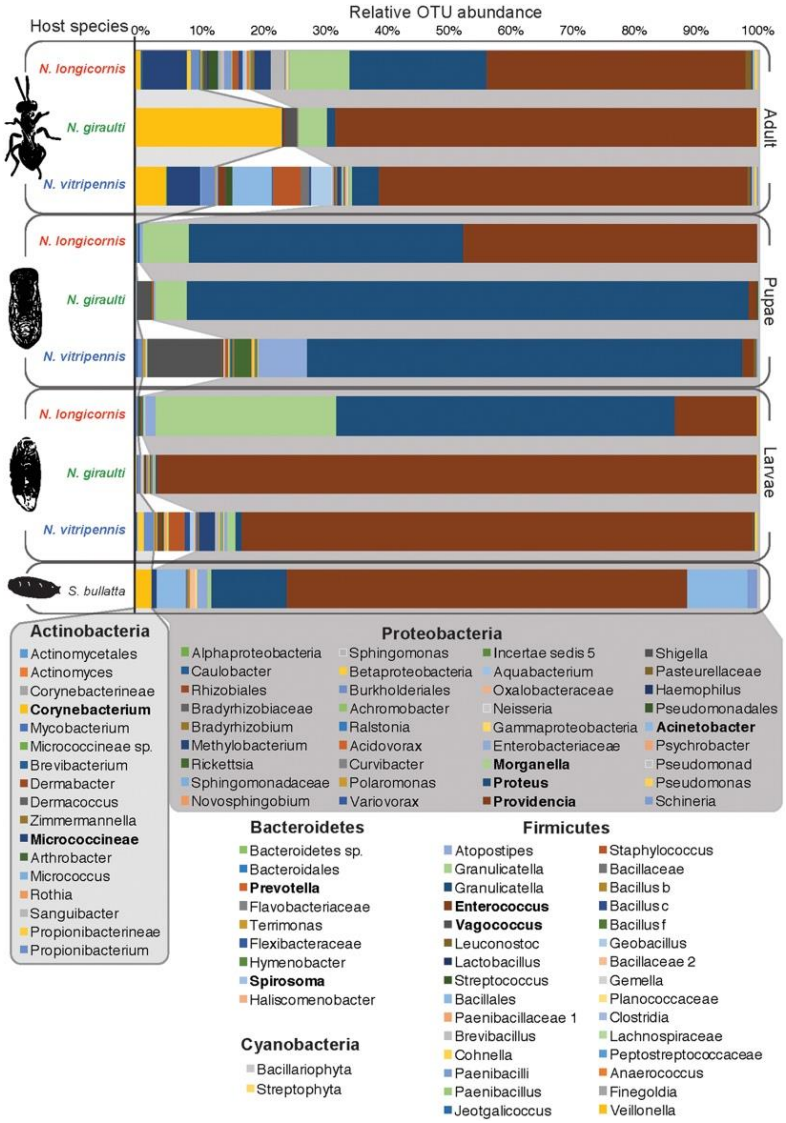

Figure I-4. The relative abundance of bacterial OTUs observed in male *Nasonia* throughout development (Brucker and Bordenstein 2013). The OTUs represented across the three *Nasonia* species and their *S. bullata* fly host are dominated by Actinobacteria, Firmicutes, and especially Proteobacteria. Three genera, *Providencia*, *Proteus*, and *Morganella*, are particularly dominant across all samples. However, their relative abundances differ according to host species and developmental stage. The unparasitized *S. bullata* fly host is similarly dominated by Proteobacteria, specifically the genus *Providencia*. Emboldened OTUs are observed at higher frequencies in one or more samples. It is important to note that many of the rarer OTUs have also been observed in other studies (Brucker and Bordenstein 2012a and personal communication).

Ongoing studies are now testing the functional significance of the microbiota in different species of *Nasonia* to determine their role in host development, e.g., through immune regulation, nutrition, and other mechanisms. In addition, transplantations of *Nasonia* microbiotas between host species will elucidate whether interspecific microbiotas alter host development traits such as larval size, larval and pupal development time or adult viability in comparison to intraspecific

microbiotas. In this context, studies in *D. melanogaster* have demonstrated that axenic individuals suffer from developmental defects along with smaller body size and an altered nutrient metabolism (Shin et al. 2011; Newell and Douglas 2014). These defects can be rescued by the acetic acid bacterium *Acetobacter pomorum*, which promotes larval growth and reduces lipid and sugar levels by modulating insulin signaling (Shin et al. 2011). In addition, *Lactobacillus plantarum* promotes larval growth in conditions of nutrient scarcity by enhancing protein assimilation and TOR-dependent hormonal growth signals (Storelli et al. 2011). In turn, the *Drosophila* innate immune response is fine-tuned to maintain gut microbiota homeostasis and responds to bacterial pathogens via ROS-production triggered by bacteria-derived uracil, which is released by various opportunistic pathogens but not autochthonous gut microbes (Ryu et al. 2008; Lee et al. 2013).

The microbial community is not limited to bacteria. *Nasonia* also harbors a diverse set of viruses (Bordenstein and Bordenstein, personal communication) and fungi, and their functional effects on the holobiont await further investigation. While no studies to date have investigated *Nasonia*'s fungal microbiota, the original draft of the *Nasonia* transcriptome revealed three novel single-stranded RNA viruses: NvitV-1, -2, -3 (Oliveira et al. 2010). These viruses were not previously found in other insect hosts, though they are related to the *Picornavirales*—a known order of insect pathogens. The observation of novel viruses in the system is interesting from the perspective that viruses are known to influence the biology of other parasitoid wasps. For instance, the virus *Leptopilina boulardi Filamentous Virus* (LbFV) manipulates the foraging behavior of its solitary parasitoid wasp host, *Leptopilina boulardi*, by inducing superparasitism (Varaldi et al. 2003, 2005, 2006). The virus is injected into the fly host together with the parasitoid eggs, allowing it to spread horizontally to uninfected individuals. In contrast to this infectious virus, polydnavirus-like particles have been integrated into the genomes of braconid and ichneumonid wasps and encode particles that contain wasp DNA and proteins which, when injected into the host with the parasitoids' eggs, enable evasion or direct suppression of the host's immune response against the parasitoid, thereby contributing significantly to parasitoid fitness (reviewed in Federici and Bigot 2003).

Establishment and transmission of the microbiota

The changes in the bacterial community throughout development raise questions as to how the *Nasonia* microbial community assembles through metamorphosis. The answer is not yet clear

in any animal system but the patterns exhibited by *Nasonia* offer an opportunity to better understand how animals change developmentally and anatomically with their microbiota. Since *Nasonia* embryos are directly deposited within fly host pupae via oviposition, both maternal and fly host microbes could contribute to the initial microbiota assembly of *Nasonia* larvae. Based on the transmission of microbes in *Drosophila* (Bakula 1969), it is possible that *Nasonia* acquire their first non-endosymbiotic bacteria through ingestion of the chorion during hatching. Alternatively, the microbial community could be passaged via maternal deposition of calyx fluid and venom (Huger et al. 1985; Werren et al. 1986). During this event, rare microbes could be introduced into the *Nasonia* microbiota. Subsequent colonization of the microbiota would then occur through feeding on the fly host. However, the excretion of the larval gut content prior to pupation presents a marked bottleneck for the microbiota. As larvae and pupae develop, it is possible that *Nasonia* species-specific innate immune genes regulate this community, which would parallel species-specific antimicrobial regulation of the microbiota in *Hydra* (Franzenburg et al. 2013). On the other hand, the innate immune response of honey bees has been shown to be strongly reduced during the pupal stage compared to larvae and adults (Gatschenberger et al. 2013). If this pattern is consistent across the order Hymenoptera, then a weaker immune regulation during the pupal stage could be influential in the mechanisms that establish the new host species-specific microbiota.

An important aspect that is often overlooked is that microbiota composition may not be regulated solely by host mechanisms, but also through interactions between the microbes themselves. From the microbial perspective, a host organism represents an ecosystem consisting of different microhabitats (i.e., niches) (Sicard et al. 2014), and microbes can be expected to differ in their preference for particular niches. Given that the *Nasonia* microbiota consists at least partly of bacteria acquired from its fly host during larval development, one might ask whether the transfer to *Nasonia* as a new host results in fitness consequences for the microbes. While some might be opportunistic and able to find suitable niches, *Nasonia* may represent a dead-end for other microbes, either due to host factors or competition with other bacteria. The latter may be due to competition for a shared resource/niche and/or by direct interference, for instance via the production of bacteriocidal toxins. Moreover, there may be indirect interactions, mediated through host mechanisms. A particular bacterium may, for instance, activate or suppress the host innate immune system, which then affects the proliferation of other bacteria.

An as yet unexplored but highly relevant aspect is the role of heritable symbionts in the establishment and composition of the *Nasonia* microbiota. *Wolbachia*, for instance, are generally highly abundant in various host tissues, thereby limiting available niches and resources for other bacteria (Dittmer et al. 2014, 2016). It is also known to influence other aspects of its host environment, such as immunity, apoptosis and iron homeostasis (Braquart-Varnier et al. 2008; Brownlie et al. 2009; Kremer et al. 2009, 2012; Kambris et al. 2010; Pan et al. 2012).

Germ-free and gnotobiotic rearing

A powerful aspect of the *Nasonia* model lies in the ability to selectively rear (or co-rear) *Nasonia* hosts in germ-free (Brucker and Bordenstein 2012b; Shropshire et al. 2016), gnotobiotic (harboring a known, controlled microbiota) and transbiotic (harboring the microbiota of a different species) conditions with methodology described in **CHAPTER IV**. The ability to inoculate germ-free *Nasonia* larvae with monocultures or whole microbial communities will enable high precision studies that deconstruct the effects of specific microbial functions in *Nasonia*. These studies have the benefit of being implemented at any stage throughout the *Nasonia* developmental process, which is important to understand the assembly and regulation of the *Nasonia* microbiota. Specific host genes could also be knocked down to observe their direct effects on microbiota assembly and host-microbe interactions in the four different *Nasonia* species. With rising interest in utilizing CRISPR genome editing in *Nasonia* (Lynch 2015), host gene addition and removal could soon be incorporated into the toolbox available for deciphering hologenomic interactions. With the unique environmental controls afforded by the *Nasonia* rearing system, there is ample opportunity to study microbiota influences on *Nasonia* development and fitness. With these tools at hand, the *Nasonia* model could also be used to experimentally test hologenomic evolution, for instance by exposing a wasp population to a selective pressure (e.g., an environmental stressor) and subsequently monitor (i) whether changes in the microbiota correlate with changes in host life history traits or behavior and (ii) whether this shift in the microbial community persists over multiple generations, as long as the selective pressure persists.

Phylosymbiosis

Microbiota composition is shaped by both host and environmental factors (e.g., immunity and diet, respectively (Ley et al. 2008; Ochman et al. 2010; Chandler et al. 2011; Colman et al. 2012; Ridley et al. 2012). While the first can be considered deterministic, the latter would be rather stochastic. However, it can be challenging to disentangle these two components and to precisely determine the relative roles of the host versus the environment on the establishment of a species' microbial community. Controlled conditions can provide evidence for host-microbiota interactions by removing confounding variations in diet, age and gender, for instance. Indeed, under a controlled experimental design, three *Nasonia* species were found to harbor distinguishable microbiotas whose beta-diversity relationships parallel host phylogeny at all developmental stages (Figure I-3A) (Brucker and Bordenstein 2012a,c). The congruence of host phylogeny and dendrograms reflecting relationships in microbiota composition has since been dubbed "phylosymbiosis" (Brucker and Bordenstein 2013). For a particular set of closely related species, phylosymbiosis predicts that intraspecific microbial communities are more similar than interspecific communities (Bordenstein and Theis 2015). Based on this premise, one could hypothesize that (i) microbiota-based models should predict host species origin with high accuracy, and (ii) various topological congruence analyses of host phylogeny and microbiota dendrograms will reveal significant degrees of phylosymbiosis. Furthermore, if phylosymbiosis were driven by both evolutionary and ecological forces, we might also observe that experimental transplants of autochthonous (intraspecific) versus allochthonous (interspecific) microbiota will drive reductions in host survival and fitness (**CHAPTER III and V**). In addition to *Nasonia*, the pattern of phylosymbiosis is evident in *Hominidae* (Ochman et al. 2010; Moeller et al. 2016), *Hydra* (Fraune and Bosch 2007; Franzenburg et al. 2013), sponges (Easson and Thacker 2014), ants (Sanders et al. 2014), and bats (Phillips et al. 2012) and further detailed in **CHAPTER III**. One future area of investigation will be to understand the factors influencing phylosymbiosis, e.g., fine-tuned host immune mechanisms and/or different transmission modes (i.e., through maternal transmission or environmental acquisition).

The microbiota and reproductive isolation

Our growing knowledge of the many ways in which microbial symbionts can induce changes in host phenotypic traits raises the question - to what extent do the microbiota contribute

to host diversification, reproductive isolation barriers, and speciation (see Brucker and Bordenstein 2012c; Vavre and Kremer 2014; Shropshire and Bordenstein 2016 for recent reviews)? Isolation barriers can be either pre-mating or post-mating. Pre-mating reproductive barriers may be driven by ecological or behavioral isolation. For instance, particular bacterial symbionts can confer novel traits (e.g., increased thermal tolerance or adaptation to new host plants), allowing their insect host to exploit new ecological niches (Montllor et al. 2002; Ferrari et al. 2004; Tsuchida et al. 2004). Niche expansions such as these can result in geographically or sympatrically isolated populations and, given enough time, lead to speciation. In addition, the microbiota has been implicated in behavioral changes related to mate choice, which may result in symbiont-driven behavioral isolation due to differences in courtship or mate discrimination (reviewed in Shropshire and Bordenstein 2016). For example, *Wolbachia* plays a crucial role in driving pre-mating isolation between semispecies of the *Drosophila paulistorum* species complex (Miller et al. 2010). In addition, the gut microbiota influences kin recognition and mating investment in several *Drosophila* species (Lize et al. 2014). Specifically, both *D. bifasciata* and *D. melanogaster* are able to distinguish between mates that have a more similar or dissimilar microbiota to themselves (Sharon et al. 2010; Lize et al. 2014). This results in a tendency for assortative mating in *D. melanogaster* after feeding on different food sources (Sharon et al. 2010), although this behavior was replicated only in inbred laboratory lines (Najarro et al. 2015). Similarly, mate selection in scarab beetles is dependent upon immune competence that the females sense in the bacterial-derived male pheromones secretions (Leal, 1998; Vasanthakumar et al. 2008; Andert et al. 2010).

In contrast, post-mating reproductive barriers may be driven by genetic conflicts between host and microbes (i.e., *Wolbachia*) or a breakdown in holobiont complexes. In *Nasonia*, both types occur. *Wolbachia*-induced CI in this system is a pre-eminent case of symbiont-assisted isolation in which nearly complete CI levels (Figure I-2) between the *Nasonia* species cause F1 hybrid lethality that is reversible by curing the *Wolbachia* infections. In other words, the interspecific F1 isolation is essentially undone with antibiotics that restore production of viable F1 hybrids (Breeuwer and Werren 1990, 1995; Bordenstein et al. 2001; Raychoudhury et al. 2010a). The study system is notable in that it provided the opportunity to investigate whether *Wolbachia*-induced CI evolved early or late in the speciation process, i.e., before or after other interspecific pre- or post-mating barriers. While the "older" species pair, *N. vitripennis* and *N. giraulti*, diverged ~1 mya and evolved other post-mating barriers such as high F2 hybrid mortality and abnormal

courtship behavior (Breeuwer and Werren 1995; Bordenstein et al. 2001); the very young species pair, *N. giraulti* and *N. longicornis*, diverged only ~400,000 years ago and produce viable and fertile hybrids (Bordenstein et al. 2001). This observation indicates that *Wolbachia*-induced reproductive isolation via CI preceded the evolution of other post-mating barriers in the younger species pair, and therefore is the first major step in the speciation process (Bordenstein et al. 2001). The even younger species pair, *N. giraulti* and *N. oneida*, represents an interesting case in this context: *N. oneida* females show strong mate discrimination against *N. giraulti* males, but not vice versa, resulting in strong but incomplete and asymmetrical pre-mating isolation (Raychoudhury et al. 2010a). Moreover, the mate discrimination phenotype in *N. oneida* is recessive and lost in F1 hybrid females (Raychoudhury et al. 2010a). The impact of *Wolbachia* on this speciation event is unfortunately blurred by the recent *Wolbachia*-mitochondrial sweep from *N. giraulti* into *N. oneida* (Raychoudhury et al. 2009), which eliminated any *Wolbachia*-induced incompatibilities that may have existed previously. Therefore, pre-mating isolation is the only barrier currently preventing hybridization between the two species.

An additional microbiota-mediated reproductive barrier has recently been uncovered in *Nasonia*, manifested as strong F2 hybrid lethality in interspecies crosses after curing of *Wolbachia* (Brucker and Bordenstein 2013). Specifically, hybrid lethality between *N. vitripennis* and *N. giraulti* is reversed through removal of the *Nasonia* gut microbiota and can be reinstated by inoculating germ-free hybrids with *Nasonia*-derived bacterial cultures (Brucker and Bordenstein 2013). *Nasonia* hybrid lethality was also characterized by an altered gut microbiota in which a rare microbial genus became abundant in hybrids. The change in bacterial community structure was coupled with aberrant host immune gene expression (specifically differential regulation of serine proteases, antimicrobial peptides, and several signaling molecules from the IMD and Toll pathways) compared to the parental species (Brucker and Bordenstein 2013). In this case, hybrid breakdown at the holobiont level led to severe mortality. This is the first study, to our knowledge, in which the microbial community contributes to hybrid mortality (Figure I-2).

Changes in the microbiota could also result in other microbe-dependent reproductive barriers, similar to phenotypes observed in various animal systems, e.g., in terms of development time, behavior, and fecundity (Brucker and Bordenstein 2012c). For example, species-specific cuticular hydrocarbons help in mate discrimination in *Nasonia* (Buellesbach et al. 2013), but the

impact of the microbiota on mate-choice is unknown. The behavioral issues that arise in hybrids (Clark et al. 2010) may therefore have microbial underpinnings.

Chapter previews

In this dissertation, I assess the roles of microbial symbionts and whole microbial communities in the evolution of their *Nasonia* wasp host. Starting with changes in *Nasonia* host regulation of a single endosymbiont, I describe in **CHAPTER II** the underlying genetic determinant in *Nasonia* wasps that regulates the densities of *Wolbachia w*VitA. By utilizing a forward genetic approaches to determine a *Nasonia vitripennis* gene capable of suppressing *Wolbachia* densities during maternal transmission, I demonstrate how the association between *Nasonia vitripennis* and *Wolbachia w*VitA has shaped the evolution of endosymbiont density suppression within the *Nasonia* clade. The host-microbe interactions during invertebrate maternal microbial transmission may play an important role in establishing host species-specific long-term symbioses.

Expanding upon the evolutionary aspects of interactions between *Nasonia* wasps and a vertically-transmitted endosymbiont to environmentally-acquired microbial communities, I present in **CHAPTER III** the eco-evolutionary relationships between *Nasonia* wasps and their gut microbiota through the pattern of phylosymbiosis. Phylosymbiosis observes that through both vertical and horizontal microbial transmission, the animal host will maintain species-specific gut microbiota; and the evolutionary history of the host species will parallel the compositional similarities in their microbiota. Since host evolution results in a pattern of host-specific microbiota, then the host may adapt to its specific microbiota resulting in performance reductions when given microbiota transplants from other host species. The pattern of phylosymbiosis was validated in *Nasonia* wasps revealing that interactions between hosts and their gut microbiota can drive the adaptation and speciation of the host.

In order to better understand the pattern of phylosymbiosis through functional experiments, I describe in **CHAPTER IV** the optimization of a technical assay for rearing Nasonia in a germ-free environment in protein-rich media without exogenous components fetal bovine serum and penicillin. This tool was an important step for the study of microbial transplantation in *Nasonia* wasps necessary to understand the functional effects of a phylosymbiotic pattern on *Nasonia* development. With the new germ-free rearing assay, I was able to better analyze growth and

metamorphosis metrics throughout the entire *Nasonia* life cycle from early larvae to adulthood. This improvement was especially important for determining the role of interspecific microbiota transplants in the reduction of *Nasonia* development and survival. I utilized the optimized *Nasonia* germ-free rearing system in **CHAPTER V** to observe the effects of interspecific microbiota transplants over the course of *Nasonia* development. I observed developmental delays from interspecific transplants during the transition between the 2nd and 3rd instar larval stages that resulted in decreased pupation and, ultimately, decreased survival to adulthood. These results support an evolutionary aspect of phylosymbiosis in which host association with its specific gut microbiota acts on adaptive host-microbiota interactions.

The major conclusions and advancements proposed for understanding the role of host-microbe interactions in animal evolution are discussed in **CHAPTER VI** along with future experimentation to better understand mechanisms of host-microbe interactions that were not fully elucidated in the previous chapters.

CHAPTER II. THE MATERNAL EFFECT GENE *WDS* CONTROLS *WOLBACHIA* TITER IN *NASONIA*[∴]

Abstract

Maternal transmission of intracellular microbes is pivotal in establishing long-term, intimate symbioses. For germline microbes that exert negative reproductive effects on their hosts, selection can theoretically favor the spread of host genes that counteract the microbe's harmful effects. Here, we leverage a major difference in bacterial (*Wolbachia pipientis*) titers between closely related wasp species with forward genetic, transcriptomic, and cytological approaches to map two quantitative trait loci that suppress bacterial titers via a maternal effect. Fine mapping and knockdown experiments identify the gene *Wolbachia density suppressor* (*Wds*), which dominantly suppresses bacterial transmission from mother to embryo. *Wds* evolved by lineage-specific non-synonymous changes driven by positive selection. Collectively, our findings demonstrate that a genetically simple change arose by positive Darwinian selection in less than a million years to regulate maternally transmitted bacteria via a dominant, maternal effect gene.

Introduction

Many animals harbor microorganisms that participate in beneficial processes as diverse as nutritional uptake and metabolism (Ley et al. 2006; Turnbaugh et al. 2006), immune cell development (Round et al. 2011; Ivanov et al. 2008), and pathogen resistance (Candela et al. 2008; Fukuda et al. 2011). However, even innocuous microbes can become harmful when not properly regulated (Calderone and Fonzi 2001; Mitchell 2011). Moreover, intracellular symbionts that are maternally transmitted over multiple host generations can impose long-term, negative fitness effects on their hosts (Fleury at al. 2000; Min and Benzer 1997). In these intimate and enduring symbioses, hosts are predicted to evolve suppression that reduces the harmful effects of the symbiont (Koehncke et al. 2009; Jaenike 2009). However, little is known about the genes and evolutionary forces that underpin the regulation of maternally transmitted symbionts, despite the repeated and independent origins of maternal transmission in diverse host taxa (Funkhouser and Bordenstein 2013). Reverse genetic studies in insects suggest immune or developmental genes may evolve to affect endosymbiont densities (Login et al. 2011; Serbus et al. 2011; Newton et al.

[∴] This chapter was published in *Current Biology* (2018) 28(11):1692-1702 with Ananya Sharma and Seth Bordenstein as co-authors. Lisa Funkhouser-Jones was co-first author.

2015); but, to the best of our knowledge, no studies have utilized forward genetic approaches to identify the gene(s) underlying variation in host regulation of maternally transmitted symbionts.

Here, we utilize a major host interspecific difference in titers of the maternally transmitted bacteria *Wolbachia* and quantitative trait loci analyses to identify a maternal effect, suppressor gene in the *Nasonia* model. *Nasonia* (order Hymenoptera) is a genus of parasitoid wasps comprised of four closely related species, with *N. vitripennis* last sharing a common ancestor with the other three species approximately one million years ago (Campbell et al. 1993; Raychoudhury 2010a; Gadau et al. 2002). In the lab, interspecific crosses of *Nasonia* species with the same or no *Wolbachia* produce viable and fertile hybrid females, which permits the transfer of genetic or cytoplasmic material (including intracellular *Wolbachia*) between *Nasonia* species. Consequently, *Nasonia* is a powerful model for studying the quantitative genetics of interspecific variation in host traits, such as wing size (Gadau et al. 2002; Loehlin et al. 2010), head shape (Werren et al. 2016), and sex pheromones (Nielhuis et al. 2013).

Wolbachia (order Rickettsiales) live intracellularly in 40%–52% of all arthropod species (Zug and Hammerstein 2012; Weinert et al. 2015), and they are predominantly transmitted transovarially with occasional transfer between host species on an evolutionary timescale (Werren et al. 1995; Vavre et al. 1999). In most insects, including in *Nasonia*, *Wolbachia* function as reproductive parasites that manipulate host reproduction through a variety of mechanisms to achieve a greater proportion of infected females in the host population (Werren et al. 2008; Serbus et al. 2008). Both efficient maternal transmission and host reproductive manipulation often depend on sufficiently high within-host *Wolbachia* densities (Perrot-Minnot and Werren 1999; Dyer et al. 2005); however, overproliferation of *Wolbachia* can drastically reduce lifespan in *Drosophila* (Min and Benzer 1997), mosquitoes (McMeniman et al. 2009; Suh et al. 2009), and terrestrial isopods (Le Clec'h et al. 2012). Thus, co-adaptation between arthropod hosts and *Wolbachia* strain(s) can promote genetic and phenotypic changes that impact transmission of *Wolbachia* densities (Mouton et al. 2003; Kondo et al. 2005; Rio et al. 2006; Chafee et al. 2011). When co-adapted host and *Wolbachia* pairs are disrupted through experimental transfer of *Wolbachia* into a naive host, control of the symbiosis is often lost, leading to overproliferation and expanded tissue tropism of *Wolbachia*, changes in bacteriophage activity, and/or fitness costs not observed in the original host species (Le Clec'h et al. 2012; Chafee et al. 2011; Bian et al. 2013).

Each *Nasonia* species is naturally infected with different *Wolbachia* strains that were primarily acquired through horizontal transfer; in rare cases, the *Wolbachia* have since co-diverged with their host wasp species (Raychoudhury et al. 2009). Introgression of a specific *Wolbachia* strain (*w*VitA) from one *Nasonia* species (*N. vitripennis*) to a naive, closely related species (*N. girault*i) results in a major perturbation of the symbiosis in which the relative *Wolbachia* densities increase by two orders of magnitude, and there is an associated reduction in fecundity in *N. girault*i (Chafee et al. 2011). Importantly, *w*VitA densities and *Nasonia* fecundity return to normal when *w*VitA is crossed back into an *N. vitripennis* genomic background from the high-density *N. girault*i line (IntG). Since both the native *N. vitripennis* and the wVitA-infected *N. girault*i IntG lines have the same cytotype, the interspecific *Wolbachia* density variation is established by variation in the host nuclear genomes (Chafee et al. 2011). In this study, we utilize several forward genetic techniques in *Nasonia* to dissect the genetic, evolutionary, and cytological basis of maternal regulation of *Wolbachia*. The varied approaches culminate in the characterization of two quantitative trait loci and the discovery of *Wolbachia* density suppressor (*Wds*), a positively selected, maternal effect gene that suppresses the transmission of *Wolbachia*.

Materials and Methods

Nasonia parasitoid wasps

Experiments were performed with *N. vitripennis* strain 12.1, *N. girault*i strain IntG12.1 or hybrids of these two species. *N. vitripennis* 12.1 is singly-infected with native *Wolbachia* strain *w*VitA and was derived from the double-infected *N. vitripennis* R511 (*w*VitA and *w*VitB) after a prolonged period of diapause (Perrot-Miot et al. 1996). *N. girault*i strain IntG12.1 was generated by backcrossing *N. vitripennis* 12.1 females to uninfected *N. girault*i Rv2x(u) males for nine generations (Chafee et al. 2011), producing hybrids with an *N. girault*i genome and an *N. vitripennis* cytoplasm harboring *w*VitA. All *Nasonia* were reared at 25°C in constant light on *Sarcophaga bullata* fly hosts reared in house on bovine liver from Walnut Hills Farm (Tennessee, USA).

Quantitative analysis of Wolbachia densities

Genomic DNA was extracted from pupae or adult *Nasonia* using the Gentra Puregene Tissue Kit (QIAGEN) according to the manufacturer's protocol. Real-time quantitative PCR

(qPCR) was performed on a CFX96 Real-Time system (Bio-Rad) using a total reaction volume of 25 µl: 12.5 µL of iQ SYBR Green Supermix (Bio-Rad), 8.5 µL of sterile water, 1.0 µL each of 5 µM forward and reverse primers, and 2 µL of target DNA in single wells of a 96-well plate (Bio-Rad). All qPCR reactions were performed in technical duplicates and included a melt curve analysis to check for primer dimers and nonspecific amplification. Selective amplification was performed using primers previously described for the *Wolbachia* groEL gene (Bordenstein et al. 2006) and *Nasonia* NvS6K gene (Bordenstein and Bordenstein 2011). Standard curves for each gene were constructed as previously described (Bordenstein and Bordenstein 2011) using a log10 dilution series of larger PCR products of known concentrations for each gene. groEL and S6K copy numbers for each sample were calculated based on the following standard curve equations: groEL: $y = -3.367x + 35.803$ and S6K: $y = -3.455x + 35.908$, where y = averaged Ct value between technical duplicates and x = log starting quantity of template DNA. *Wolbachia* density was calculated by dividing groEL copy number by S6K copy number for each sample. Since diploid female *Nasonia* have twice the number of S6K copies than males, all experiments comparing *Wolbachia* densities were performed on either all male or all female samples to eliminate S6K copy number as a confounding factor in the statistical analyses.

Microsatellite marker genotyping

Primers used to amplify microsatellite markers that differ in size between *N. vitripennis* and *N. giraulti* are listed in Appendix A. Microsatellite markers not previously published were identified by aligning *N. vitripennis* and *N. giraulti* genomic sequences using the Geneious alignment tool in Geneious Pro v5.5.8 (Biomatters). The Geneious primer design tool was then used to generate primer sets spanning each microsatellite. All PCR reactions were run on a Veriti Thermal Cycler (Applied Biosystems) with a total reaction volume of 15 µl: 7.5 µL of GoTaq Green Master Mix (Promega), 3.6 µL of sterile water, 1.2 µL of 5 µM forward and reverse primers (see Appendix A for annealing temp.), and 1.5 µL of target DNA. PCR products were run on 4% agarose gels in TBE buffer (Sigma) at 90 V for 2.5 to 6 hours, stained with GelRed (Biotium) according to manufacturer's protocol, and imaged on a Red Personal Gel Imager (Alpha Innotech). New markers were validated based on predicted band size using *N. vitripennis* 12.1 and *N. giraulti* IntG as controls.

Phenotypic selection introgression and genotyping

N. vitripennis 12.1 females (low *w*VitA density) were backcrossed with *N. giraulti* IntG males (high *w*VitA density) for nine generations. For each generation of backcrossing, five female pupal offspring were pooled from each hybrid mother (N = 13 – 35 hybrid females depending on survival at each generation), and the pupal *Wolbachia* densities were measured using qPCR. Sisters of the pupae with the lowest *Wolbachia* densities were then used as mothers in the next round of backcrossing (N = 60 – 80 hybrid females). Two independent selection lines were maintained simultaneously along with control lines of pure-breeding *N. vitripennis* and *N. giraulti*. After eight generations of selection, the three females from each introgression line that produced ninth-generation offspring with the lowest *Wolbachia* densities were pooled and their DNA extracted using the DNeasy Blood and Tissue Kit (QIAGEN) with the protocol for purification of DNA from insects. To obtain enough DNA for microarray hybridization, we used the REPLI-g Mini Kit (QIAGEN) with the protocol for 5 μL of DNA template to amplify genomic DNA overnight at 30°C, then purified the DNA using ethanol precipitation. The final concentration for each sample was diluted to 1 μg/μl and a total of 10 μL was sent to The Center for Genomics and Bioinformatics at Indiana University to be processed on a *Nasonia* genotyping microarray (Roche NimbleGen) tiled with probes for 19,681 single nucleotide polymorphisms and indels that differ between *N. vitripennis* and *N. giraulti* (Desjardins et al. 2013).

For each sample, the proportion of *N. vitripennis* alleles at each marker was determined based on the ratio of hybridization to the *N. vitripennis*-specific probe versus hybridization to the *N. giraulti*-specific probe, as previously described (Desjardins et al. 2013). To verify species-specificity of these markers for our *Nasonia* strains, we also genotyped *N. vitripennis* 12.1 and *N. giraulti* IntG control females on the array, and markers that did not display the correct specificity within one standard deviation of the median were removed from subsequent analyses (5,301 markers total). The remaining markers were then manually mapped back to the most recent *Nasonia* linkage map (Desjardins et al. 2013). Since all introgression females received one copy of their diploid genome from their *N. giraulti* father, the theoretical maximum proportion of *N. vitripennis* alleles at each marker cluster for experimental samples is 0.5. The proportion of *N. vitripennis* alleles was averaged for every 22 consecutive markers across each chromosome, and heatmaps were generated using the HeatMap function in MATLAB (MathWorks). Areas were considered enriched for *N. vitripennis* alleles at ≥ 0.2.

QTL analysis

F2 hybrid females (N = 191) were generated by backcrossing F1 *N. vitripennis*/*N. girault*i hybrids to *N. girault*i IntG males. F2 females were then backcrossed again to *N. girault*i IntG and allowed to lay offspring. Five female pupae from each F2 female were pooled and their *Wolbachia* densities measured using qPCR. Females that produced offspring with densities within the highest and lowest quartile of the density distribution (N = 42 for each quartile) were selectively genotyped with 47 microsatellite markers spread across chromosomes 1, 2 and 3 with an average distance of 3 cM between markers (Table A-1). Phenotypic information for all 191 F2 females was included in the mapping analyses to prevent inflation of QTL effects due to the biased selection of extreme phenotypes (Lander and Botstein 1989). QTL analyses were performed in R (version 3.0.2) with package R/qtl (Broman et al. 2003). Significance thresholds for our dataset were calculated by using a stratified permutation test with the scanone function (1000 permutations). To identify significant QTL and their interactions, we first conducted a one-dimensional, one-QTL scan and a two-dimensional, two-QTL scan using the EM algorithm with a step size of 1 cM and an assumed genotype error probability of 0.001. Two significant QTLs were identified, one each on chromosomes 2 and 3, which were predicted to act additively. The positions of identified QTL were then refined using multiple QTL modeling with the multiple imputation algorithm (200 imputations, step size = 1 cM) assuming a model with two additive QTLs. 95% Bayes credible intervals were calculated for each QTL after multiple QTL modeling using the bayesint function.

Marker-assisted segmental introgressions

Marker-assisted segmental introgression lines were generated by repeatedly backcrossing hybrid females to *N. girault*i IntG males for nine generations while selecting for *N. vitripennis* alleles at three microsatellite markers on chromosome 3 (MM3.17, NvC3-18, and MM3.37). After the ninth generation, families that maintained an *N. vitripennis* allele at one or more of these markers were selected, and siblings were mated to each other to produce lines containing homozygous *N. vitripennis* regions at and around the markers. Individual adult females from each segmental line were genotyped and phenotyped separately (N = 10 – 15 females per line). Females were hosted as virgins, five male pupal offspring per female were pooled, and pupal *Wolbachia* densities were measured using qPCR. Variation across plates for a single experiment was reduced by including a set of parental DNA controls on all plates. The parental fold-change was then

calculated by dividing the average *N. girault*i control density by the average *N. vitripennis* control density. To calculate the sample fold-change, the absolute density for each sample was divided by the average density of the *N. vitripennis* control. To determine how "effective" each segmental introgression line was at reducing densities, we calculated the percent effect on density suppression for each sample using the following equation:

$$\%\ effect\ \ on\ density\ suppresion = \left(1 - \frac{sample\ fold\ change}{parental\ fold\ change}\right) \times 100$$

Each female was genotyped with markers across the region of interest, all females with identical genotypes across all markers were grouped together, and their percent effects on density suppression were averaged.

For the two subsequent rounds of introgression lines (R1 to R10 and R6-1 to R6-3), 300 IntC3 line virgin females or 800 R6 line virgin females, respectively, were backcrossed to IntG males. The resulting virgin F1 females produced haploid, recombinant F2 males. These recombinant males were mated to IntG females to produce heterozygous female offspring with the recombinant genotype. Siblings were then mated to each other and genotyped for two more generations to produce recombinant lines containing homozygous *N. vitripennis* introgressed regions reduced in size.

A subset of the genes within the 32-gene candidate region were genotyped using sequencing primers (Table A-5) to amplify PCR products 250-750 bp for each of the R6 recombinant lines (R6-1 to R6-3) for Sanger sequencing (GENEWIZ). All PCR reactions were run on a Veriti Thermal Cycler (Applied Biosystems) with a total reaction volume of 15 µl: 7.5 µL of GoTaq Green Master Mix (Promega), 3.6 µL of sterile water, 1.2 µL of 5 µM forward and reverse primers (see Table A-5 for annealing temp.), and 1.5 µL of target DNA and purified using the QIAquick PCR Purification kit (QIAGEN). At least 6 distinct single nucleotide polymorphisms (SNPs) between *N. vitripennis* and *N. girault*i alleles were used to characterize the allele for each recombinant line using Geneious Pro v5.5.8 (Biomatters).

RNA-seq of ovaries

One-day old adult, virgin females from *Nasonia* strains *N. vitripennis* 12.1, *N. girault*i IntG, and *N. vitripennis*/*N. girault*i introgression line IntC3 were hosted as virgins on *S. bullata* pupae for 48 hours to stimulate feeding and oogenesis. Females were then dissected in RNase-free 1X

PBS buffer, and their ovaries were immediately transferred to RNase-free Eppendorf tubes and flash-frozen in liquid nitrogen. Forty ovaries were pooled for each replicate and 4-5 biological replicates were collected per *Nasonia* strain. Ovaries were manually homogenized with RNase-free pestles, and their RNA was extracted using the Nucleospin RNA/Protein Kit (Macherey-Nagel) according to the manufacturer's protocol for purification of total RNA from animal tissues. After RNA purification, samples were treated with RQ1 RNase-free DNase (Promega) for 1 hour at 37°C, followed by an ethanol precipitation with 1/10th volume 3M sodium acetate and 3 volumes 100% ethanol incubated overnight at −20°C. PCR of samples with *Nasonia* primers NvS6KQTF4 and NVS6KQTR4 (Bordenstein and Bordenstein 2011) revealed some residual DNA contamination, so DNase treatment and ethanol precipitation were repeated. After the second DNase treatment, PCR with the same primer set confirmed absence of contaminating DNA. Sample RNA concentrations were measured with a Qubit 2.0 Fluorometer (Life Technologies) using the RNA HS Assay kit (Life Technologies). All samples were run multiplexed on two lanes of the Illumina HiSeq3000 (paired-end, 150 bp reads, ∼30M reads) at Vanderbilt's VANTAGE sequencing core. Raw reads were trimmed and mapped to the *N. vitripennis* genome Nvit_2.1 (GCF_000002325.3) in CLC Genomics Workbench 8.5.1, allowing ten gene hits per read using a minimum length fraction of 0.9 and a minimum similarity fraction of 0.9. The number of reads generated for each sample and the percentage of reads that mapped to the *N. vitripennis* genic and intergenic regions are provided in Table A-2. Significant differential gene expression was determined in CLC Genomics Workbench 8.5.1 at $\alpha = 0.05$ for unique gene reads using the Empirical analysis of DGE tool, which is based on the edgeR program commonly used for gene expression analyses (Robinson et al. 2010).

RT-qPCR validation of RNA-seq results

One-day old adult, virgin females from *N. vitripennis* 12.1, *N. giraulti* IntG, and IntC3 were hosted with two *S. bullata* pupae and honey to encourage ovary development. After 48 hours, ovaries were removed in RNase-free PBS, flash-frozen in liquid nitrogen then stored at −80°C. 4-5 replicates of fifty ovaries per replicate were collected for each *Nasonia* strain. Total RNA was extracted from each sample using Trizol reagent (Invitrogen) with the Direct-zol RNA Miniprep kit (Zymo Research) then treated with the DNA-free DNA Removal kit (Ambion) for one hour at

37°C. After ensuring with PCR that all DNA had been removed, RNA was converted to cDNA using the SuperScript VILO cDNA Synthesis kit (Invitrogen).

RT-qPCR was performed on a CFX96 Real-Time system (Bio-Rad) using a total reaction volume of 25 µl: 12.5 µL of iTaq Universal SYBR Green Supermix (Bio-Rad), 8.5 µL of sterile water, 1 µL each of 5 µM forward and reverse primers (Table S6), and 2 µL of target cDNA in single wells of a 96-well plate (Bio-Rad). All RT-qPCR reactions were performed in technical duplicates and included a melt curve analysis to check for nonspecific amplification. The 60S ribosomal protein L32 (also known as RP49) was used as an expression control. All primers for RT-qPCR are provided in Table S6. Expression values for each candidate gene were calculated using the ΔΔCt method of relative quantification (Livak and Schmittgen 2001) with RP49 as the reference gene. Fold-change was determined by normalizing expression values to the mean expression value of *N. giraulti* IntG for each gene.

RNAi of candidate genes

To generate DNA template for dsRNA synthesis, primers with a T7 promoter sequence on the 5′ end of each primer were used to amplify a 450-700 bp region of the targeted genes (Table S6) by PCR using *N. vitripennis* whole-body cDNA as template. PCR amplicons were separated by electrophoresis on a 1% agarose gel, excised, and purified using the QIAquick Gel Extraction kit (QIAGEN). The purified PCR products were used as template for a second PCR reaction with the same gene-specific T7 primers, then purified using the QIAquick PCR Purification kit (QIAGEN). After quantification with the Qubit dsDNA Broad Range Assay kit (Thermo Fisher Scientific), approximately 1 µg of the purified PCR amplicon was used as template for dsRNA synthesis with the MEGAScript RNAi kit (Ambion). The dsRNA synthesis reaction was incubated for six hours at 37°C, treated with RNase and DNase for one hour at 37°C, then column-purified according to the manufacturer's protocol.

For injection, the dsRNA was used at a final concentration standardized to 750 ng/µL dsRNA. A Nanoject II (Drummond Scientific) was used to inject 23 nL of dsRNA (or MEGAScript kit elution buffer) into the ventral abdomen of virgin, female *Nasonia* at the red-eyed, yellow pupal stage. After emerging as adults, injected females were given honey and hosted individually on two *S. bullata* pupae for 48 hours. On the third day after emergence, they were transferred to new vials where they were presented with a single *S. bullata* pupae that was only exposed at the anterior end.

After five hours, the pupae were opened and ten male embryos were collected in a 0.2 mL PCR tube for each female and stored at −80°C. The females were hosted on two pupae overnight, and then the same process was repeated again on the fourth day.

The number of *Wolbachia* bacteria per male embryo from injected females three and four days post emergence was determined using qPCR with *Wolbachia* groEL primers as described above. *Wolbachia* titers were not normalized to *Nasonia* gene copy number because early embryos have varying numbers of genome copies depending on how many rounds of mitotic division they have undergone (Pultz et al. 2005). To determine the knock-down efficiency of each dsRNA injection, RNA extraction and RT-qPCR of black pupae, five days post injection, were performed with 14-17 biological replicates from each treatment group as described above using the gene-specific RT-qPCR primers in Table A-6.

Wds phylogeny and selection analyses

N. giraulti and *N. longicornis* nucleotide sequences of *Wds* were obtained from NCBI genomic scaffold sequences GL276173 and GL277955, respectively, and indels were manually extracted in Geneious Pro v11.0.3 (Biomatters) based on homology to *N. vitripennis* gene LOC1006079092. Protein alignment of Wds amino acid sequences for the three *Nasonia* spp. and its homolog in *T. sarcophagae* (TSAR_005991) was performed using the Geneious alignment tool. MEGA7.0.26 (Kumar et al. 2016) was used to identify the JTT model as the best model of protein evolution for the alignment based on corrected Akaike information criterion (AICc). PhyML (Guindon et al. 2010) and MrBayes (Huelsenbeck and Ronquist 2001) were executed in Geneious with default parameters to construct a maximum likelihood tree with bootstrapping and a Bayesian tree with a burn-in of 100,000, respectively.

To identify residues under positive selection in Wds, Ka/Ks values were calculated based on a pairwise alignment of the *N. vitripennis* and *N. giraulti* Wds coding sequences using a sliding window analysis (window = 30 AA, step size = 1 AA, Standard Code for genetic code input) in the SWAKK bioinformatics web server (Liang et al. 2006). Analysis of Wds for protein structures and conserved domains was performed using the SMART online software at http://smart.embl-heidelberg.de (Letunic and Bork 2018). Protein pIs were predicted using the online ExPASY Compute pI/Mw tool.

Imaging Wolbachia in Nasonia

For *Wolbachia* staining in ovaries, virgin, female *Nasonia* were hosted on *S. bullata* pupae for two to three days before dissection to encourage ovary development. Females were dissected in 1X phosphate-buffered saline (PBS) solution, where ovaries were removed with forceps and individual ovarioles were separated with fine needles. Ovaries were fixed in 4% formaldehyde in PBS with 0.2% Triton X-100 (PBST) for 20 minutes at room temperature then transferred to a 1.5 mL Eppendorf tube containing PBST. Samples were washed quickly three times with PBST then incubated in PBST plus 1 mg/ml RNase A for three hours at room temperature then overnight at 4°C. After removing the RNase A solution, ovaries were incubated at room temperature for 15 minutes in PBST with 1:300 SYTOX green nucleic acid stain (Thermo Fisher Scientific) before washing twice with PBST, 15 minutes each time. Ovaries were then transferred to a glass slide and mounted in ProLong Gold antifade solution (Thermo Fisher Scientific) and covered with a glass coverslip sealed with nail polish. Ovary images in Figure I-2 are representative of three independent experiments performed on different days with 2 – 3 females per species.

For *Wolbachia* staining in embryos, virgin, female *Nasonia* were hosted on a single *S. bullata* pupae for five hours. The host puparium was peeled away, and embryos were transferred with a probe to a glass vial containing 5 mL heptane. After shaking for two minutes, 5 mL methanol was added to the vial and shaken for another two minutes. Dechorionated embryos that sunk to the bottom of the vial were transferred to a 1.5 mL Eppendorf tube with methanol, then were serially rehydrated in increasing ratios of methanol to PBST for 1 min each (90% MeOH:10% PBST, 75% MeOH: 25% PBST, 50% MeOH: 50% PBST, 25% MeOH:75% PBST) before a final wash in 100% PBST for 5 mins. Embryos were then blocked in PBST + 0.2% BSA (PBST-BSA) for 30 mins then PBST-BSA + 5% normal goat serum (PBANG) for 1 hour followed by a 2-hour incubation in PBANG + 1 mg/ml RNase. Embryos were stained overnight at 4°C with monoclonal mouse *anti*-human Hsp60 antibody (Sigma; 1:250), which cross-reacts with *Wolbachia* but not insect proteins (Taylor and Hoerauf 1999; McGraw et al. 2002). After washing in PBST-BSA (4X, 15 mins each), embryos were incubated in goat *anti*-mouse Alexa Fluor 594 (Thermo Fisher Scientific; 1:500) for 2 hours, washed again in PBST-BSA (4X, 15 mins each), then mounted to coverslips with Prolong Diamond Antifade Mountant (Thermo Fisher Scientific). Embryo images in Figure I-2 are representative of two independent experiments performed on different days.

All images were acquired on a Zeiss LSM 510 META inverted confocal microscope at the Vanderbilt University Medical Center Cell Imaging Shared Resource core and processed with Fiji software (Schindelin et al. 2012). Quantification of *Wolbachia* in *Nasonia* oocytes and nurse cells of stage 3 egg chambers was performed by calculating corrected total cell fluorescence with ImageJ software 1.47v. *Nasonia* oocyte images taken at the same relative z stack slice were traced and the area integrated intensity was measured and compared to a background region (a traced region next to the egg chamber that has no fluorescence). Corrected total cell fluorescence was calculated as integrated intensity of the oocyte – (area of the oocyte $*$ mean fluorescence of the background region). Quantification of *Wolbachia* in *Nasonia* nurse cells was also measured by counting the total number of fluorescent puncta, representative of *Wolbachia* and absent in *Wolbachia*-free *Nasonia*, in the *Nasonia* nurse cell cytoplasms. Images of Hsp60-stained embryos were false-colored green in Fiji.

Quantification and statistical analyses

All statistical analyses, unless otherwise noted, were performed in GraphPad Prism 6.07 (GraphPad Software, La Jolla, CA). Outliers were removed from the results on embryonic *Wolbachia* titers and Wds RT-qPCR using the ROUT method, Q = 1%. Non-parametric tests were used on all data since most data did not pass a Shapiro-Wilk test for normality or sample sizes were too small. Mann-Whitney U tests were used for comparisons between two groups, whereas a Kruskal-Wallis test was used to compare multiple groups. If the Kruskal-Wallis test was significant ($p \leq 0.05$), a post hoc Dunn's test of multiple comparisons was used to calculate significance for all pairwise combinations within the group. All averages are reported as mean ± SEM. For all quantifications of pupal *Wolbachia* densities, sample size "N" represents one pool of five pupae. For any data referring to adult *Nasonia* (genotyping, RNAi or RT-qPCR), sample size "N" denotes individual *Nasonia*. Statistical parameters for each experiment are reported in the results section and in any related figure legends.

Data and software availability

The accession number for the RNA-seq data reported in this paper is Bioproject: PRJNA430433.

Results

N. vitripennis dominantly suppresses w*VitA titers through a maternal genetic effect*

To determine the inheritance pattern of *w*VitA densities, we reciprocally crossed *N. vitripennis* (low-density) and *N. giraulti* IntG (high-density) individuals, and we measured the *Wolbachia* densities of F1 female hybrids using qPCR for a single-copy *Wolbachia* gene (*groEL*) normalized to a *Nasonia* gene (*NvS6K*) (Figure II-1A). The average F1 female pupal *Wolbachia* densities from pure-breeding *N. vitripennis* (n = 5) and *N. giraulti* control families (n = 5) were 0.057 ± 0.004 and 4.805 ± 1.071 (mean ± SEM), respectively, which represents an 84-fold interspecific difference in *Wolbachia* titers and is consistent with previous studies (Chafee et al. 2011). Interestingly, while F1 hybrid females from both crosses had identical genotypes (i.e., heterozygous at all loci) and the same cytotype (*N. vitripennis*), the average *Wolbachia* densities in reciprocal F1 hybrid females were significantly different at 0.149 ± 0.029 versus 1.746 ± 0.187 (Figure 1A; n = 10 for both crosses; Kruskal-Wallis test: H = 24.99, df = 3, $p < 0.0001$; Dunn's multiple comparisons test: p = 0.03).

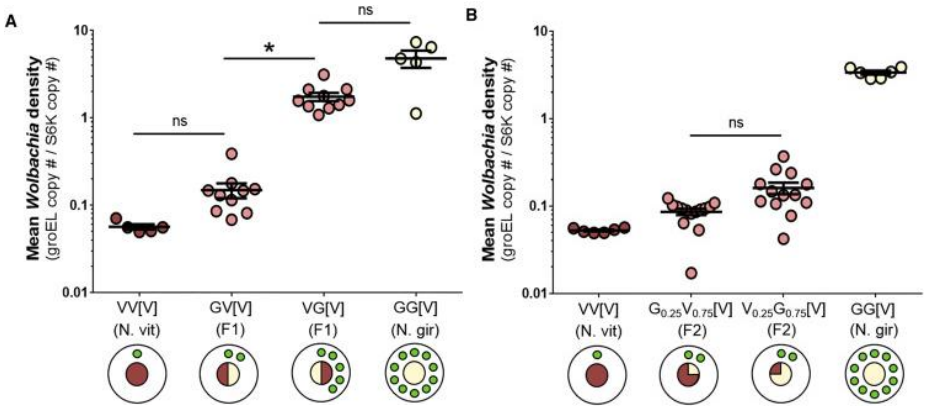

Figure II-1. Disparities in *w*VitA titers are established through a maternal genetic effect. (A) *w*VitA densities in female pupae from parental *N. vitripennis* 12.1 and *N. giraulti* IntG, and their reciprocal F1 hybrids. (B) *w*VitA densities in F2 pupae from F1 females backcrossed to their paternal line. For each cross, genotype (male × female) is followed by cytotype in brackets (V, *N. vitripennis*; G, *N. giraulti*; number, estimated proportion of genotype). For the circle diagrams, the inner circle represents the expected percentage of the nuclear genome that is of *N. vitripennis* (red) or *N. giraulti* (cream) origin. Green circles represent *w*VitA load (not drawn to scale). Error bars represent mean ± SEM. *$p < 0.05$, post hoc Dunn's test.

To test whether the difference in F1 *Wolbachia* densities was due to maternal *Wolbachia* load or to a maternal genetic effect, we backcrossed F1 females to their paternal line and pooled five female F2 pupae per F1 mother for qPCR (Figure II-1B). If a maternal genetic effect

regulates *Wolbachia* densities, F2 pupae from both experimental lines should have similar *Wolbachia* levels since F1 hybrid mothers are genotypically identical. Indeed, the densities of F2 pupal offspring of both low- and high-density F1 mothers were not significantly different (Figure II-1B; 0.086 ± 0.007, n = 14, and 0.161 ± 0.024, n = 13, respectively; Dunn's multiple comparisons test: p = 0.18), supporting the inference that maternal nuclear genotype plays an important role in regulating *Wolbachia* densities. Furthermore, since the densities of both F2 hybrid groups were more similar to the *N. vitripennis* control (0.053 ± 0.001, n = 6) than to the *N. girault*i control (3.364 ± 0.174, n = 6), the *N. vitripennis* suppression gene(s) producing the low *Wolbachia* density phenotype is dominant (Figure II-1B).

Disparities in embryonic w*VitA levels between N. vitripennis and N. girault*i *are established during oogenesis*

We previously showed variation in *w*VitA loads between *N. vitripennis* and *N. girault*i in early embryos, with strict posterior localization of *w*VitA in *N. vitripennis* that is perturbed in *N. girault*i (Chafee et al. 2011). Since the *w*VitA density disparity is partially controlled through a maternal genetic effect (Figure II-1B), we reasoned that an embryonic disparity in *w*VitA densities between *N. vitripennis* and *N. girault*i is likely established in the egg chamber during oogenesis (Figure II-2A). Indeed, nucleic acid staining with SYTOX Green revealed that fewer *w*VitA bacteria are present in stage three *N. vitripennis* egg chambers (Figure II-2B) than in *N. girault*i ones at the same stage (Figure II-2E; Figure II-3). Once in the oocyte, *w*VitA localizes to the posterior end at low density in *N. vitripennis* (Figure II-2B), but it occurs at high density in the posterior end with an expanded distribution toward the anterior end of the oocyte in *N. girault*i (Figure II-2E). The lack of puncta in ovaries from uninfected *N. vitripennis* confirms that the SYTOX nucleic acid dye effectively stains *Wolbachia* but no other cytoplasmic elements, such as mitochondria (Figure II-2D). Altogether, the distribution and density of *w*VitA in oocytes of these two *Nasonia* species mirror their embryonic *w*VitA patterns (Figures II-2C and II-2F), suggesting that *Wolbachia* density differences are established during oogenesis and regulated through maternal effect genes, rather than zygotic genes expressed later in embryonic development.

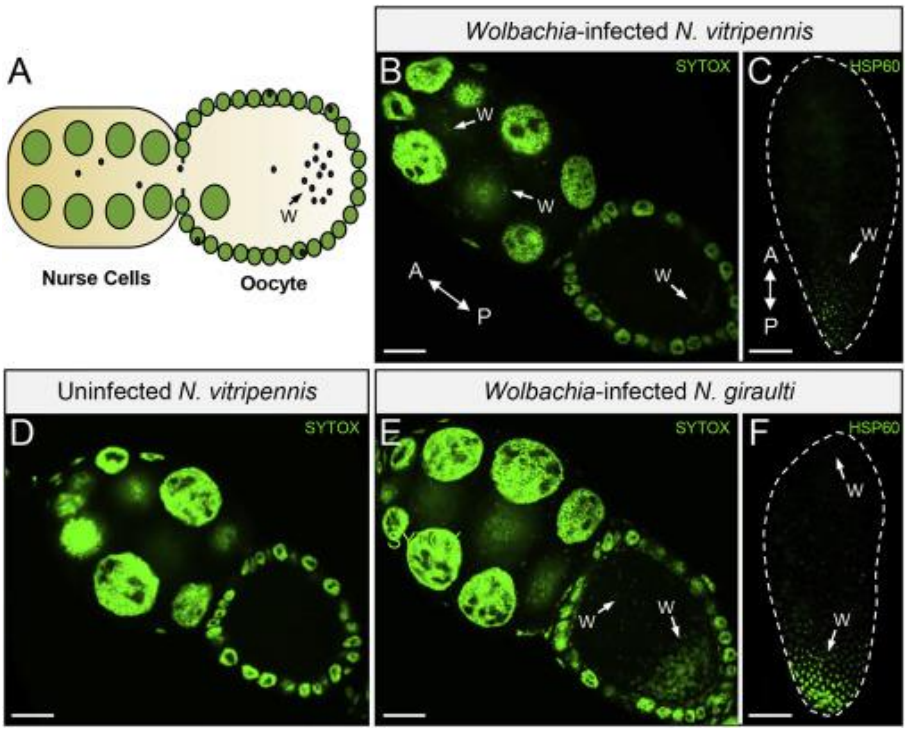

Figure II-2. Disparities in *w*VitA titers begin during oogenesis. (A) Diagram of a *Nasonia* egg chamber. Large green circles represent nurse cell nuclei and small black circles represent *Wolbachia* (black arrow labeled with "W"). (B) Stage 3 egg chambers with host and *Wolbachia* DNA stained with SYTOX Green from *w*VitA-infected *N. vitripennis* 12.1. A, anterior; P, posterior; scale bar, 15 μm. Examples of *Wolbachia* bacteria are labeled with a "W" and white arrows. (C) An embryo with *Wolbachia* stained with HSP60 from *w*VitA-infected *N. vitripennis* 12.1. Scale bar, 50 μm. (D) Stage 3 egg chambers with host and *Wolbachia* DNA stained with SYTOX Green from uninfected *N. vitripennis* 12.1T. Scale bar, 50 μm. (E) Stage 3 egg chambers with host and *Wolbachia* DNA stained with SYTOX Green from *w*VitA-infected *N. girault*i IntG. Scale bar, 15 μm. (F) An embryo with *Wolbachia* stained with HSP60 from *w*VitA-infected *N. girault*i IntG. Scale bar, 50 μm. All embryo and ovary images are representative of two and three independent experiments, respectively.

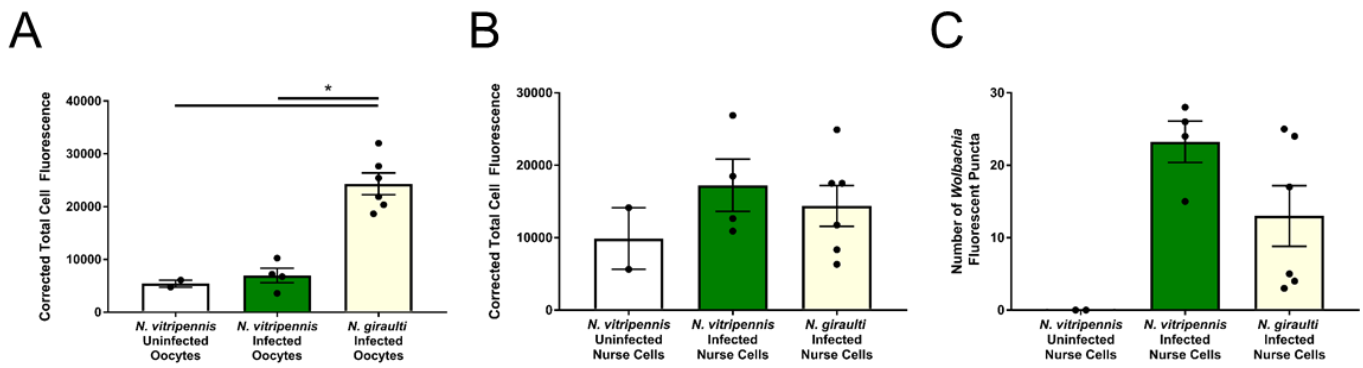

Figure II-3. Quantification of fluorescence in *Wolbachia*-infected *Nasonia* oocytes. (A) Bars represent the average corrected total cell fluorescence of *Wolbachia* in *N. vitripennis* 12.1 and *N. girault* IntG oocytes from stage 3 egg chambers. A *Wolbachia*-cured *N. vitripennis* line serves as a negative control. (B) Bars represent the average corrected total cell fluorescence of *Wolbachia* in *N. vitripennis* 12.1 and *N. girault* IntG nurse cell cytoplasms. A *Wolbachia*-cured *N. vitripennis* line serves as a negative control. (C) Bars represent counts of *Wolbachia* indicated fluorescent puncta in *N. vitripennis* 12.1 and *N. girault* IntG nurse cell cytoplasms. A *Wolbachia*-cured *N. vitripennis* line served as a negative control. * $p<0.05$, Kruskal Wallis test with Dunn's multiple correction. Error bars are mean ± S.E.M.

Phenotype-based selection and introgression identify two maternal suppressor genomic regions

In an initial approach to determine the location and number of loci that suppress *w*VitA densities in *N. vitripennis*, we selected upon the low-density phenotype of this species while serially backcrossing hybrid females to *N. girault* IntG males (Figure II-4A). Since the phenotype is controlled through a maternal genetic effect, hybrid females were selected based on the *w*VitA densities of their offspring, with sisters of the low-density offspring used as mothers in the next round of introgression (Figure II-4A). Two independent selection lines were generated simultaneously to help discriminate between *N. vitripennis* regions maintained due to selection (present in both lines) versus those possibly maintained through chance (present in only one line).

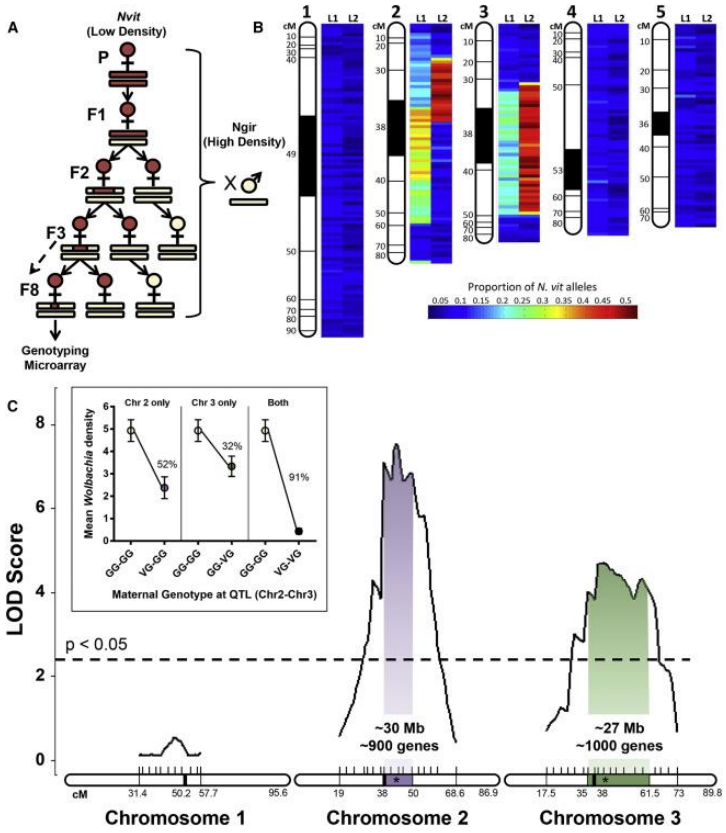

Figure II-4. Two genomic regions interact additively to suppress *w*VitA titers. (A) Schematic of introgression using density phenotype (red female, low; cream female, high) as proxy for maternal genotype (red bar, *N. vitripennis*; cream bar, *N. giraulti*). Eighth generation females with lowest embryonic *Wolbachia* densities were genotyped on a *Nasonia* microarray. (B) Heatmap of the proportion of *N. vitripennis* alleles across the genome in a pool of three females from each introgression line (L1 or L2). The proportion of *N. vitripennis* alleles is scaled from 0 to 0.5, where 0 = no *N. vitripennis* alleles and 0.5 = all females were heterozygous. Areas were considered enriched for *N. vitripennis* alleles at ≥0.2. (C) Plot of LOD score after QTL mapping of F2 females. Shaded regions represent the 95% Bayes credible interval for significant QTL peaks (star). The thick black line within each chromosome diagram denotes the centromere, while the vertical black lines above the chromosomes denote the locations of *Nasonia* molecular markers used for genotyping. Dashed line represents genome-wide significance threshold at $\alpha = 0.05$. (Inset) *Wolbachia* density (mean ± SEM) of offspring based on maternal genotype at each QTL peak (V, *N. vitripennis*; G, *N. giraulti*). Percent reduction in densities is compared to offspring of F2 homozygous *N. giraulti* females. All maps are based on the *Nasonia* genetic map (Desjardins et al. 2013).

For each independent line, DNA from three females that produced ninth-generation offspring with the lowest *Wolbachia* densities were pooled and genotyped on a *Nasonia* genotyping microarray composed of 19,681 sequence markers that differ between *N. vitripennis* and *N. giraulti* (Desjardins et al. 2013). Both selection lines (L1 and L2) displayed an enrichment of *N. vitripennis* alleles along the central portions of chromosomes 2 and 3 of *Nasonia*'s five chromosomes (Figure II-4B). On the most recent *N. vitripennis* linkage map

(Desjardins et al. 2013), the area of enrichment on chromosome 2 for L1 occurs between 38 and 51.1 cM, while enrichment in L2 extends from 25.6 to 38 cM (Figure II-4B). Although overlap in *N. vitripennis* allele enrichment between L1 and L2 on chromosome 2 occurs at 38 cM, the exact position and size of the overlap cannot be determined due to the fact that it falls within the poorly assembled heterochromatic regions flanking the centromere (Desjardins et al. 2013). For chromosome 3, the areas of enrichment for *N. vitripennis* alleles between L1 and L2 coincide starting at 35 cM and ending at 47.5 cM.

QTL analysis validates the two maternal effect suppressor regions

To validate the *Wolbachia* density-suppressing chromosomal regions determined through phenotypic selection and a gentoyping microarray, we performed an independent quantitative trait locus (QTL) analysis in which F1 hybrid females were backcrossed to high-density *N. giraulti* IntG males to obtain 191 F2 recombinant females. Each F2 female was phenotyped by measuring the *Wolbachia* densities of her F3 pupal offspring. Since the most informative individuals in QTL mapping are those with the most extreme phenotypes (Lander and Botstein 1989), we selectively genotyped F2 females with the lowest (0.072–0.409, n = 42) and highest (2.958–10.674, n = 42) F3 pupal *Wolbachia* titers with a total of 47 microsatellite markers across chromosomes 1, 2, and 3 and an average distance between markers of 3 cM (Appendix A). Using genotype data for selected individuals and phenotype data for all F2 females, we identified two significant QTL regions at a genome-wide significance level of $\alpha = 0.05$ (LOD > 2.29): one QTL peak on chromosome 2 at 43 cM ($p < 0.001$) and the other on chromosome 3 at 41.5 cM ($p < 0.001$; Figure II-4C). Strikingly, the 95% Bayes credible interval on chromosome 2 corresponds to the same region identified by the genotyping microarray as enriched for *N. vitripennis* alleles in introgression line 1 (38–51.1 cM), while the 95% Bayes credible interval on chromosome 3 also contains a region that was enriched for *N. vitripennis* alleles (35–47.5 cM) in both introgression lines. Thus, the microarray and QTL analyses complement each other and confirm that suppressor genes of major effect for *w*VitA density are located near the centromeric regions on chromosomes 2 and 3.

As a negative control, we genotyped the same individuals with markers located on *Nasonia* chromosome 1, which was not enriched for *N. vitripennis* alleles after the selection introgression. In the QTL analysis, the highest peak on chromosome 1 was not statistically significant (Figure II-

4C), indicating again that chromosomes 2 and 3 are likely the only chromosomes harboring genes of major effect for the *w*VitA density trait.

To determine the effect of each QTL on density suppression, the average percent reduction in F3 pupal *Wolbachia* densities was calculated for the F2 females with *N. vitripennis* alleles at markers close to one or both of the calculated QTL peaks. Females with *N. vitripennis* chromosome 2 or chromosome 3 QTLs produced offspring with a 52% or 32% reduction in densities, respectively, compared to offspring of females that were homozygous *N. giraulti* at both QTLs (Figure II-4C, inset). Furthermore, these effects acted additively for a 91% reduction in densities in offspring of females with *N. vitripennis* alleles at both loci compared to offspring of F2 females with *N. giraulti* alleles at both loci (Figure II-4C, inset).

Marker-assisted introgression confirms and narrows the maternal effect suppressor QTL on chromosome 3

To validate the QTLs on chromosomes 2 and 3 and narrow the gene candidate regions, we independently introgressed the QTL regions from *N. vitripennis* into an *N. giraulti* IntG background for at least nine generations using marker-assisted selection (similar to Figure II-3A). After the ninth generation, we conducted sibling matings to produce segmental introgression lines that were homozygous *N. vitripennis* for the marker of interest. Unfortunately, generating *N. vitripennis* homozygous lines for the chromosome 2 region was not possible due to hybrid sterility, so we focused exclusively on the chromosome 3 region.

The initial homozygous and heterozygous introgression lines generated from sibling matings identified a candidate region 3.4 Mb in size containing 288 genes (line IntC3) that suppressed *w*VitA densities by 60%, while lines lacking this region had little to no density suppression (Figure II-5). Surprisingly, the percent effect of the chromosome 3 homozygous introgression on *Wolbachia* suppression was nearly double that observed in the QTL study (60% versus 32%; Figure II-4C, inset). However, the QTL study was performed on F2 hybrid females while the introgression lines underwent at least nine generations of backcrossing. If there is an *N. vitripennis*-specific negative regulator of the *Wolbachia* suppressor gene on a different chromosome, then the allele would likely be present in F2 hybrids but would have recombined out with subsequent backcrossing to *N. giraulti* IntG. The stronger phenotype could also be due to the homozygous introgression lines having two copies of the *N. vitripennis* chromosome 3 candidate

region, while F2 hybrid females were heterozygous. However, this is unlikely since heterozygous introgression females had the same level of *Wolbachia* suppression as their homozygous counterparts (Figure II-5, C3-3 and C3-4 versus C3-5 and C3-6; Kruskal-Wallis test: H = 1.39, df = 3, p = 0.71).

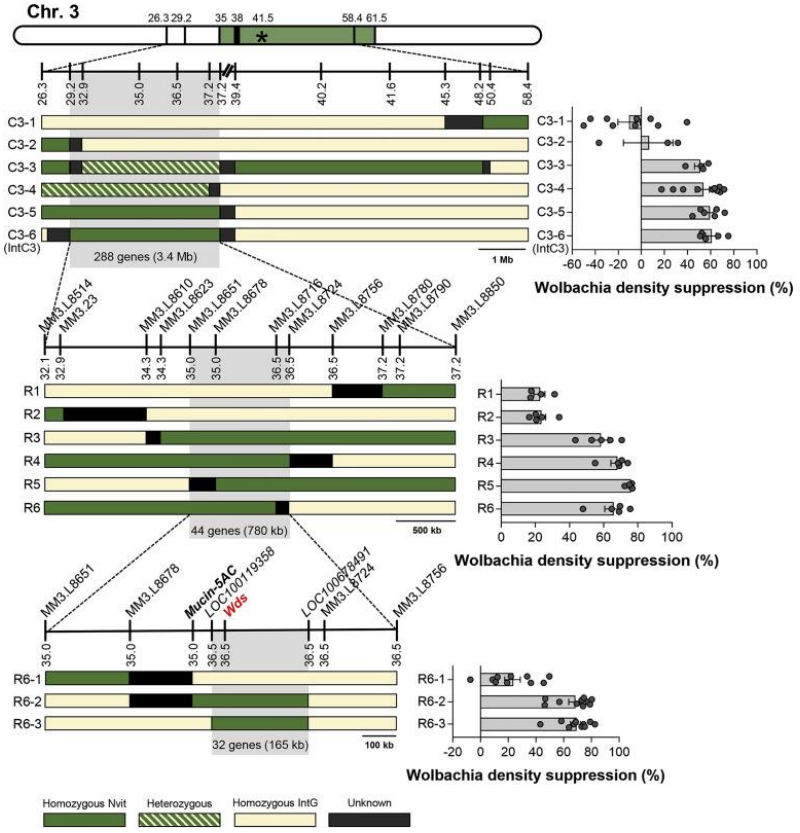

Figure II-5. Segmental introgression lines narrow the chromosome 3 candidate region to 32 genes. The star and colored region on the chromosome map represent the QTL peak and 95% Bayes credible interval, respectively. The thin vertical black lines in the chromosome map denote the locations of *Nasonia* molecular markers used for genotyping, while the thick black line represents the centromere. Diploid recombinant genotypes are depicted as haplotypes, where green bars represent *N. vitripennis*homozygous regions, dashed bars are heterozygous regions, solid cream bars are *N. girault*i IntG homozygous regions, and black bars are recombination breakpoints between two markers. Line graphs represent chromosome length in megabases and are drawn to scale except for centromeric regions (broken dashes at top of the figure). Names of the molecular markers (MMs) used for genotyping are provided above the line graphs, and their locations (in cM) based on the genetic map from [40] are located below the line graphs. The bar graphs show the mean percent effect on density suppression in pupal offspring from all individual mothers with the same haplotype. Gray shading indicates density suppressor candidate regions based on presence of *N. vitripennis* genes correlated with high percent effect on density suppression. Error bars denote mean ± SEM.

Line IntC3 was further backcrossed to *N. girault*i IntG to generate four recombinant lines (R3, R4, R5, and R6) that suppressed *w*VitA densities by 58%–78% (depending on the line) with

an overlapping candidate region of 780 kb and 44 genes (Figure II-5). Finally, line R6 was backcrossed to *N. giraulti* IntG to obtain three recombinant lines, two of which caused 67% (R6-2) and 68% (R6-3) density suppression. The overlapping *N. vitripennis* region in lines R6-2 and R6-3 was 165 kb and contained only 32 genes (Figure II-5).

RNA-Seq identifies a single candidate gene (Wds) based on expression differences in Nasonia ovaries

To identify candidate genes within the 165 kb, 32-gene region that were differentially expressed in the maternal germline of *N. vitripennis* and *N. giraulti*, we performed high-throughput RNA sequencing (RNA-seq) on four independent pools of 40 ovary samples from the parental *N. vitripennis* line 12.1, the introgression line IntC3, and five independent pools from the parental *N. giraulti* line IntG (Table A-2). Seven genes in the 32-gene candidate region exhibited significant differences in expression among the three aforementioned lines (Table A-3). However, since the density trait is controlled by a dominant *N. vitripennis* maternal effect allele (Figure II-1B), we reasoned that the most likely candidate gene(s) would be upregulated in *N. vitripennis* compared to *N. giraulti*.

Analysis of the RNA-seq data indicated that only one of the seven genes (LOC100679092) was consistently and significantly overexpressed in *N. vitripennis* and IntC3 (low-density) ovaries compared to *N. giraulti* IntG (high-density) ovaries, which was confirmed in independent biological replicates by qRT-PCR (79-fold and 92-fold higher expression in *N. vitripennis* and IntC3 than *N. giraulti* IntG, respectively; Figure II-6).

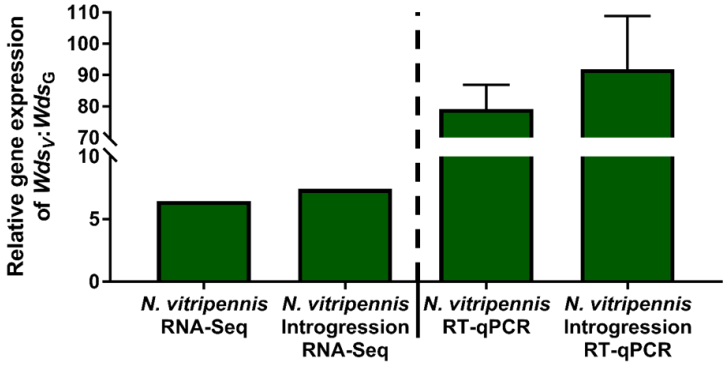

Figure II-6. RT-qPCR validation of *Wdsv* expression in ovaries of N. vitripennis and IntC3 compared to IntG. Bars represent the average fold change of *N. vitripennis* ovarian gene expression of Wds_v compared to *N. giraulti* IntG expression. Error bars are mean ± S.E.M.

The RNA-seq data also validated the same predicted gene splicing model for LOC100679092 for both *N. vitripennis* and *N. giraulti*, indicating that the expression differences are not due to species-specific alternative splicing of the gene. As an uncharacterized gene with no known protein domains, we hereby name the gene *Wds* for *Wolbachia* density suppressor gene.

Wds *controls embryonic* w*VitA densities via a maternal effect*

Parental RNAi has successfully been used in *Nasonia* to examine the effects of maternal genes on embryonic development (Lynch et al. 2006; Verhulst et al. 2010). If the *N. vitripennis* allele of *Wds* (*Wds*$_v$) was responsible for suppressing *Wolbachia* titers, we expected that knockdown of *Wds*$_v$ transcripts in IntC3 mothers would result in reduced density suppression and, consequently, an increase in *w*VitA levels in the resulting embryos. Indeed, injection of IntC3 mothers with double-stranded RNA (dsRNA) against *Wds*$_v$ significantly increased offspring embryonic *w*VitA densities (696 ± 67.9, n = 24) by 56% or 63% compared to embryonic *w*VitA densities from mothers injected with dsRNA against a control bacterial gene, maltose transporter subunit E (*malE*) (447 ± 52.1, n = 24) or buffer-injected females (426 ± 50.3, n = 23), respectively (Figure II-7A; Kruskal-Wallis test: H = 13.1, df = 3, $p < 0.01$; Dunn's multiple comparisons test: p = 0.006 and p = 0.027 compared to *Wds*$_v$ group). This increase coincided with a 57% knockdown in *Wds*$_v$ gene expression in RNAi females compared to the buffer-injected controls (Figure II-7B; Mann Whitney U test, p = 0.0015). Furthermore, we compared embryonic *w*VitA densities from mothers injected with dsRNA against *Nasonia* gene *LOC100679394* (*Mucin-5AC*), a gene that was significantly upregulated in *N. vitripennis* but immediately outside the chromosome 3 candidate region. Embryos from mothers injected with dsRNA against *Mucin-5AC* did not produce significantly higher *w*VitA densities (459 ± 75.9, n = 25) compared to embryos from either *malE*-RNAi (447 ± 52.1, n = 24) or buffer-injected females (426 ± 50.3, n = 25; Figure II-7A), even though *Mucin-5AC*-RNAi mothers had a 71% decrease in *Mucin-5AC* gene expression versus buffer-injected controls (Figure 8; Mann-Whitney U test, p = 0.0003).

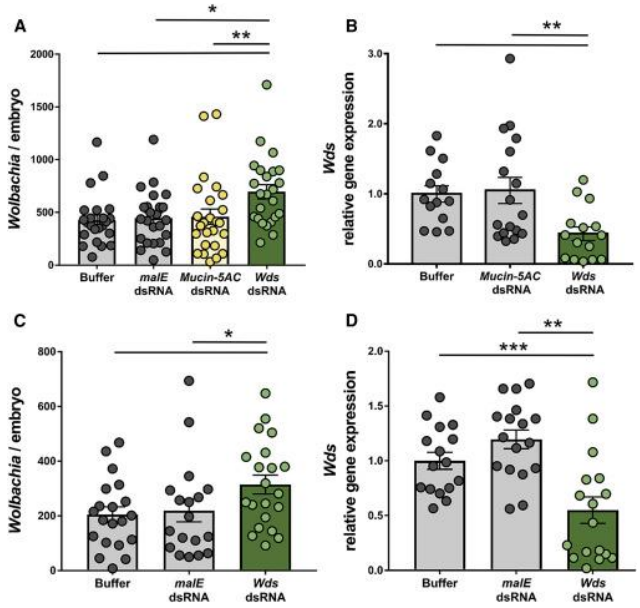

Figure II-7. The *N. vitripennis* allele of *Wds* suppresses densities of vertically transmitted *Wolbachia*. (A) Number of *w*VitA *Wolbachia* per embryo from IntC3 females that were buffer injected, injected with dsRNA against control genes *MalE* or *Mucin-5AC*, or injected with dsRNA against Wds_v. $^{*}p < 0.05$ and $^{**}p < 0.01$, post hoc Dunn's multiple comparisons test. (B) Relative gene expression of Wds_v in late pupae of *Wds*-RNAi and *Mucin-5AC*-RNAi females normalized to Wds_v expression in buffer-injected females. $^{**}p < 0.01$, Mann-Whitney U test. (C) Number of *w*VitA *Wolbachia* per embryo from R6-3 females that were buffer injected, injected with dsRNA against control gene *MalE*, or injected with dsRNA against Wds_v. $^{*}p < 0.05$, Mann-Whitney U test. (D) Relative gene expression of Wds_v in late pupae of *Wds*-RNAi and *MalE*-RNAi females normalized to Wds_v expression in buffer-injected females. $^{**}p < 0.01$ and $^{***}p < 0.001$, Mann-Whitney U test. All error bars represent mean ± SEM.

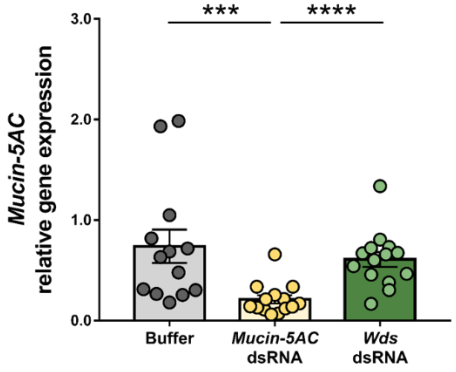

Figure II-8. Relative gene expression of *Mucin-5AC* in late pupae. Relative gene expression of *Mucin-5AC* in late pupae of *Mucin-5AC*-RNAi and *Wds*-RNAi females normalized to *Mucin-5AC* expression in buffer-injected females. $^{***}p < 0.001$, and $^{****}p < 0.0001$, Mann-Whitney U test. Error bars represent mean ± S.E.M.

To further validate the effect of Wds_v on *Wolbachia* densities, females from recombinant line R6-3 (homozygous *N. vitripennis* for the 32-gene candidate region only) were injected with

dsRNA against *Wds*$_v$. Knockdown of *Wds*$_v$ in R6-3 females again significantly increased embryonic *w*VitA densities (314 ± 34.4, n = 21) by 43% or 54% compared to embryonic *w*VitA densities from mothers injected with dsRNA against the control bacterial gene *malE* (219 ± 39.2, n = 19) or from buffer-injected females (204 ± 28.4, n = 20), respectively (Figure II-7C; Mann-Whitney U test, p = 0.049 and p = 0.023 compared to the *Wds*$_v$ group). This increase coincided with a 45% knockdown in *Wds*$_v$ gene expression in RNAi females compared to the buffer-injected controls (Figure II-7D; Mann-Whitney U test, p = 0.0041).

Accelerated evolution and positive selection impact Wds in N. vitripennis

The *Nasonia* genus is comprised of four closely related species, with *N. vitripennis* sharing a common ancestor with the other three species approximately one million years ago (Campbell et al. 1993; Raychoudhury et al. 2010a). Wds protein sequences are 95% identical between *N. vitripennis* and *N. giraulti* with ten amino acid differences (and no insertions or deletions [indels]) of 201 total amino acids (Figure II-9A). Between the more closely related *N. giraulti* and *N. longicornis* species that diverged approximately 400,000 years ago (Campbell et al. 1993), Wds is 99% identical with two amino acid differences that evolved specifically in *N. giraulti* (Figure II-9A). Interestingly, Wds in *Trichomalopsis sarcophagae*, the wasp species most closely related to *Nasonia* (Werren and Loehlin 2009), shares 95% amino acid identity to the *N. vitripennis* protein, but 97% and 98% identity to the *N. giraulti* and *N. longicornis* proteins, respectively (Figure II-9A). Taken together, there are seven unique amino acid changes in *N. vitripennis* that led to accelerated protein sequence evolution in *Wds*$_v$ (Figures II-9A and II-9B). Furthermore, three of those seven amino acid changes fall within a region of high positive selection based on a sliding window analysis of the Ka/Ks ratio (Figure II-9C) (Liang et al. 2006). Additionally, these changes are associated with a shift in the isoelectric point (pI) of the Wds protein, an important factor in protein evolution (Alende et al. 2011). The pI drops from 9.24 in *N. vitripennis* to 8.75 in *N. giraulti*. In contrast, the pI difference for the Mucin-5AC control is minimal (ΔpI = 0.04).

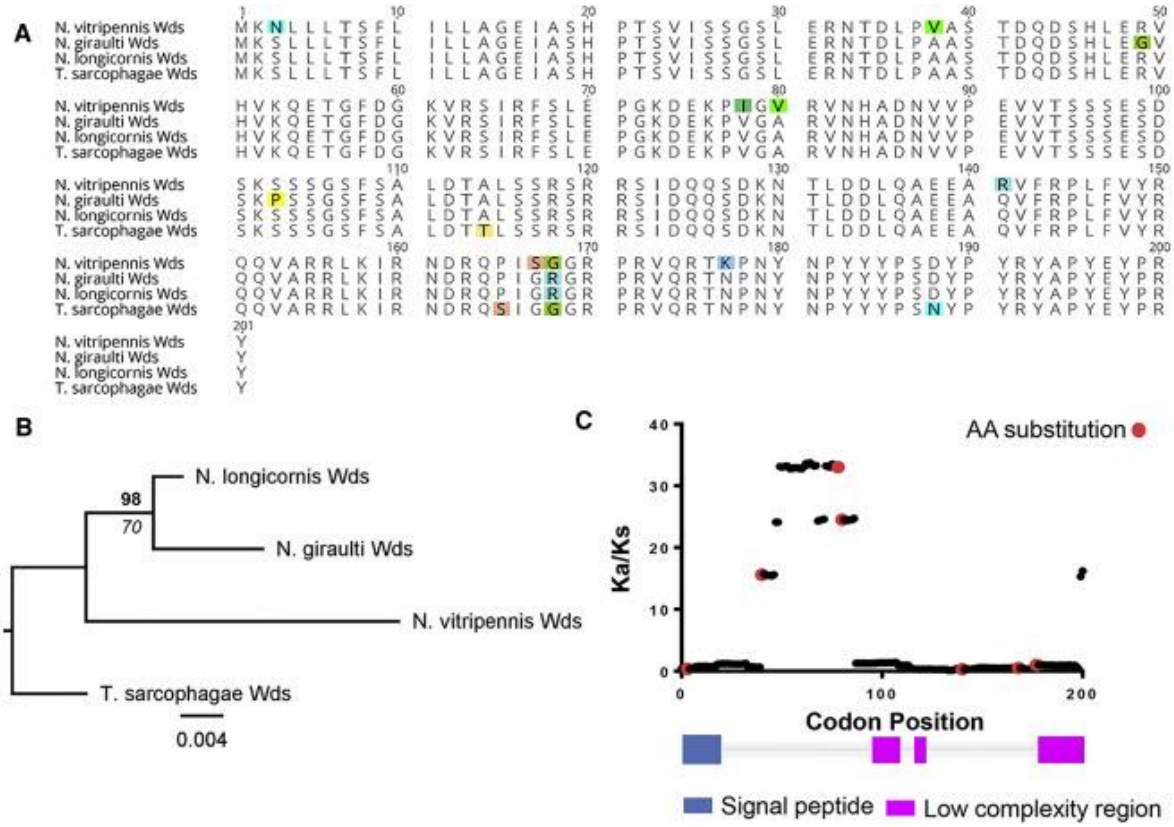

Figure II-9. The *N. vitripennis* allele of *Wds* is under positive selection. (A) Alignment of Wds protein homologs from *N. vitripennis* (RefSeq: XP_008213336.1), *N. girault* (GenBank: GL276173.1), *N. longicornis* (GenBank: GL277955.1), and *Trichomalopsis sarcophagae* (GenBank: OXU27029.1). (B) Amino acid phylogeny of Wds across the *Nasonia* genus and *Trichomalopsis sarcophagae*. Bold text above branch denotes Bayesian posterior probability. Italic text below branch denotes maximum likelihood bootstrap value. Scale bar denotes amino acid substitutions per site. (C) Plot of Ka/Ks ratios based on a sliding window analysis across the *N. vitripennis* and *N. girault Wds* coding sequences. Red circles indicate the locations of the seven amino acid substitutions unique to *N. vitripennis* Wds. Diagram below illustrates location of the predicted signal peptide and low-complexity regions of the Wds protein.

Overall, Wds in the *N. vitripennis* lineage experienced recent amino acid substitutions, possibly in response to acquisition of the *w*VitA *Wolbachia* strain that horizontally transferred into *N. vitripennis* after *N. vitripennis*'s divergence from its common ancestor with *N. girault* and *N. longicornis* (Raychoudhury et al. 2009). Outside of these four species, the next closest Wds orthologs are found in wasps such as *Trichogramma pretiosum*, *Copidosoma floridanum*, and *Polistes canadensis*, but they only share 29%–42% amino acid identity to Wds_v across a majority of the sequence (Table A-4). While more distant orthologs are present in other Hymenopterans such as bees and ants (Table A-4), only portions of the proteins can be

properly aligned. Therefore, our findings demonstrate a rapidly evolving, taxon-restricted gene can contribute directly to the adaptive evolution of regulating maternal symbiont transmission.

Discussion

The main goal of this study was to determine the number and types of gene(s) that control the most widespread, maternally transmitted symbiont in animals (Zug and Hammerstein 2012; Weinert et al. 2015). Unlike reverse genetic screens that mutate genes and then look for phenotypes, which may produce off-target effects unrelated to the true function of the protein, this forward genetic screen utilized an unbiased, candidate-blind approach to dissect the genetic basis of variation in host suppression of maternally transmitted *Wolbachia*. We found that suppression of *w*VitA in *N. vitripennis* can be mapped to two regions of the *Nasonia* genome that regulate nearly all of the *Wolbachia* density suppression.

The identification of the *Wds* gene demonstrates that host regulation of maternally transmitted symbiont density is adaptive and can proceed through lineage-specific amino acid changes in a maternal effect gene. The *N. vitripennis*-specific substitutions in Wds were possibly driven by *N. vitripennis*'s acquisition of *w*VitA after its divergence with *N. giraulti* (Raychoudhury et al. 2009). Indeed, another *N. vitripennis*-specific *Wolbachia* strain, *w*VitB, maintains its low levels after transfer to *N. giraulti* (Chafee et al. 2011), indicating that Wds_v may encode a specific regulator of *w*VitA. Furthermore, *N. giraulti* maintains its native *w*GirA *Wolbachia* strain at comparable levels to *w*VitA in *N. vitripennis* (Chafee et al. 2011), but whether Wds_g is involved in regulating *w*GirA remains to be tested.

The Wds protein has areas of low complexity and a predicted signal peptide at its N terminus (Figure 6C), but otherwise it does not contain any characterized protein domains that allude to its function. Staining of *w*VitA in *Nasonia* ovaries revealed a trend of higher *Wolbachia* titers in the nurse cells of *N. vitripennis* than *N. giraulti* (Figures II-3B and II-3C) concurrent with significantly lower *Wolbachia* levels in *N. vitripennis* oocytes than in *N. giraulti* oocytes (Figure II-3A). Thus, Wds_v may operate by hindering *w*VitA trafficking between nurse cells and the developing oocyte in *N. vitripennis*, perhaps by preventing *w*VitA binding to microtubule motor proteins responsible for *Wolbachia* transport into the oocyte (Ferree et al. 2005; Serbus and Sullivan 2007). Furthermore, in *Drosophila*, *Wolbachia w*Mel bacteria in the oocyte increase proportionally faster than those in the nurse cells (Ferree et al. 2005). If the same is true for *Nasonia*, then high *w*VitA densities in *N. giraulti* could be a result of increased *w*VitA trafficking

to the oocyte (due to a lack of repression by Wds_g) compounded with faster proliferation once in the oocyte.

Alternatively, Wds_v could suppress *Wolbachia* replication by upregulating a host immune response or by downregulating host pathways that *Wolbachia* rely upon for growth. For example, inhibiting host proteasome activity in *Drosophila* significantly reduces *Wolbachia* oocyte titers (White et al. 2017), presumably due to a reduction in the availability of amino acids, a key nutrient that *Wolbachia* scavenges from its host (Caragata et al. 2014). However, if Wds_v regulates a general host pathway that impacts *Wolbachia* replication (such as host proteolysis), then we would expect both *w*VitA and *w*VitB titers to increase when transferred to *N. giraulti*. Instead, the strain specificity of Wds_v suggests a more direct interaction with *Wolbachia*, such as a competitive inhibitor of motor protein binding and nurse cell-to-oocyte trafficking, as discussed above.

Conclusion

The findings presented here indicate that keeping maternally transmitted symbionts in check can have a simple genetic basis, even for obligate intracellular bacteria that must be regulated within host cells and tissues. Moreover, a single maternal effect gene with a major consequence on the density phenotype demonstrates how natural selection can rapidly shape the evolution of density suppression of maternally transmitted symbionts in invertebrates. Future studies are warranted to tease apart the specific host-*Wolbachia* interactions driving *Wolbachia* regulation in *Nasonia* and to determine whether these interactions are paralleled in other insect-*Wolbachia* symbioses.

CHAPTER III. PHYLOSYMBIOSIS: RELATIONSHIPS AND FUNCTIONAL EFFECTS OF MICROBIAL COMMUNITIES ACROSS HOST EVOLUTIONARY HISTORY[†]

Abstract

Phylosymbiosis was recently proposed to describe the eco-evolutionary pattern whereby the ecological relatedness of host-associated microbial communities parallels the phylogeny of related host species. Here, we test the prevalence of phylosymbiosis and its functional significance under highly controlled conditions by characterizing the microbiota of 24 animal species from four different groups (*Peromyscus* deer mice, *Drosophila* flies, mosquitoes, *Nasonia* wasps) and re-evaluate the phylosymbiotic relationships of seven species of wild hominids. We demonstrate three key findings. First, intraspecific microbiota variation is consistently less than interspecific microbiota variation, and microbiota-based models predict host species origin with high accuracy across the dataset. Interestingly, the age of host clade divergence positively associates with the degree of microbial community distinguishability between species within the host clades, spanning recent host speciation events (~one million years ago) to more distantly related host genera (~108 million years ago). Second, topological congruence analyses of each group's complete phylogeny and microbiota dendrogram reveal significant degrees of phylosymbiosis, irrespective of host clade age or taxonomy. Third, experimental transplants of autochthonous (intraspecific) versus allochthonous (interspecific) microbiota among closely related wasp species and more divergent mice species yield reductions in host survival and digestive performance, respectively. Consistent with selection on host-microbiota interactions driving phylosymbiosis, there are survival and performance reductions when interspecific microbiota transplants are conducted between closely-related and divergent host species pairs. Overall these findings indicate that the composition and functional effects of an animal's microbial community can be closely allied with host evolution, even across wide-ranging timescales and diverse animal systems reared under controlled conditions.

[†]This chapter was published in *PLoS Biology* (2016) 14(11):e2000225 with Seth Bordenstein as co-author. Robert Brucker, Kevin Kohl, and Andrew Brooks were co-first authors.

Introduction

A large body of literature has documented genetic and environmental influences on the composition of host-associated microbial communities (Brucker and Bordenstein 2012a; Brucker and Bordenstein 2013; Burns et al. 2015; David et al. 2014; Franzenburg et al. 2013; Ley et al. 2008; Mueggeet al. 2011; Org et al. 2015; Rawls et al. 2006; Sanders et al. 2014). Although environmental factors are considered to play a much larger role than host genetics and evolutionary history (Davenport et al. 2016), host influences and their functional consequences are poorly elucidated and thus require systematic study across host-microbiota systems. Several outstanding questions remain regarding the nature of host effects on microbiota assembly. Are host-microbiota associations stochastically assembled, or might there be deterministic assembly mechanisms that predict these associations? How rapidly do microbiota differences form between closely related host species, and are interspecific microbiota differences prone to decay over time? Can host-driven assembly of the microbiota be isolated from confounding variables such as diet, age, sex and endosymbionts? If there are microbiota differences between species, are they functional in an evolutionarily informed manner, such that mismatches between host and interspecific microbiota lead to reductions in fitness or performance, particularly when interspecific microbiota transplants are conducted between older host species pairs?

If host-associated microbial communities assemble stochastically through environmental acquisition with no host-specific influence, then microbiota compositions across related host species will not differ from expectations based on random community assemblies and dispersal limitations. Therefore, in a common environment, microbiota will form independent of host species (Figure III-1A), and any interspecific differences in microbiota composition would be arbitrary. In contrast, if hosts influence a sufficient amount of the composition of the microbiota, then under controlled rearing conditions intraspecific microbial communities will structure more similarly to each other than to interspecific microbial communities (Figure III-1B). Similarly, if microbial communities are randomly established or are not distinguishable with regard to host evolutionary relationships, then dendrograms illustrating β-diversity distance between microbial communities will not parallel the phylogeny of the host species (Figure III-1C). However, if microbial communities are distinguishable, then host clades with greater genetic divergence may exhibit more distinguishable microbiota. In this case, there will be congruence between the host phylogeny and microbiota dendrogram (Figure III-1D). As this outcome at the whole microbial

community level is not likely due to coevolution, cospeciation, or cocladogenesis from a last common ancestor, "phylosymbiosis" was proposed as an alternative term that does not presume that members of the microbial community are constant, stable, or vertically transmitted from generation to generation (Brucker and Bordenstein 2012a,c). Rather, phylosymbiosis refers to an eco-evolutionary pattern in which evolutionary changes in the host associate with ecological changes in the microbiota.

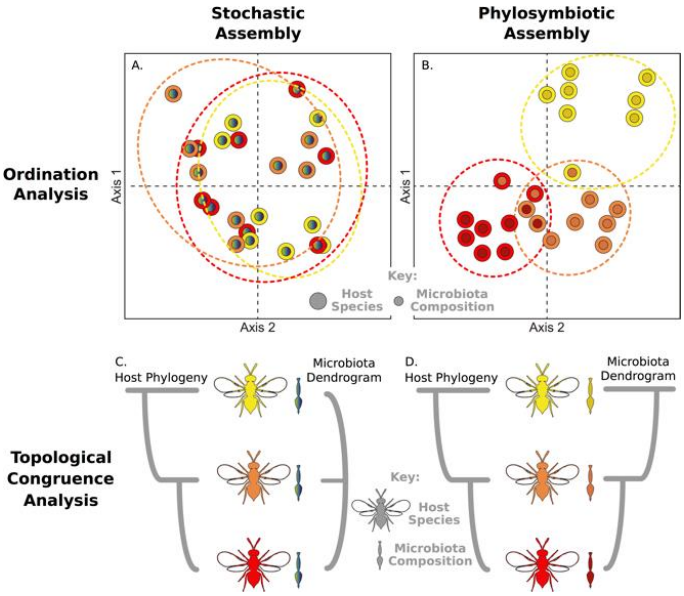

Figure III-1. Analyses and predictions that can distinguish stochastic host-microbiota assembly from phylosymbiosis under controlled conditions. Two-dimensional ordination plots depict hypothetical microbiota similarity under (A) stochastic versus (B) phylosymbiotic models. Dashed lines represent host-specific clustering. Topological congruence analyses between host phylogeny (evolutionary relatedness) and microbial community dendrogram (ecological relatedness) depict the pattern expected for (C) stochastic versus (D) phylosymbiotic host-microbiota assembly.

Phylosymbiosis leads to the explicit prediction that as host nuclear genetic differences increase over time, the differences in host-associated microbial communities would also increase. Indeed, phylosymbiosis has been observed in natural populations of sponges (Easson et al. 2014), ants (Sanders et al. 2014), bats (Phillops et al. 2012), and apes (Moeller et al. 2014; Ochman et al. 2010). However, other studies on termites (Dietrich et al. 2014), flies (Chandler et al. 2011; Wong et al. 2013; Staubach et al. 2013), birds (Hird et al. 2015), and mice (Baxter et al. 2015) have not observed patterns of phylosymbiosis or host-specific microbial signatures. In natural population studies, determining the forces driving phylosymbiosis is equivocal as both environmental and host effects can covary and contribute to microbiota assembly. Importantly, major effects of the

environment, age, or sex may overwhelm the ability to detect phylosymbiosis. Indeed, diet is a stronger determinant of whole microbial community structure than genotype in lab-bred mice (Carmody et al. 2015). Additionally, conjecture about the formation of host-specific communities should be resolved in a wider context, especially its functional significance, as microbiotas may be inconsequential to host biology or uniquely situated for certain host phenotypes and fitness. Thus, the prevalence and functional significance of phylosymbiosis is uncertain and requires reductionist approaches to discriminate among the frequently confounded variables of host, environment, development, sex, and endosymbiont status.

Here, we quantify phylosymbiosis under laboratory conditions, controlling for environmental and host rearing variation. Prior investigations of interspecific gut microbial communities across multiple related species have not typically controlled for these confounding variables with the exception of male *Nasonia* wasps (Brucker and Bordenstein 2012a; Brucker and Bordenstein 2013) and *Hydra* (Franzenburg 2013; Fraune and Bosch 2007). Specifically, we reared 24 species in the laboratory while controlling for sex (virgin females), age, diet, and endosymbionts, thus removing major environmental variables and isolating the contribution of host species on microbiota assembly. The experimental systems, or "host clades," span four species of *Nasonia* parasitic jewel wasps, six species of *Drosophila* fruit flies, eight species of *Anopheles*, *Aedes*, and *Culex* mosquitoes, and six species of *Peromyscus* deer mice. An externally derived dataset with seven members of the hominid lineage (Ochman et al. 2010) provides another mammalian and multi-genus clade for reference and facilitates examination of natural populations where phylosymbiosis was previously documented. Together, the five host clades include 31 distinct taxa and span a range of estimated divergence times from 0.2-108 million years. Lastly, we test the significance of host-specific microbiota associations through a series of microbial transplants with autochthonous (intraspecific) and allochthonous (interspecific) microbiota in *Nasonia* and *Peromyscus* to test the hypothesis that phylosymbiosis represents a functional association. We expect that an experimentally-mediated disruption of phylosymbiosis will have functional costs that may, though not necessarily, lower host fitness/performance in an evolutionarily informed manner. Our findings demonstrate that a consistent set of experimental and bioinformatic approaches can isolate the degree of host-driven phylosymbiosis while avoiding potentially confounding variables in comparative microbiota studies.

Materials and Methods

Nasonia husbandry and sample collection

Nasonia were reared as previously described (Brucker and Bordenstein 2013). Four strains were used: *Nasonia vitripennis* (strain 13.2), *N. longicornis* (IV7U-1b), *N. giraulti* (RV2x(u)), *N. onida* (NAS_NONY(u)). To collect individuals for microbiota analysis, virgin females were sorted as pupae into sterile glass vials and collected within the first 24 hours of eclosing as adults. Subsequently, they were rinsed with 70% ETOH for two minutes, a 1:10 bleach solution for two minutes, followed by two rinses in sterile water. Individuals were then placed in 1.5 ml tubes and flash frozen in liquid nitrogen. They were then stored at -80°C until DNA extractions. Fifty individuals were collected per strain.

Drosophila husbandry and sample collection

Nine strains of *Drosophila* were obtained from the University of California San Diego *Drosophila* Species Stock Center. Six strains were used in the microbiome analysis because they were *Wolbachia*-free: *Drosophila melanogaster* (Strain Dmel, stock number 14021-0248.25), *D. simulans* (Dsim, 14021-0251.195), *D. yakuba* (Dyak, 14021-0261.01), *D. erecta* (Dere, 14021-0224.01), *D. pseudoobscura* (Dpse, 14011-121.94), and *D. mojavensis* (Dmow, 15081-1352.22). The three strains that tested positive for *Wolbachia* (method described below) were: *D. sechellia* (14021-0248.25), *D. ananassae* (14021-0371.13), and *D. willistoni* (14030-0811.24). All strains were reared on a Cornmeal media (*Drosophila* Species Stock Center: http://stockcenter.ucsd.edu/info/food_cornmeal.php) with a sterile Braided Dental Roll (No. 2, Crosstex®, Atlanta, GA, U.S.A) inserted into the surface of the media. All stocks were incubated at 25°C with a 12 hour light dark cycle and monitored every 24 hours. Every 14 days, stock vials were cleared of any emerged adults and six hours later, ten virgin females and three males were transferred to new food vials. This conditioning on the same food was done for five generations before setting up media vials for sample collection. For each of the six strains, five virgin females were mated with two males and allowed to oviposit for 24 hours; afterwards the parents were removed and the vials were incubated as per above.

After 12 days, vials were cleared and virgin females were collected every 4-6 hours over a 36-hour period. All females were rinsed with 70% ETOH for two minutes, a 1:10 bleach solution for two minutes, followed by two rinses in sterile water. Individual pupae were then placed in 1.5

ml tubes and flash frozen in liquid nitrogen. They were then stored along with their corresponding water sample at -80°C until DNA extractions. Approximately 25-30 virgin adult females were collected per strain.

Mosquito husbandry and sample collection

Mosquitoes were acquired from the Malaria Research and Reference Reagent Resource Center as eggs on damp filter paper within 24 hours of being laid. Eight strains were used: *Anopheles funestus* (strain name FUMOZ), *An. furauti s.s* (FAR1), *An. quadrimaculatus* (GORO), *An. arabiensis* (SENN), *An. gambiae* (MALI NIH), *Aedes aegypti* (COSTA RICA), *Ae. Albopictus* (ALBO), and *Culex tarsalis* (YOLO F13). Eggs were floated in 350ml of sterile water with 1.5 ml of 2% yeast slurry, and autoclaved within a sterile and lidded clear plastic container. Containers were enclosed within a larger sterile clear container and placed inside an incubator set at 25°C with a 12 hour light dark cycle and monitored every 24 hours. After 48 hours the hatched larvae were sorted out and 100-150/spp. were placed in new sterile water (150 ml) with 30 mg of powdered koi food (Laguna® Goldfish & Koi all season pellets). Water level was maintained at 150 ml and larvae were feed 30 mg of powdered koi food every day for a total of 13 days. All pupae were discarded (frozen and autoclaved) on day 10 and new pupae were collected every 12 hours on day 11, 12 and 13. Water samples were also collected and frozen for microbial analysis on day 11.

To collect individuals for microbiota analysis, pupae were sorted according to gender and all females were rinsed with 70% ETOH for two min, then 1:10 bleach solution for two min, followed by two rinses in sterile water. Individual pupae were then placed in 1.5 ml tubes and flash frozen in liquid nitrogen. They were then stored along with their corresponding water sample at -80°C until DNA extractions. Ten to 25 individuals were collected per strain.

Peromyscus husbandry and sample collection

Fecal samples were collected from the *Peromyscus* Genetic Stock Center at the University of South Carolina. Six stock species of *Peromyscus* were used: *P. maniculatus* (stock BW), *P. polionotus subgriseus* (PO), *P. leucopus* (LL), *P. californicus insignis* (IS), *P. aztecus hylocetes* (AM), and *P. eremicus* (EP). All mice were reared using their standard care practices at the stock center on the same mouse chow diet. Cages were cleaned at regular intervals for all species, and

all species were caged within the same facility. Individuals from non-mating cages of females (5-6 per cage) were used for collections.

Fecal pellets were collected on a single morning from individual mice directly into a sterile tube and placed on dry ice before being stored at -80ºC for 24hr. Samples were then shipped overnight on dry ice and again stored at -80°C until DNA extractions. One to three pellets from 15 individuals were collected per strain.

In order to eliminate the introduction of confounding factors and exclude any subjects that had a pinworm infection at the time of sample collection, we conducted a screen to confirm the pinworm status of each mouse. Pinworm status was confirmed by PCR. Primers utilized to amplify the 28s rDNA D1 and D2 domains of multiple pinworm species were developed and confirmed with positive DNA samples of *Syphacia obvelata* and *Aspiculuris tetraptera* (received from, Feldman Center for Comparative Medicine at the University of Virginia). The C1 primer 5'-ACCCGCTGAATTTAAGCAT-3' and the D1 primer 5'-TCCGTGTTTCAAGACGG-3' amplified under the following reaction conditions: 94°C for 1 minute; 35 cycles of 94°C for 30 seconds, 55°C for 30 seconds, 72°C for 30 seconds; and a final elongation time at 72°C for 2 minutes. The resultant samples were then visualized a 1% agarose gel. Of the 84 fecal specimens analyzed, eight of the samples showed amplification at 750bp corresponding to the expected amplification size of the pinworm DNA sequence. For confirmation the 750bp bands were extracted using a Wizard Gel Extraction Kit (Promega Corporation, Madison, WI, USA) and sequenced for confirmation (GENEWIZ, inc, New Jersey, USA). Sequence results confirmed the presence of *Aspiculuris tetraptera* infection, and these eight samples and were excluded from further analysis.

Wolbachia screens of stock insect lines

The presence or absence of *Wolbachia* was checked using two replicates of three individuals per species. DNA extraction was performed with PureGene DNA Extraction Kit (Qiagen) and fragments of the 16S rDNA gene were PCR amplified using primer set WolbF and WolbR3 (Nishiguchi 2002). Only stock strains that were *Wolbachia* negative were used in the experiments.

Insect DNA extraction

Individual insects (and the mosquitos' corresponding water samples) were mechanically homogenized with sterile pestles while frozen within their collection tube. The samples were then thawed to room temperature for 30 seconds and flash frozen again in liquid nitrogen with additional mechanical homogenization. The samples were finally processed using the ZR-Duet™ DNA/RNA MiniPrep Kit (Zymo Research, Irvine, CA, U.S.A.). Samples where then quantified using the dsDNA BR Assay kit on the Qubit® 2.0 Fluorometer (Life Technologies)

DNA isolation from mouse samples

The PowerSoil® DNA isolation kit (Mo Bio Laborotories, Carlsbad, CA, USA), was utilized to extract DNA from 20 mg of mouse fecal material per sample according to manufacturer's protocol after being mechanically homogenized with sterile pestles while frozen within their collection tube. Samples where then quantified using the dsDNA BR Assay kit on the Qubit® 2.0 Fluorometer (Life Technologies)

PCR, library prep, and sequencing

Total genomic DNA was quantified using dsDNA HS Assay kit on the Qubit. Using two µl of DNA, a 20 µl PCR reaction of 28S general eukaryotic amplification was conducted on each sample, with only 25 cycles. Products were purified using Agencourt® AMPure® XP, quantified using the dsDNA HS Assay kit on the Qubit, and compared to the amount of 16S amplification from the same DNA volume and PCR reaction volume as previously described [2]. PCR amplification of the bacteria 16S rRNA was performed with the 27F 5'-AGAGTTTGATCCTGGCTCAG-3' and 338R 5'-GCTGCCTCCCGTAGGAGT-3' "universal" bacterial primers with the NEBNext® High-Fidelity 2X PCR Master Mix, duplicate reactions were generated per sample which were pooled together post amplification. For sequencing runs 1 (*Peromyscus*) and 2 (*Nasonia*, Mosquito, *Drosophila*) 16S PCR products that were made into libraries had their concentrations normalized relative to about 1000 ng/ml and 2000 ng/ml of the 28S quantity for library prep respectively.

Using the Encore® 384 Multiplex System (NuGEN, San Carlos, CA, U.S.A), each samples' 16S product was ligated with Illumina® NGS adaptors and a unique barcode index (after the reverse adaptor). The samples were then purified using Agencourt® AMPure® XP, quantified using

the dsDNA HS Assay kit on the Qubit. Samples were subsequently pooled.

Each pooled library was run on the Illumina® MiSeq using either the MiSeq Reagent Kit V2 or V3 for paired end reads. Run 1 was conducted at the University of Georgia Genomics Facility and run 2 was conducted at Vanderbilt Technologies for Advance Genomics (VANTAGE).

Sequence quality control

Sequence quality control and OTU analyses were carried out using QIIME version 1.8.0 (Lo et al. 2002). Forward and reverse paired-end sequences were joined and filtered if: they fell below an average Phred quality score of 25, contained homopolymers runs or ambiguous bases in excess of 6 nucleotides, or were shorter than 200 base pairs. Sequences were also removed if there were errors in the primer sequence, or if barcodes contained errors and could not be assigned to a sample properly. A total of 5,065,121 reads passed quality control for the meta-analysis, with an average read length of 310 ± 48 nucleotides. *Drosophila*: 648,676 reads, average length 315 ± 23. *Hominid*: 1,292,542 reads, average length 247 ± 38. Mosquito: 664,350 reads, average length 328 ± 19. *Nasonia*: 864,969 reads, average length 322 ± 15. *Peromyscus*: 295,752 reads, average length 347 ± 12.

OTU analysis

Chimeric sequences were evaluated and removed using the UCHIME algorithm (Caporaso et al. 2010) for the intersection of *de novo* and GreenGenes 13_5 non-chimeras (Edgar et al. 2011). The sequences were then clustered into Operational Taxonomic Units (OTUs) at 94, 97, and 99 percent similarity using the USEARCH open-reference method (McDonald et al. 2012). OTUs were mapped at the respective percent against the GreenGenes 13_5 database and screened for a minimum group size of two counts with dereplication based on full sequences (Edgar et al. 2011). Representative sequences were chosen as the most abundant representative in each OTU cluster and aligned using GramAlign (Edgar 2010). A phylogenetic tree of the representative sequences was built in QIIME (Lo et al. 2002) with the FastTree method and mid-point rooting (Russell et al. 2008). Taxonomy was then assigned to the OTU representatives with the UCLUST method against the GreenGenes 13_5 database (Edgar et al. 2011). OTU tables were constructed in QIIME (Lo et al. 2002) and sorted by sample ids alphabetically.

Sample and OTU quality control

OTU tables were screened to remove any OTUs classified as Chloroplast, Unassigned and *Wolbachia*. Individual samples were assessed for low sequence coverage affecting community profiles and diversity, and for processing errors based on minimum count thresholds assessed against group means. Following rarefaction, counts were subsequently chosen as the highest rarefaction number allowed by the smallest sample's count representation in each respective clade and the meta-analysis. Alpha diversity was measured using Shannon and Chao1 metrics generated with the QIIME alpha_rarefaction script. Plots of alpha diversity at a range of rarefied levels were used to assess and remove samples with low diversity.

Meta-analysis

The PCoA (Figure III-2A) components for the meta analysis were constructed using the QIIME jackknifed_beta_diversity script. The OTU table first underwent rarefaction, followed by the computation of Bray-Curtis beta-diversity distances for each rarefied table. PCoA plots of the first three coordinate dimensions were generated using a custom Python script. Individual samples are each depicted as a point and are colored by host clade of origin.

The community profile (Figure III-2B) for the meta-analysis was generated using a custom python script and BIOM tools (Price et al. 2010). OTU tables were first converted to relative abundance for each sample, and bacterial taxonomy was collapsed at the class level. Bacterial classes were sorted alphabetically, and a stacked bar chart representing the relative abundance for each sample was constructed.

The network analysis (Figure III-2C) was visualized using Cytoscape (McDonald et al. 2010). OTU tables were first collapsed by bacterial taxonomy at the genus level, and QIIME's make_otu_network script was used to construct connections between each bacterial genus to individual hosts based on relative abundance. Network files were then imported into Cytoscape, where the network was computed using and edge-weighted force directed layout. Nodes were colored by host clade, and connections were colored by key bacterial phylum observed in high abundance (i.e. Actinobacteria, Bacteroidetes, Firmicutes, Proteobacteria) and gray for additional phylum.

Alpha diversity plots (Figure III-2D) were prepared using the Phyloseq package (Cline et al. 2007). OTU tables collapsed by host species were imported into Phyloseq, and the plot_richness

function was used to generate box and whisker plots of shannon alpha-diversity. Plots were colored by host clade of origin.

Microbiota dendrograms

Microbiota dendrograms were constructed using the QIIME jackknifed_beta_diversity script. OTU table counts were first collapsed by host species of origin to get representative species microbiota profiles. The pipeline script performed 1,000 rarefactions on each table, and calculated Bray-Curtis beta-diversity distances for each. Bray-Curtis distance matrices were UPGMA clustered to give dendrograms of interspecific relatedness. The role of 97% versus 99% OTU clustering cutoffs, and weighted and unweighted UniFrac beta-diversity measures (Figure B-2) were evaluated for Robinson-Foulds and Matching Cluster concordance with host phylogeny.

Host phylogenies

Host phylogenetic trees were constructed using sequences for each host species' cytochrome oxidase gene downloaded from the NCBI. Cytochrome oxidase (COI) was chosen as a highly conserved molecular marker and is widely used for inter-specific phylogenetic comparison (McMurdie and Holmes 2013). Sequences were initially aligned using Muscle v3.8.31(Patwardhan et al. 2014). Gap positions generated through inserts and deletions were removed, and overhanging sequence on 5' and 3' ends were trimmed. Models of molecular evolution were evaluated using jModelTest v2.1.7 (Edgar 2004), and the optimal model was used for final alignment and tree building in RaxML v8.0.0 (Darriba et al. 2012). The *Nasonia* and *Peromyscus* clades were carried out using the same methodology except for final alignment and tree building in PhyML v3.0 (Stamatakis 2014), and for *Peromyscus* the arginine vasopressin receptor 1A (AVPR1A) gene was concatenated with COI to further resolve the phylogeny. All trees are concordant with well-established phylogenies from literature references noted in the results section.

Robinson-Foulds and matching cluster congruency analyses

Quantifying congruence between host phylogeny and microbiota dendrogram relationships (Figure III-3) was carried out with a custom python script and the TreeCmp program (Guindon et al. 2010). The topologies of both trees were constructed, and the normalized Robinson-Foulds

score (Bogdanowicz and Giaro 2013) and normalized Matching Cluster score (Everard et al. 2014) were calculated as the number of differences between the two topologies divided by the total possible congruency score for the two trees. Next, 100,000 random trees were constructed with the same number of leaf nodes, and each was compared to the host phylogeny. The number of trees which had an equivalent or better score than the actual microbiota dendrogram were used to calculate the likelihood of seeing phylosymbiosis under stochastic assembly. Normalized results of both statistics have been provided to facilitate comparison. Matching Cluster and Robinson-Foulds p-values were determined by the probability of 100,000 randomized bifurcating dendrogram topologies yielding equivalent or more congruent phylosymbiotic patterns than the microbiota dendrogram.

Intraspecific versus interspecific beta-diversity distances

Within each clade, the Bray-Curtis distances calculated by the jackknife_beta_diversity script (Figure III-4A) were separated by those that compared microbiota within a host species and those that compared between host species. The box and whisker plots were constructed in python. Coloring indicates host clade of origin, and all intraspecific and interspecific distances are represented for each clade. These distances were then compared between the groups using a nonparametric two-tailed Mann-Whitney-U test implemented in Scipy (Bogdanowicz et al. 2012; Millman and Aivazis 2011).

ANOSIM clustering

To evaluate intraspecific clustering (Figure III-4B), the ANOSIM test was used to calculate the distinguishability of Bray-Curtis distances based on species of origin. Bray-Curtis distance matrices were generated using the QIIME jackknifed_beta_diversity script, on tables of individuals rarefied 1,000 times. The QIIME script compare_categories was used to calculate ANOSIM scores using the Bray-Curtis distance matrix and host species as categories. 1,000 permutations were used to calculate the significance of clustering for each clade. Three-dimensional PCoA plots were generated in Python using components generated from Bray-Curtis distance matrices in QIIME, and the first three components are shown. Points are colored by host species within each clade, and colors correlate with the species labels in Figure III-3 for reference.

Correlation of ANOSIM clustering and clade age

A general linear regression was performed to test the correlation between age of clade origin and the intraspecific clustering measured through ANOSIM R-statistic scores. Cladogenesis Age was Log10 transformed to normalize the distance scale between samples (1, 10, 100MYA). The regression was carried out in STATA v12.0 to determine the coefficient (R^2) and significance (P-value).

Random forest analyses

OTU tables were first collapsed at each bacterial taxonomic level (i.e. Phylum…Genus) using the QIIME script summarize_taxa. Then both the raw OTU table and each collapsed table underwent ten rarefactions to an even depth using the QIIME script multiple_rarefactions_even_depth. RFC models were constructed with the supervised_learning script for 1,000 rounds of ten-fold Monte-Carlo cross validation on each table. At each level the results were collated and averages taken for the ten rarefied tables. Host species were used as the category for RFC model distinguishability, testing the ability to assign samples to their respective host species. The average class error for each clade was subtracted from 100 to get the percent accuracy of the models at each taxonomic level. The same methodology was used for constructing RFC models for the meta-analysis, with the only exception being that host species, host clade, and vertebrate/invertebrate categories were tested for distinguishability.

Microbiota transplants

Peromyscus: We tested the effects of allochthonous microbial communities on host performance by conducting a series of microbial transplants from various donor rodent species into a single recipient species, the oldfield mouse (*Peromyscus polionotus*). We obtained virgin, female *Peromyscus* species (*P. polionotus, P. maniculatus, P. leucopus, P. eremicus, P. californicus*) from the Peromyscus stock center. We also obtained three female individuals of *Neotoma lepida* (*Neotoma* is the sister genus of *Peromyscus*) from Dr. M. Denise Dearing (University of Utah). Additionally, we obtained six female individuals of wild, outbred *Mus musculus* from Dr. Wayne Potts (University of Utah). The founding animals of this colony were collected from near Gainesville, Florida, USA, and the animals have been randomly bred in captivity for roughly 13 generations and are still highly outbred (Oliphant 2007; Meagher et al.

2000). All rodent species were maintained on powdered laboratory rodent chow (Formula 8904, Harlan Teklad, Madison, WI), except for woodrats, which were fed powdered rabbit chow (Formula 2031, Harlan Teklad, Madison, WI), given that woodrats are herbivorous. All procedures involving rodents were approved under the University of Utah Institutional Animal Care and Use Committee protocol #12-12010.

To conduct microbial transplants, we followed a protocol that was previously established to transplant the microbiota from *Neotoma lepida* into *Rattus norvegicus* (Lozupone and Knight 2005). First, donor feces were collected from 3-6 individuals of each donor species by placing rodents in wire-bottom metabolic cages overnight and collecting feces the next morning. Feces were then ground with a mortar and pestle and mixed into powdered laboratory chow (Formula 8904, Harlan Teklad, Madison, WI) at a ratio of 15% w/w. Recipient animals (5-6 individuals per group) were fed food containing feces of a particular donor species for two nights. Then, recipient animals were fed normal laboratory diets for 6 days, which is a sufficient time for the clearance of transient, ingested microbes (Gaukler et al. 2016). We then measured food intake and dry matter digestibility by placing animals into wire-bottom metabolic cages. Animals were presented with a known amount of powdered rodent chow overnight. The next morning, remaining food was weighed, and feces were collected, dried overnight, and weighed. Food intake was calculated as g dry food presented – g dry food remaining. Dry matter digestibility was calculated as (g dry food ingested – g dry feces produced)/ g dry food ingested.

We investigated whether microbial communities from more distantly related hosts affected performance metrics in recipients. We compared food intake using ANOVA and Tukey's HSD test across recipient groups. We also conducted correlations of dry matter digestibilities and estimated divergence times based off of previously published phylogenies (Stepphan et al. 2004; Kohl et al. 2016). We performed correlations using both untransformed divergence times and log-transformed divergence times.

Nasonia: We tested the effects of allochthonous microbial communities on host survival by exposing two recipient species (*N. vitripennis* or *N. giraulti*) to a suspension of heat-inactivated microbes isolated from three donor *Nasonia* species (*N. vitripennis*, *N. giraulti*, and *N. longicornis*). We reared *Nasonia* in an *in vitro* rearing system (Shropshire and van Opstal 2016) and inoculated germ-free larvae in 6 mm diameter transwell inserts with autochthonous microbiota, allochthonous microbiota, and sterile PBS for the first 8 days after embryo hatching.

Microbiota were purified from fourth instar larvae of *Nasonia* by filtration through a 5um filter and centrifugation at 10,000 rpm for three minutes. The pellet was suspended in sterile Phosphate Buffer Saline (PBS) solution at a concentration of 5 x 10^6 CFU of microbiota bacteria (determined by tryptic soy agar plating) per milliliter. 20 µL of this microbiota suspension was added to transwell inserts for each of the 8 inoculation days. *Nasonia* rearing media was replaced daily just before the inoculations.

Measurements of *Nasonia* survival from 1st instar larvae to adulthood were determined using transwell insert images taken with an AmScope MT1000 camera. For each transwell, live larval counts were recorded three days post embryo hatching. Adult counts were determined by recording the number of remaining larvae and pupae in each transwell sample 20 days after embryo hatching (5-7 days after first adult eclosion) and subtracting that number from the larval counts previously recorded. Normalized adult survival per transwell sample was calculated as the percent survival of *Nasonia* from 3 days to 20 days after embryo hatching divided by the average percent survival of the autochthonous microbiota treatment group. We compared survival between the autochthonous and allochthonous treatment groups using Mann Whitney U tests.

Results

Host clade differentiates microbial communities

Phylosymbiosis predicts that host clades will harbor distinguishable microbial communities (*e.g*. jewel wasps vs. fruit flies vs. deer mice, etc.), and that more closely related host clades will exhibit more similar microbial communities (*e.g.* insects vs. mammals). Indeed, at a broad scale, we found that host clades harbored relatively distinct microbial communities (Figure III-2A, ANOSIM, R=0.961, P<1e-6). Further, there was significant microbiota differentiation between the mammalian and invertebrate host clades in the Principle Coordinate Analysis (PCoA; Figure III-2A, ANOSIM, R=0.905, P<1e-6). The PCoA shows insect groups separating along two dimensions of a plane, with the mammals distinguished orthogonally from that plane in a third dimension, suggesting that variance in insect microbial communities is fundamentally different than that in mammals. As is well established, the gut communities of mammals were dominated by the bacterial classes Clostridia (Firmicutes) (Figure III-2B, Hominid 42%, *Peromyscus* 37%) and Bacteroidia (Bacteroidetes) (Figure III-2B, Hominid 15%, *Peromyscus* 37%), while the insect clades were dominated by Proteobacteria (Figure III-2B, *Drosophila* 78%, Mosquito 69%,

Nasonia 77%). This same bacterial divide is also seen in the network analysis with significant clustering of the insect microbial communities around Proteobacteria, and the mammal microbial communities around subsets of shared and unique Firmicutes and Bacteroidetes (G-test, P<1e-6, Figure III-2C). Microbial diversity as measured by the Shannon index (Shannon 1948) was approximately 35% higher in mammalian hosts compared to insects, indicating more diverse symbiont communities among the mammalian clades (Figure III-2D; Nested ANOVA: Phylum effect [mammals vs invertebrates]: $F_{1,302}$=419.82, P<0.001; Clade effect nested within Phylum: $F_{3,298}$=18.46, P<0.001; Species effect nested within Clade and Phylum: $F_{26,272}$=7.94, P<0.001).

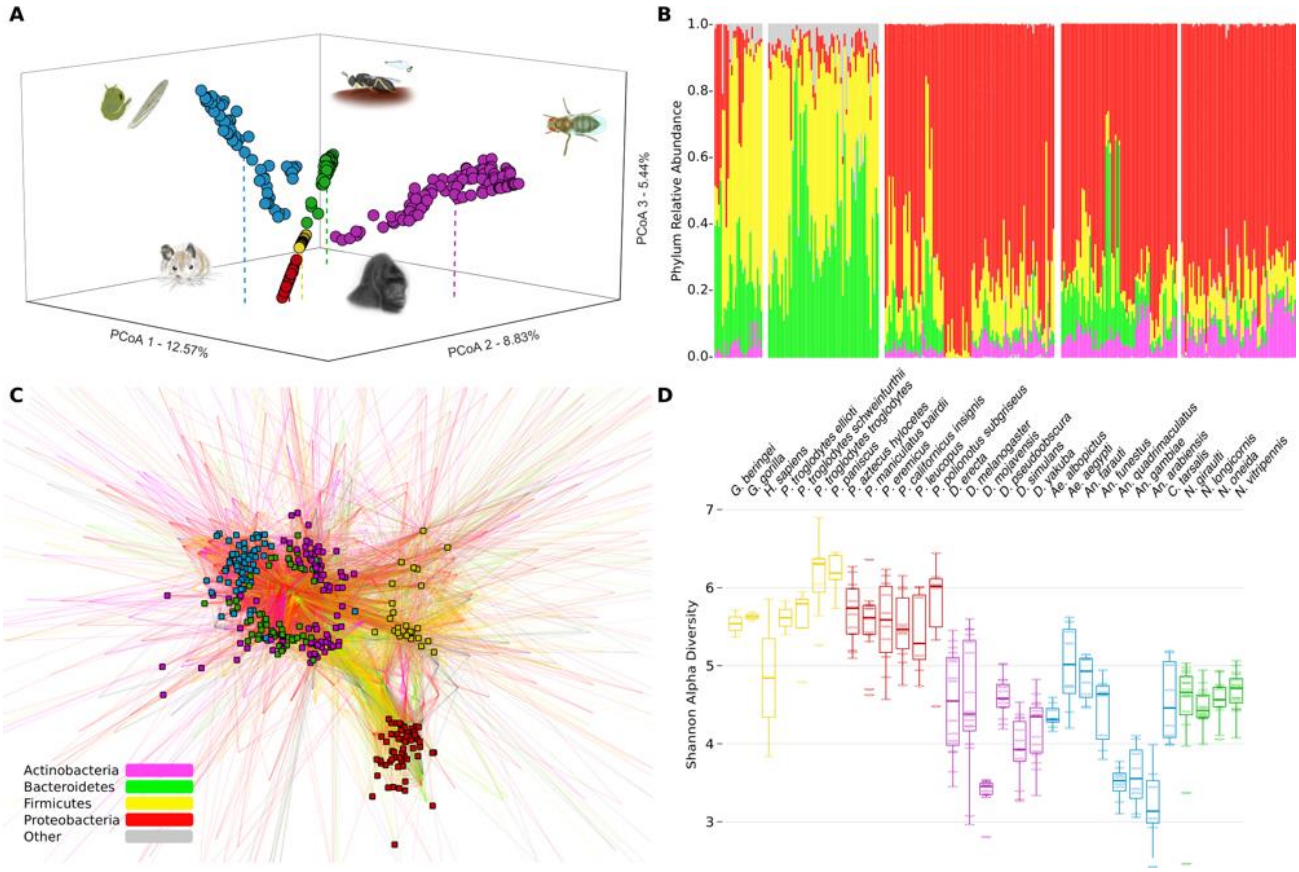

Figure III-2. Meta-analysis of microbiota variation across five host clades. (A) PCoA analysis of Bray-Curtis ecological similarity in three dimensions based on 99% OTU cutoff, with colors depicting clade of origin, (B) Phylum level taxonomic profiles of microbiota relative abundance for all samples, with a key provided in C. (C) Network analysis in which small squares depict samples, with their color indicating clade of origin. Lines connect genus-level OTUs to samples and are weighted by occurrence and colored by OTU phylum. (D) Shannon alpha diversity for each host species. Small ellipses depict individual samples and dark lines indicate the species median diversity. The lower and upper end of each box represent the 25th and 75th quartiles respectively. Whiskers denote the 1.5 interquartile range.

We implemented a Random Forest Classifier (RFC) supervised learning algorithm to quantify the degree to which individual microbial communities can be classified into their respective host clade. RFC models show a strong ability to classify microbial communities to their correct host clades (98.5% Classification Accuracy). Additionally, models distinguish mammals and insect samples with high accuracy (95.9% Classification Accuracy). Cross-validation prevents overfitting by ensuring that classification accuracy is assessed using only samples excluded from model training. We also used RFC models to identify the most distinguishing bacterial taxonomic level for both inter-clade distinction and the divide between mammals and insects. Genera provided the strongest ability to predict host clade (99.0% Classification Accuracy); however, the major groups of insects and mammals were better distinguished by family level community classification (98.3% Classification Accuracy). Taken together, these results illustrate that evolutionary relationships of the host clades broadly covary with differences in microbial communities. While differentiation of the five clades could in part be attributable to varied experimental conditions for each animal group, since they were reared separately, clustering of the vertebrate microbial communities from the invertebrate microbial communities is independent of rearing conditions and suggests a host-assisted structuring of microbial communities.

Intraspecific microbial communities are distinguishable within host clades

Phylosymbiosis predicts that an individual's microbial community will exhibit higher similarity to the communities from individuals of the same host species than to those from different host species. The degree of similarity will be variable but should correlate with divergence time or genetic relatedness of the host species. Pairwise comparisons of beta-diversity distances between all individuals within each host clade reveal that the average distance between microbial communities within a species is always less than between species (Figure B-1). Summarized beta diversity distances also reveal lower intraspecific vs. interspecific separation, with significant differences observed for all clades (Figure III-3A, Each dataset: Mann Whitney U $P < 1e\text{-}6$).

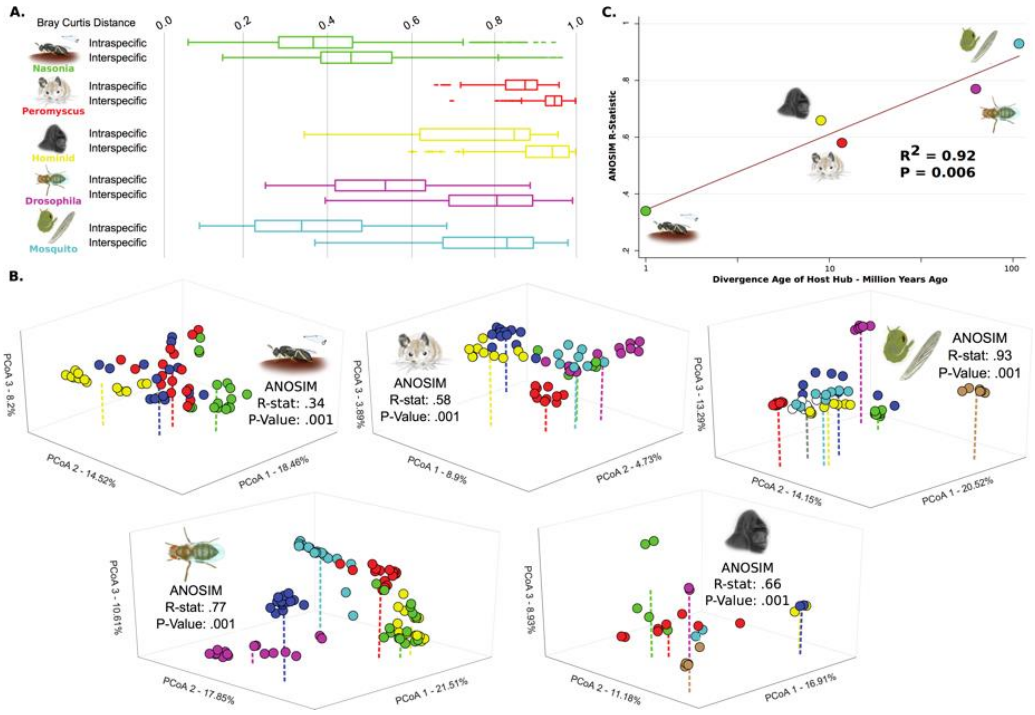

Figure III-3. Intraspecific versus interspecific microbial community variation within and between host clades. (A) Box-and-whisker plot of intraspecific and interspecific Bray-Curtis distances between samples for each clade. Boxes represent the 25th to 75th quartiles with the central line depicting the group median, and whiskers showing the 1.5 interquartile extent. (B) PCoA of Bray-Curtis distances with first three most distinguishing dimensions shown. Colors represent different species and correspond to the colors in Figure III-3. (C) Regression analysis measuring the correlation between the evolutionary age of host clade divergence on a log scale and the ANOSIM R values of intraspecific microbiota distinguishability from part B for each host clade.

We evaluated the intraspecific microbiota clustering through Bray-Curtis beta-diversity interrelationships with PCoA and statistically assessed the strength of interspecific microbiota distinguishability with ANOSIM (Figure III-3B). Visualization of the first three principle components revealed that individual samples clustered around their respective species' centroid position. In all host clades, each host species harbored significantly distinguishable microbial communities (Figure III-3B, ANOSIM P<0.001 for all host clades). Notably, the ANOSIM R values of interspecific microbiota distinguishability within a host clade positively correlated with the maximal age of divergence of the species in the host clades (Figure III-3C, Regression Analysis Log Transformed Clade Age, R^2=0.92, P=0.006; Untransformed Clade Age, R^2=0.70, P=0.048). Thus, host clades with higher total divergence times between species had stronger degrees of microbiota distinguishability across host species, while less diverged host clades exhibited less microbiota distinguishability. For example, with an estimated host divergence time of 108 million

years (Neafsey et al. 2015), mosquitoes showed the greatest distinguishability of their microbiota. Conversely, in *Nasonia* jewel wasps, which only diverged between 200,000 and one million years ago (Werren et al. 2010), the relative strength of clustering was less distinct but still statistically significant. The three intermediate age clades showed corresponding intermediate levels of clustering: *Drosophila* with an estimated divergence time of 62.9 million years (Clarke et al. 2007), Hominids that diverged 9 million years ago (Steiper and Young 2006), and *Peromyscus*, which diverged 11.7 million years ago (Weber and Hoekstra 2009). Therefore, the phylosymbiotic prediction that host species will exhibit significant degrees of specific microbiota assembly was supported in these observations, even under highly controlled conditions in the laboratory models. Microbiota specificity was maintained among very closely related and very divergent species, and a connection was observed between the magnitude of host genetic divergence and microbiota similarity.

Supervised classification: microbiota composition predicts host species

As microbiota distinguishability was supported within species across all five animal clades, it should be possible to model the strength of how well communities of bacteria predict their host species and how specific members of the microbiota affect these predictions. We therefore used RFC models trained on host clades to evaluate the classification accuracy, i.e., distinguishability explained by microbiota differences between species, and the expected predicted error (EPE), which measures the improvement of RFC species distinguishability compared to random classification. RFC results indicated that the OTU (*Drosophila*, *Peromyscus*) and genus taxonomic levels (Hominid, Mosquito, *Nasonia*) have the highest classification accuracy, while significant EPE was observed for all clades (EPE>2, Supplementary Table 1). The mosquito and *Drosophila* host clades exhibited the strongest genus level results (Mosquito, Classification Accuracy=99.8%, EPE=558.9; *Drosophila*, Classification Accuracy=97.2%, EPE=31.7). Other host clades demonstrated significant, but comparatively lower strength models. The reduced predictive power of these models may be due to a number of factors, such as a lower number of host species (*Nasonia*, Classification Accuracy=88.7%, EPE=13.4), uneven sample representation from each species (Hominid, Classification Accuracy=53.4%, EPE=2.1), and lower sequencing coverage (*Peromyscus*, Classification Accuracy=61.4%, EPE=2.5).

To determine the most distinguishing genera of the bacterial community, we examined the resulting loss of model Classification Accuracy when each genus is excluded from RFCs to assess the contribution to Model Accuracy. Distinguishability within the *Drosophila*, *Nasonia*, and Mosquito clades was driven primarily by genera in Proteobacteria, which represent five (14.0% Model Accuracy), seven (11.3% Model Accuracy), and eight (18.2% Model Accuracy) of the top ten genera respectively. Three of the ten most distinguishing genera in *Drosophila* females are from the Acetobacteraceae family (9.5% Model Accuracy), previously recognized to be "core" microbiota members (Wong et al. 2013; Shin et al. 2011). Three of the twenty most distinguishing genera in *Nasonia* females were closely related symbionts from the Enterobacteriaceae family (genera: *Proteus*, *Providencia*, *Morganella*; 3.1% Model Accuracy), consistently found in our previous studies of *Nasonia* males (Brucker and Bordenstein 2012a; Brucker and Bordenstein 2013; Wong et al. 2013; Shin et al. 2011). Eight genera from the phylum Proteobacteria dominate mosquito female distinguishability, primarily three Gammaproteobacteria of the order Pseudomonadales (8.2% Model Accuracy), and three Betaproteobacteria of the family Comamonadaceae (5.9% Model Accuracy). Hominid interspecific distinguishability was driven by the phylum Firmicutes, particularly of the order *Clostridiales* that contains three of the most distinguishing genera (1.5% Model Accuracy). The genus *Allobaculum* confered nearly double the distinguishing power of any other bacteria in *Peromyscus* (3.8% Model Accuracy), and it is associated with low fat diet, obesity, and insulin resistance in mice (Weber and Hoekstra 2009). As may be expected, genera of the abundant phyla Firmicutes and Bacteroidetes dominated the majority of distinguishability in *Peromyscus* (10.6% Model Accuracy), but genera from Proteobacteria in the family Helicobacteraceae comprised four of the top eleven genera (4.4% Model Accuracy). Overall, microbiota composition can be used to predict host species with high accuracy, and genera commonly observed in other studies of these host clades underlie interspecific distinguishability.

Phylosymbiosis is common within host clades

The major prediction of phylosymbiosis is that phylogenetic relatedness will positively correlate with beta-diversity relationships of microbial communities among related host species. Microbiota dendrograms were constructed by collapsing host species' total communities at a 99% OTU cutoff from individual samples to generate a cumulative microbial community for each

species, and then comparing relationships of their beta-diversity metrics. The Matching Cluster and Robinson-Foulds tree metrics were utilized to calculate host phylogenetic and microbiota dendrogram topological similarity, with normalized distances ranging from 0.0 (complete congruence) to 1.0 (complete incongruence; (Bogdanowicz and Giaro 2013)). Matching Cluster weights topological congruency of trees, similar to the widely used Robinson-Foulds metric (Bogdanowicz and Giaro 2013; Robinson ad Foulds 1981). However, Matching Cluster takes into account sections of subtree congruency, and therefore is a more refined evaluation of small topological changes that affect incongruence. Significance of the Matching Cluster and Robinson-Foulds analyses was determined in a comparable manner to a previous analysis by generating the probability of randomized bifurcating dendrogram topologies yielding equivalent or more congruent phylosymbiotic patterns than the microbiota dendrogram (Ley et al. 2008). Additionally using the same methodology, Matching Cluster and Robinson-Foulds metrics were evaluated for Bray-Curtis, unweighted UniFrac (Lozupone and Knight 2005), and weighted UniFrac (Lozupone and Knight 2005) beta-diversity dendrograms at both 99 and 97 percent clustered OTUs (Supplementary Fig 2). The Cytochrome Oxidase I gene was used to construct the phylogeny for each host clade, which compared well to established phylogenetic or phylogenomic trees for all species included in the study (*Nasonia* (Werren et al. 2010); *Drosophila* (Clark et al. 2007); Hominids (Steiper and Young 2006); Mosquitos (Neafsey et al. 2015)). *Peromyscus* was further resolved with an additional marker (Arginine Vasopressin Receptor 1A - AVPR1A) to reflect the latest phylogenetic estimates (Weber and Hoekstra 2009; Kohl et al. 2016).

Nasonia female wasps exhibited an equivalent phylogenetic tree and microbial community dendrogram, representing exact phylosymbiosis (*Nasonia* wasps, Figure III-4A). These results parallel previous findings in *Nasonia* males (Brucker and Bordenstein 2012a; Brucker and Bordenstein 2013). Despite congruency, the *Nasonia* clade has limited topological complexity with only four species, therefore resulting in a relatively marginal significance. Mice also show nearly perfect congruence with the exception of *P. eremicus* (Figure III-4B). *Drosophila* fruit flies (Figure III-4C) showed the lowest topological congruency but were still moderately significant. Four of the six species show correct topological relationships, while the microbial community relationships of *D. pseudoobscura* and *D. erecta* are topologically swapped. These results are different from previous findings in *Drosophila* that utilized a different experimental design, set of taxa, and sequencing technology (Wong et al. 2013). However, the evidence for phylosymbiosis

is tentative in *Drosophila* as unlike other clades, there is no significant congruence for either unweighted and weighted UniFrac metrics (Figure B-2). Previous studies detected no pattern of phylosymbiosis across *Drosophila* species (Wong et al. 2013), which could be attributed to *Drosophila's* constant replenishment of microbes from the environment (Chandler et al. 2011; Staubach et al. 2013), or the dominance by the bacterial genus *Acetobacter* which is important for proper immune and metabolic development (Wong et al. 2013). The two additional clades, mosquitoes and hominids, showed significant phylosymbiosis (Figure III-4D,E). Specifically, the mosquitoes showed accurate separation of *Culex* and *Aedes* genera from *Anopheles,* and the topological departures from phylosymbiosis appeared in two of the bifurcations between closely related species. The hominid microbial community dendrogram reflects the correct branching of *Gorilla* from *Homo sapiens,* followed by bonobos and chimpanzees, with the exception that one of the chimpanzee subspecies grouped more closely with the bonobo lineage. These results are similar to previous observations that the relationships of the microbial communities parallel those in the host phylogeny (Ochman et al. 201). With the exception of *Drosophila* that yielded limited evidence for host-microbiota congruence, significant degrees of phylosymbiosis were observed across clades with varying tree similarity metrics and microbiota beta-diversity analyses.

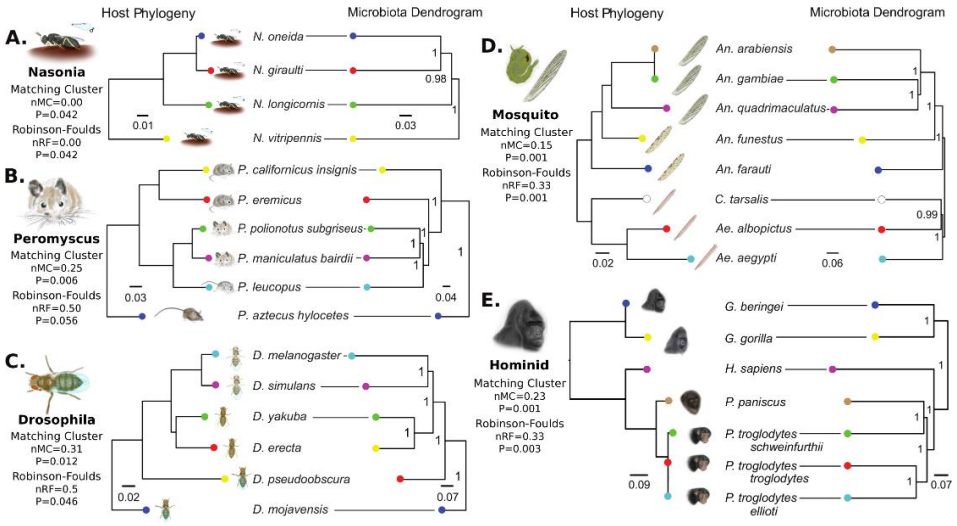

Figure III-4. Phylosymbiosis between host phylogeny and microbiota dendrogram relationships. Topological congruencies are quantified by the normalized Robinson-Foulds (RF) metric, which considers symmetry in rooted tree shape to quantify topological similarity on a scale from 0 (complete congruence) to 1 (incomplete incongruence). The normalized Matching Cluster (MC) metric is a refined version of the RF metric that sensitively accounts for incongruences between closely related branches. Horizontal lines connect species that share congruent positions in both host phylogeny and microbiota dendrograms.

Phylosymbiosis represents a functional association

Microbiota-host distinguishability and topological congruence does not strictly imply that the symbiotic associations are fitness directed, though it naturally follows that a particular host species may be more ideally suited for an autochthonous versus allochthonous microbiota. We therefore performed a series of microbial transplants to test the prediction that inoculated microbiota from a different species would decrease aspects of host performance or fitness in contrast to inoculated microbiota from the same species. Moreover, if there is selection on host-microbiota interactions such that microbiotas are uniquely situated for resident host backgrounds, then transplanted microbiota from a divergent species could drive more pronounced reductions in host biology than transplanted microbiota from a closely related species.

In *Peromyscus*, we followed a previously established protocol (Kohl et al. 2016) to transplant the microbial communities from six rodent donor species into a single recipient species, *P. polionotus*, as well as a control group where the microbial communities from *P. polionotus* were introduced to intraspecific individuals of *P. polionotus.* Inventories of fecal microbiota from donor and recipient mice revealed that portions of the donor microbiota successfully transferred. The estimated amount of transplanted OTUs and their relative abundance ranged from 6.5-26.2% and 11.4-40.7%, respectively, when analyzed at the 99% OTU cutoff level. Variation in the transfer of foreign microbes was dependent on donor species and its divergence from the recipient species (Figure B-3). We then measured dry matter digestibility, or the proportion of food material that is digested by the animal. Consistent with selection on host-microbiota interactions, mice that were inoculated with microbial communities from more distantly-related hosts exhibited decreased dry matter digestibilities (Figure III-5). These results were only significant when the group receiving feces from *P. eremicus* donors was removed (Figure III-5). Notably, the microbiota of *P. eremicus* is not congruent with our predictions of phylosymbiosis (Figure III-4). Thus, only the taxa showing phylosymbiosis exhibited the functional trend with digestibility. Distantly related donor species (*N. lepida* and *M. musculus*) did not drive significance, as the correlation remained statistically significant when investigating only *Peromyscus* donors (excluding *P. eremicus*; Figure III-5).

In the most extreme cases in which mice were inoculated with the microbial communities from *P. californicus* or *M. musculus*, there was approximately a 3% decrease in dry matter digestibility, which is on par with the decrease in digestibility observed as a result of helminth

infections in *Peromyscus* (Munger and Karasov 1989). Animals must consume more food to meet energy demands when faced with decreases in digestibility. Indeed, mice inoculated with microbial communities from *P. californicus* or *M. musculus* exhibited significantly higher food intakes than the control group (Figure B-4; Tukey's HSD test: P=0.001 for *P. californicus* -> *P. polionotus*; P=0.044 for *M. musculus* -> *P. polionotus*). The mice inoculated with the microbes from *P. eremicus* performed just as well, if not better, than the control groups in terms of dry matter digestibility (Fig 5), but still had slightly higher food intakes (Figure B-4).

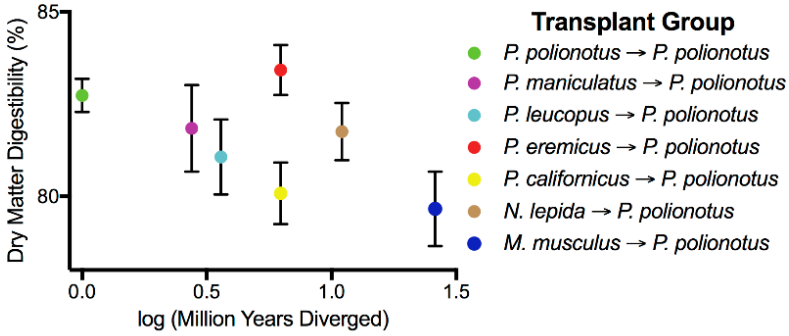

	R^2	P-value
All data	0.32	0.19
Remove *P. eremicus* → *P. polionotus*	0.70	**0.036**
Peromyscus donors only	0.09	0.61
Peromyscus, excluding *P. eremicus* → *P. polionotus*	0.94	**0.029**

Figure III-5. Effects of allochthonous and autochthonous microbial communities on the digestive performance of recipient mice. Dry matter digestibility is calculated as (g dry food ingested – g dry feces produced)/ g dry food ingested. Divergence times between P. polionotus and donor species were determined from previously published phylogenies (Stephhan et al. 2004; Kohl et al. 2016). Points represent mean values ± s.e.m. for each group (n = 5-6 recipients per group).

In *Nasonia*, we used an *in vitro* rearing system to transplant heat-inactivated microbial communities from three *Nasonia* donor species into larvae of *N. vitripennis* or *N. giraulti* (Shropshire and van Opstal 2016). We then measured the survival of the recipients from first instar larva to adulthood. In both *N. vitripennis* and *N. giraulti* hosts, interspecific microbiota transplantations exhibited significant decreases in survival to adulthood when compared to intraspecific microbial transplantations (Figure III-6). Specifically, *N. giraulti* with a *N. vitripennis* microbiota yielded a 24.5% average survival decrease in comparison to a *N. giraulti* microbiota (Figure III-6A, Mann-Whitney U, P=0.037). Interestingly, *N. giraulti* with a microbiota from the more closely related *N. longicornis* exhibited a similar, but non-significant survival reduction

(23.7%, Figure III-6A, Mann-Whitney U, P=0.086). *N. vitripennis* with a *N. girault*i or *N. longicornus* microbiota exhibited a 42.6% (Figure III-6B, Mann-Whitney U, P<0.0001) and 23.3% (Figure III-6B, Mann-Whitney U, P=0.003) average survival decrease in comparison to a *N. vitripennis* microbiota, respectively (Figure III-6A, Mann-Whitney U, P<0.0001). Comparisons were also made between non-inoculated hosts and those inoculated with interspecific backgrounds (*N. girault*i background: *N. vitripennis* inoculum p=0.07, *N. longicornis* inoculum p=0.26; *N. vitripennis* background: *N. girault*i inoculum p=0.001, *N. longicornis* inoculum p=0.15).

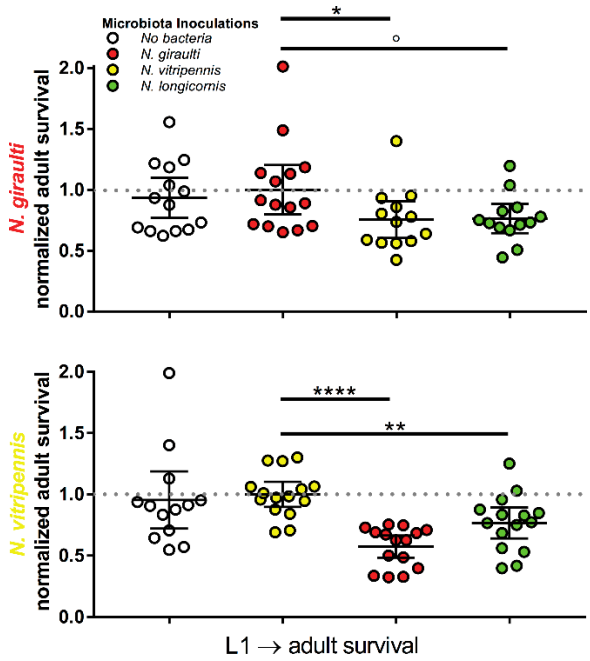

Figure III-6. Effects of allochthonous and autochthonous microbial communities on the survival of *Nasonia* wasps. (A) Normalized larval-to-adult survival of *N. girault*i wasps harboring no, self, or foreign microbiota. (B) Normalized larval-to-adult survival of *N. vitripennis* wasps harboring no, self, or foreign microbiota. Adult survival is calculated as (# of 1st instar larvae in a transwell – # of adults in a transwell)/ # of 1st instar larvae in a transwell. Adult survival was normalized to the average survival of the autochthonous microbiota transplantation. Circles represent individual transwell samples and the dashed line represents the average survival of the autochthonous microbiota transplantation normalized to 1. Mann Whitney U statistics, °p<0.1, *p<0.05, ** p<0.01, and **** P<0.0001.

Discussion

Under the phylosymbiosis hypothesis, host-associated microbial communities form, in part, as a result of interactions with the host rather than through purely stochastic processes associated with the environment. Specifically, we predicted that given closely-related animals reared in controlled environments, the relationships of the microbiota would be congruent with the evolutionary relationships of the host species. Previous evidence for phylosymbiosis under

controlled regimes existed in *Nasonia* (Brucker and Bordenstein 2012a; Brucker and Bordenstein 2013) and *Hydra* (Fraune and Bosch 2007), and wild populations of sponges (Easson and Thacker 2014), ants (Sanders et al. 2014), and apes (Moeller et al. 2014; Ochman et al. 2010) also exhibited this pattern. Here, in a comprehensive analysis of phylosymbiosis in a diverse range of model systems, we report the widespread occurrence of this pattern under strictly controlled conditions as well as a functional basis in the context of host digestive performance in mice and survival in wasps. These results represent the first evidence for phylosymbiosis in *Peromyscus* deer mice, *Drosophila* flies, a variety of mosquito species spanning three genera, and *Nasonia* wasp females with the inclusion of *N. oneida*. Previous studies in *Nasonia* measured male phylosymbiosis and did not include *N. oneida* (Brucker and Bordenstein 2012a; Brucker and Bordenstein 2013). By rearing closely related species from the same host clade in a common environment, and by controlling age, developmental stage, endosymbiont status, and sex, the experiments rule out confounding variables that can influence microbiota relationships in comparative analyses. Eliminating these variables is important because they often substantially correlate with interspecific differences. Thus, our findings demonstrate that a uniform experimental and bioinformatic methodology can excavate host effects on phylosymbiosis from other potentially confounding variables in comparative microbiota studies.

We observed marked differences in microbial diversity and community structure between mammalian and invertebrate host clades. Mammalian communities were more diverse and dominated by Bacteroidetes and Firmicutes, while insect-associated communities were less diverse and primarily dominated by Proteobacteria. These results are consistent with previous microbial inventories conducted in mammals and insects (Ley et al. 2008; Yun et al. 2014). Together, these findings suggest large-scale differences in the host-microbiota interactions between mammals and insects. These differences across host phyla could be due to a variety of possibilities including host genetics, diet, age, and rearing environment.

To separate out confounding variables that structure host-microbiota assemblages and rigorously test phylosymbiosis, we utilized an experimental design within four host clades that isolated the effects of host evolutionary relationships from other effects (i.e. diet, age, rearing environment, sex, endosymbionts). We found that host species consistently harbored distinguishable microbiota within each host clade. Additionally, we found significant degrees of congruence between the evolutionary relationships of host species and ecological similarities in

their microbial communities, which is consistent with the main hypothesis of phylosymbiosis. These results importantly expand previous evidence for this eco-evolutionary pattern and demonstrate that related hosts reared under identical conditions harbor distinguishable microbial assemblages that can be likened to microbial community markers of host evolutionary relationships. It is conceivable that recently diverged species, i.e. those younger than several hundred thousand years, would have less genetic variation and fewer differences in microbiota composition. Furthermore, divergent hosts may have vast differences in physiology that overwhelm the likelihood of observing phylosymbiosis. Surprisingly, we observed phylosymbiosis to varying degrees in all host clades, and the age of clade divergence positively correlates with the level of intraspecific microbiota distinguishability. Thus, as host species diverge over time, microbial communities become more distinct (Brucker and Bordenstein 2012a,c), and thus the limits of detecting phylosymbiosis may occur at extreme scales of incipient or ancient host divergence times.

The mechanisms by which phylosymbiosis is established requires systematic investigation. Perhaps the most apparent regulator of host-microbiota interactions is the host immune system. A previous study of phylosymbiosis in *Hydra* demonstrated that anti-microbial peptides of the innate immune system are strong dictators of community composition, and expression of anti-microbial peptides are necessary for the formation of host-specific microbiota (Franzenburg et al. 2013). Further, genome-wide association studies in humans (Blekhman et al. 2015, mice (Org et al. 2015), and *Drosophila* (Chaston et al. 2016) have identified a large-immune effect in which host immune genes can explain variation in microbial community structure. Interestingly, host immune genes often exhibit rapid evolution and positive selection compared to genes with other functions (Obbard et al. 2009; Nielsen et al. 2005). While this trend is often explained by the host-pathogen arms race (Obbard et al. 2009), it is also likely due to host evolutionary responses for recruiting and tending a much larger collection of nonpathogenic microbes.

Other host pathways may also underlie the observed species-specific microbiota signatures. Hosts produce glycans and mucins on the gut lining that may serve as biomolecular regulators of microbial communities (Hooper and Gordon 2001; McLoughlin et al. 2016). For example, knocking out the gene for α1–2 fucosyltransferase inhibits production of fucosylated host glycans on the gut surface, and significantly alters microbial community structure (Kashyap et al. 2013). Additional knockout studies have demonstrated the roles of circadian clock genes (Liang

et al. 2015), microRNAs (Liu et al. 2016), and digestive enzymes (Malo et al. 2010) in determining microbial community structure. These various physiological systems might also interact with one another and even evolved in tandem to regulate microbial community structure.

Alternatively, rather than hosts "controlling" their microbiota, microbes may be active in selecting which host niches to colonize. For example, hosts have been compared to ecological islands, where environmental selection of the microbiota through niche availability may occur (Costello et al. 2012). However, given the large number of studies that demonstrate the role of microbes in improving host performance (McFall-Ngai et al. 2013), we find it unlikely that hosts would assume a solely passive role in these interactions. An elegant study allowed microbial communities from various environments (soil, termite gut, human gut, mouse gut, etc.) to compete within the mouse gut (Seedorf et al. 2014). This study found that a foreign community of the human gut microbiota exhibited an early competitive advantage and colonized the mouse gut first. Later, the mouse gut microbiota dominated and outcompeted the human gut microbiota (Seedorf et al. 2014). Thus, community assembly is not a monolithic process of host control but likely a pluralistic combination of host control, microbial control, and microbe-microbe competition. In this context, both population genetic heritability and community heritability measurements of the microbiota will be useful in prescribing the varied genetic influences of a foundational host species on microbiota assembly (van Opstal and Bordenstein 2015).

The acquisition route of microbes could also influence our understanding of phylosymbiosis. If phylosymbiosis is observed when the microbiota is acquired horizontally from other hosts, the environment, or some combination of the two, then phylosymbiosis is presumably influenced by host-encoded traits such as control of or susceptibility to microbes. However, maternal transmission of microbes is argued to be a common trend in animals (Funkhouser and Bordenstein 2013). For example, sponges exhibit vertical transmission of a diverse set of microbes in embryos (Sharp et al. 2007). Transmission of full microbial communities is unlikely in most systems, given that the communities of developing animals tend to exhibit markedly lower diversity and distinct community structure compared to adults (Brucker and Bordenstein 2012a; Pantoja-Feliciano et al. 2013; Yatsunenko et al. 2012). Thus, it is improbable that phylosymbiotic relationships are explained simply by community drift over host evolutionary divergence. There could be a subset of microbial taxa that are more likely to be transmitted from mother to offspring that in turn affect what other microbes colonize. For instance in humans, the family

Christensenellaceae is situated as a hub in a co-occurrence network containing several other gut microbes and has a significant population genetic heritability (Goodrich et al. 2014). When *Christensenella minuta* is introduced into the guts of humanized-mice, the microbial community structure was significantly altered (Goodrich et al. 2014). This microbe, as well as others, can therefore be likened to a keystone taxon or "microbial hub" that can impact community structure despite their low abundance (Goodrich et al. 2014; Agler et al. 2016; Fischer and Mehta 2014). Thus, one could hypothesize that phylosymbiotic relationships in some systems may be driven by host transmission of microbial hubs that determine whole community structure through ensuing microbe-microbe interactions. However, further work is needed to test this hypothesis.

The congruent relationships between hosts and associated microbial communities are likely maintained through their positive effects on host performance and fitness but could be neutral or harmful as well. While the importance and specificity of hosts and microbes in bipartite associations has been demonstrated on host performance (Murfin et al. 2015), it is unclear whether such effects occur for hosts and their complex microbial communities. If they exist, disruption of phylosymbiosis via hybridization or microbiota transplants should lead to reduced fitness or performance. For instance, hybridization experiments demonstrate negative interactions or "hybrid breakdown" between host genetics and the gut microbiota that drives intestinal pathology in house mice (Wang et al. 2015) and severe larval lethality between *Nasonia vitripennis* and *N. giraulti* wasps (Brucker and Bordenstein 2012c). Further, transplant experiments show that all microbes are not equal for the host. An early study demonstrated that germ-free rabbits inoculated with a mouse gut microbiota exhibited impaired gastrointestinal function compared to those given a normal rabbit microbiota (Boot et al. 1985). Together, these functional studies and others suggest that interactions between hosts and their microbiota are not random and instead occur at various functional levels.

Here, we add an evolutionary component to these ideas by demonstrating that microbial communities from more evolutionarily distant hosts can be prone to more pronounced reductions in host performance or fitness. Specifically, *Peromyscus* deer mice inoculated with microbial communities from more distantly related species tended to exhibit lower food digestibility. The exception to this trend was the *P. eremicus* → *P. polionotus* group, which did not exhibit any decrease in digestibility. It should be noted that *P. eremicus* also did not follow expected trends of phylosymbiosis (Figure III-4B), which may explain the departure from our expected trend in

digestibility. For example, deviations from phylosymbiosis could be due to a microbial community assembly that is inconsequential to host performance. Therefore, transferring non-phylosymbiotic community between host species may not yield functional costs.

An alternative explanation for our results could be that hosts are acclimated to their established microbiota and the introduction of foreign microbiota either elicits a host immune response or disrupts the established microbiota, thus decreasing digestibility. One technique to distinguish between adaptation and acclimation would be to conduct experiments in germ-free *P. polionutus* recipients. However, the derivation of germ-free mammals is a difficult and expensive process (Wostmann 1996) and has not been conducted for *Peromsycus*. Earlier studies utilizing germ-free mammals demonstrate that microbial communities from evolutionarily distant hosts negatively impact gastrointestinal function (Boot et al. 1985) and immune development (Chung et al. 2012), thus supporting our hypothesis of functional matching between host and the gut microbiota.

Additionally, among very closely related species, *Nasonia* exposed to interspecific microbiota have lower fitness than those exposed to intraspecific microbiota. While this experiment utilized heat-inactivated bacteria to avoid shifts in the microbiota composition during media growth, the protocol is sufficient to test the predictions of phylosymbiosis. First, isolated microbial products can exert drastic effects on eukaryotic partners. For example, a sulfonolipid purified from bacteria can induce multicellularity in choanoflagellates (Alegado et al. 2012). Additionally, the insect immune system can respond with strain-level specificity to heat-inactivated bacteria (Roth et al. 2009). Therefore, we hypothesize that each *Nasonia* host species evolved to the products of their own gut microbiota, rather than those of gut microbiota from related host species. Together, results from the *Peromyscus* and *Nasonia* functional experiments reveal the importance of host evolutionary relationships when considering interactions between hosts and their gut microbial communities and ultimately the symbiotic processes that can drive adaptation and speciation (Bordenstein and Theis 2015; Shapira 2016). The molecular mechanisms underlying the functional bases of phylosymbiosis in various systems demand further studies.

Conclusion

Overall, we have established phylosymbiosis as a common, though not universal, phenomenon under controlled rearing with functional effects on host performance and survival. It

is worth emphasizing again that this term is explicit and different from many other similar terms, such as coevolution, cospeciation, cocladogenesis or codiversification (Theis et al. 2016). While cospeciation of hosts and specific environmentally- or socially-acquired microbes, e.g., Hominids and gut bacterial species (Moeller et al. 2016), or the bobtail squid and *Vibrio* luminescent bacteria (Nishiguchi 2002), could contribute in part to phylosymbiosis, concordant community structuring with the host phylogeny is not dependent on parallel gene phylogenies, but instead on total microbiota compositional divergence. Phylosymbiosis does not assume congruent splitting from an ancestral species because it does not presume that microbial communities are stable or even vertically transmitted from generation to generation (Brucker and Bordenstein 2012 a,c). Rather, phylosymbiosis predicts that the congruent relationships of host evolution and microbial community similarities could have varied assembly mechanisms in space and time and be newly assembled each generation (though see our discussion of transmission routes above). Moreover, the findings here imply that across wide-ranging evolutionary timescales and animal systems there is a functional eco-evolutionary basis for phylosymbiosis, at least under controlled conditions.

It may be difficult to detect phylosymbiosis in natural populations because of extensive environmental variation that overwhelms the signal. We suggest that one way to potentially overcome this challenge is to start with laboratory-controlled studies that identify (i) phylosymbiotic communities and (ii) the discriminating microbial taxa between host species. Resultantly, investigations can test whether these microbial signatures exist in natural populations, albeit perhaps in a smaller fraction of the total microbiota that is mainly derived by environmental effects. Another advantage of controlled studies is that the functional effects, both positive and negative, of a phylosymbiotic community assembly can be carefully measured in the context of host evolutionary history.

CHAPTER IV. AN OPTIMIZED APPROACH TO GERM-FREE REARING IN THE JEWEL WASP *NASONIA*[ᵛ]

Abstract

Development of a *Nasonia in vitro* germ-free rearing system in 2012 enabled investigation of *Nasonia*-microbiota interactions and real-time visualization of parasitoid metamorphosis. However, the use of antibiotics, bleach, and fetal bovine serum introduced artifacts relative to conventional rearing of *Nasonia*. Here, we optimize the germ-free rearing procedure by using filter sterilization *in lieu* of antibiotics and by removing residual bleach and fetal bovine serum. Comparison of these methods reveals no influence on larval survival or growth, and a 52% improvement in adult production. Additionally, adult males produced in the new germ-free system are similar in size to conventionally reared males. Experimental implications of these changes are discussed.

Introduction

The *Nasonia* genus (Ashmead & Smith 1904) consists of four closely related interfertile parasitoid wasp species and has been a powerful model for the study of genetics (Davies and Tauber 2015; Lynch 2015; Raychoudhury et al. 2010a), evolution (Bordenstein, O'Hara and Werren 2001; Bordenstein and Werren 2007; Brucker and Bordenstein 2013; Clark et al. 2010), endosymbiosis (Bordenstein, O'Hara, and Werren 2001; Ferree et al. 2008), development (Rivers and Losinger 2014; Verhulst et al. 2013; Zwier et al. 2012), behavior (Baeder and King 2004; Beukeboom and Van den Assem 2001; Clark et al. 2010; Drapeau and Werren 1999; Raychoudhury et al. 2010a), pheromonal communication (Diao et al. 2016; Ruther and Hammerl 2014; Steiner, Hermann, and Ruther 2006), and other areas. The design and publication of an *in vitro* system for *Nasonia* in 2012 detached *Nasonia* from its fly host, allowed for real-time monitoring of development, and provided an avenue to study how microbes influence *Nasonia* biology (Brucker and Bordenstein 2012b). These tools advanced the *Nasonia* system to explore how gut microbiota influence development and hybrid lethality (Brucker and Bordenstein 2013).

[ᵛ] This chapter was published in *PeerJ* (2016) 4:e3216. with Seth Bordenstein as co-author. Dylan Shropshire was co-first author.

Nasonia germ-free rearing involves two major components: (i) sterilizing *Nasonia* embryos and (ii) providing larvae with sterilized food in an *in vitro* system. Embryo sterilization is conducted by picking *Nasonia* embryos from pupal fly hosts (typically Sarcophaga bullata; Werren and Loehlin 2009a) and then rinsing the embryos with bleach followed by sterile water (Brucker and Bordenstein 2012b). Producing *Nasonia* Rearing Medium (NRM) involves the collection of hundreds of fly pupae, extraction of proteinaceous fluids from those pupae, addition of fetal bovine serum (FBS) and Schneider's Drosophila medium for additional nutrition, filter sterilization, and addition of antibiotics (Figure IV-1; Brucker and Bordenstein 2012b). Sterilized embryos are then placed on a transwell permeable membrane with filter-sterilized NRM underneath for feeding (Brucker and Bordenstein 2012b).

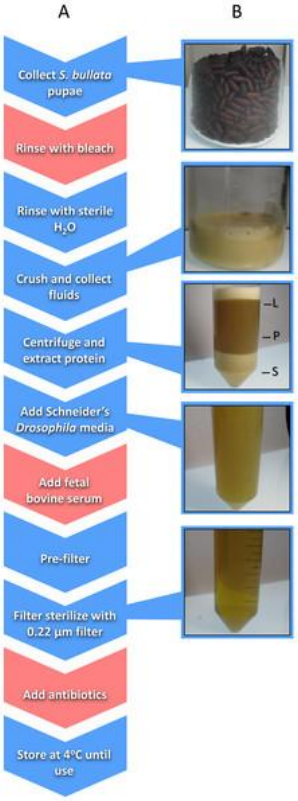

Figure IV-1. Schematic of the workflow to produce *Nasonia* Rearing Media (NRM). (A) Red boxes indicate steps present in NRMv1 but eliminated in NRMv2; blue boxes indicate steps present in both procedures. (B) shows the visual progression from *S. bullata* pupae to final NRM product. L, lipid layer; P, protein layer; S, sediment layer.

This protocol yielded similarly sized *Nasonia* to those from in vivo rearing (Brucker and Bordenstein 2012b). However, NRM production relies on introducing foreign and potentially

harmful elements such as bleach, FBS, and antibiotics. Removal of each component carries its own rationale. For example, the bleach treatment was intended to kill surface bacteria on the puparium of host flies and remove particulates (Brucker and Bordenstein 2012b). However, surface bacteria will be removed during filtration and residual bleach from the rinse may persist in the final NRM product as a toxic agent. Furthermore, FBS is added as a nutritional supplement to increase larval survival and development (Brucker and Bordenstein 2012b), but *Nasonia* do not frequently encounter components of FBS including bovine-derived hormones such as testosterone, progesterone, insulin, and growth hormones (Honn and Chavin 1975). Finally, antibiotics are a confounding variable and removing them will provide more flexibility to bacterial inoculations in the *in vitro* system.

This study removes these three major components of the original NRM and optimizes the procedure by eliminating extraneous steps and utilizing quicker approaches. These changes are validated by directly comparing germ-free *Nasonia* reared on either the original (NRMv1) or optimized (NRMv2) media for larval and pupal survival, larval growth, and adult production. The morphology of adults produced both *in vitro* and in vivo is then compared.

Materials and Methods

Nasonia rearing medium (NRMv1)

Sarcophaga bullata pupae were produced as previously described (Werren and Loehlin 2009a). Approximately 150 ml of *S. bullata* pupae were transferred to a sterile 250 ml beaker after close inspection to remove larvae, poor quality pupae, and debris. A solution of 10% Clorox bleach was then added to the beaker to cover the pupae. After five minutes, the bleach was drained from the beaker and the pupae were repeatedly rinsed with sterile millipore water until the scent of bleach was absent. Sterile millipore water was added in the beaker to approximately 2⁄3 the volume of pupae, covered, and placed in a 36 °C water bath to soften the puparium. *S. bullata* pupae were homogenized using a household kitchen blender and filtered through a 100 µm cell strainer (Fisherbrand; Thermo Fisher scientific Incorporated, Waltham, MA, USA). The filtrate was poured evenly across two 50 ml conical tubes (Falcon, Corning Incorporated, Corning, NY, USA) and centrifuged at 4 °C (25,000xG) for 5 min to separate the sediment, protein, and lipid layers, and a 22-gauge needle (BD PrecisionGlide; Becton, Dickinson and Company, Franklin Lakes, NJ, USA) was used to remove the protein layer. The protein layer was combined with 50 ml of

Schneider's Drosophila medium 1 x and 20% FBS. Using a reusable 500 ml vacuum filtration apparatus (Nalgene, Thermo Fisher scientific Incorporated, Waltham, MA, USA), the resulting product was passed through filter paper (Whatman; General Electric Healthcare Life Sciences, Maidstone, United Kingdom) with gradually smaller pore sizes (11, 6, 2.5, 0.8, and 0.45 µm). A 0.22 µm syringe filter (Costar, Corning Incorporated, Corning, NY) was used to remove bacteria. Finally, 200 µg of carbenicillin and penicillin/streptomycin were added to the medium. The final product was stored at 4 °C until use (Figure IV-1).

Nasonia rearing medium (NRMv2)

Approximately the same number of *S. bullata* pupae were collected as described above. Pupae were subsequently rinsed in sterile millipore water to remove small particulates. They were then crushed by hand through a 100 µm nylon net (EMD Millipore, Merck Millipore, Billerica, MA, USA) and the filtrate was collected in a sterile 250 ml glass beaker. Nylon powder-free non-sterile gloves were worn during this extraction. The filtrate was centrifuged at 4 °C (25,000xG) for 10 min to separate the sediment, protein, and lipid layers. Using a 22-gauge needle (BD PrecisionGlide; Becton, Dickinson and Company, Franklin Lakes, NJ), the protein layer was transferred to a sterile beaker. Schneider's Drosophila media was added to the protein extract to triple the volume and, using a reusable vacuum filtration apparatus (Nalgene; Thermo Fisher scientific Incorporated, Waltham, MA, USA), the resulting mixture was passed through filters with gradually smaller pore sizes (11, 6, 2.5, 0.8, and 0.45 µm). A 0.22 µm syringe filter (Costar; Corning Incorporated, Corning, NY, USA) was used to remove bacteria. The final product was stored at 4 °C until use (Figure IV-1). The following is a step-wise protocol for the production of NRMv2.

1. Fill a sterilized beaker with 150 ml of *S. bullata* pupa. Remove larvae, poor quality pupae, and debris.
2. In the beaker, cover pupae with sterile Millipore water, allow to sit for 1 min, and strain to remove surface particulates from the puparium surface. Some moisture will remain on the pupae.
3. Crush the pupae by hand (covered with powder-free nitrile gloves) and squeeze juices through a 100 µm nylon mesh to remove the *S. bullata* puparium.

4. Separate juices (approximately 70–90 ml) evenly into two 50 ml conical tubes and seal tightly.
5. Centrifuge the mixture for 10 min at 4 °C (25,000xG). The mixture will separate into three distinct layers: a sediment, protein, and lipid layer from bottom to top, respectively.
6. To prevent clogging during filtration, extract the protein layer using a 22-gauge sterile needle and transfer it to a sterile beaker under sterile laminar flow.
7. Add a 2:1 ratio of Schneider's Drosophila medium to the protein extract.
8. Using a vacuum filtration system, filter the media through progressively smaller pore sizes (11, 6, 2.5, 0.8, and 0.45 µm filters) to remove increasingly smaller particulates. To prevent clogging, replace filter paper when flow begins to slow.
9. Sterilize the media by filtering through a 0.22 µm syringe filter, taking care to use aseptic technique.
10. Store at 4 °C for up to 2 weeks.
11. Filter NRM through a 0.22 µm syringe filter before use to ensure sterility and remove sedimentation.

Nasonia strains and collections

N. vitripennis (strain AsymCx; *Wolbachia* uninfected) mated females were hosted on *S. bullata* pupae and housed in glass culture tubes capped with cotton at 25 ± 2 °C in constant light, as previously described (Werren and Loehlin 2009b). After 10–12 days, *S. bullata* puparіums were opened and virgin *N. vitripennis* females were collected as pupae from the resulting offspring. Upon adult eclosion, individual virgin females were isolated and provided two *S. bullata* pupae for hosting to increase the number of eggs deposited in subsequent hostings. In haplodiploids, virgin females are fecund and lay all male (haploid) offspring. Two days after initial hostings, females were provided with a new *S. bullata* pupae housed in a Styrofoam plug, allowing her to oviposit only on the anterior end of the host for easy embryo collection.

Germ-free rearing of Nasonia

N. vitripennis strain AsymCx embryos were extracted from *S. bullata* pupae parasitized by virgin females after 12–24 h. 20–25 embryos were placed on a 3 µm pore transwell polyester membrane (Costar; Corning Incorporated, Corning, NY, USA) and sterilized twice with 70 µl 10%

bleach solution and once with 70 µl 70% ethanol solution. The embryos were then rinsed three times with 80 µl sterile millipore water. After rinsing, the transwell insert was moved into a 24 well plate with 250 µl of NRM in the well. All plates were stored in a sterile Tupperware box at 25 ± 2 °C in constant light conditions for the duration of the experiment. Under sterile laminar flow, transwells were moved to new wells with 250 µl of fresh NRM every second day. Approximately 1.5 ml of NRM was used per transwell over the duration of the experiment. After eleven days, the transwells were moved to dry wells in a clean plate and the 12 empty surrounding wells were filled with 1 ml of sterile millipore water to increase humidity. Two plates with 12 transwells each (total of 24) were set up using either NRMv1 or NRMv2 by JDS for *Nasonia in vitro* rearing in May 2016. Replicate rearing and collection of larval and pupal survival data was conducted on both NRMv1 (N = 9 inserts) and NRMv2 (N = 13 inserts) by EVO in April 2015 and March 2016, respectively (Figure IV-2).

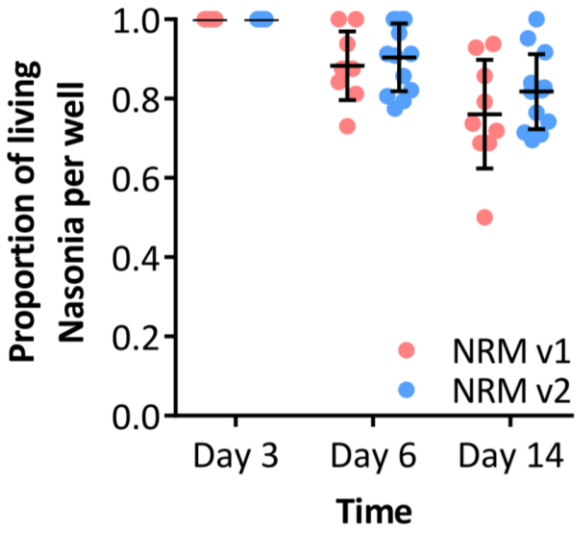

Figure IV-2. Replicate comparison of *Nasonia* germ-free larval development on NRMv1 and NRMv2. (A) The proportion of living *Nasonia vitripennis* in transwells on days 3, 6, and 14. There are no statistically significant differences in larval and pupal survival to day 14 on NRMv1 and NRMv2. R1, replicate one conducted by JDS; R2, replicate two conducted by EVO. Vertical bars with caps represent standard deviation from the mean.

Comparative analysis of development

A picture was taken of each well, every day for 20 days, under magnification using a microscope-attached AmScope MT1000 camera. A baseline for the number of larvae present in a well was determined by counting the number of larvae present in transwell pictures three days after embryo deposition on the transwell membranes (day 3). Survival estimates were determined

by counting the number of live larvae on day 6 and the number of live larvae and pupae on day 14, compared to day 3. Larvae and pupae were identified as dead if they were visibly desiccated or malformed. Larval length was determined using ImageJ software by measuring the anterior to posterior end of larvae on days 3, 6, and 14. The proportion of adults produced by a transwell was determined as follows: (the number of larvae on day 3 − the number of dead larvae and pupae remaining on day 20) ÷ the number of larvae on day 3. Pictures of conventionally reared and germ-free (NRMv2) adult males were taken, and ImageJ was used to measure head width, which is a correlate for body size in *Nasonia* (Blaul and Ruther 2012; Tsai et al. 2014).

Results

Larval growth of *Nasonia vitripennis* reared on NRMv1 was previously compared to conventionally reared *N. vitripennis* and there were no differences in larval survival or larval growth over development (Brucker and Bordenstein 2012b). Here we demonstrate, in comparisons between NRMv1 and NRMv2, that there is also no difference in larval and pupal survival to day 14 (Figure IV-2A; Mann–Whitney U (MWU) for day 6 $p = 0.19$ and day 14 $p = 0.41$) nor length, measured as the distance from the anterior to posterior end (Figure IV-2B; MWU for day 3 $p = 0.26$, day 6 $p = 0.18$, day 14 $p = 0.13$). A replicate experiment reveals that the survival results are repeatable (Figure IV-2; MWU for day 6 $p = 0.23$ and day 14 $p = 0.06$). Moreover, a visual comparison of larval sizes on NRMv1 and NRMv2 shows no major differences (Figures IV-3C–3F). These findings indicate that removal of residual bleach, FBS, and antibiotics does not have a significant impact on larval survival or development.

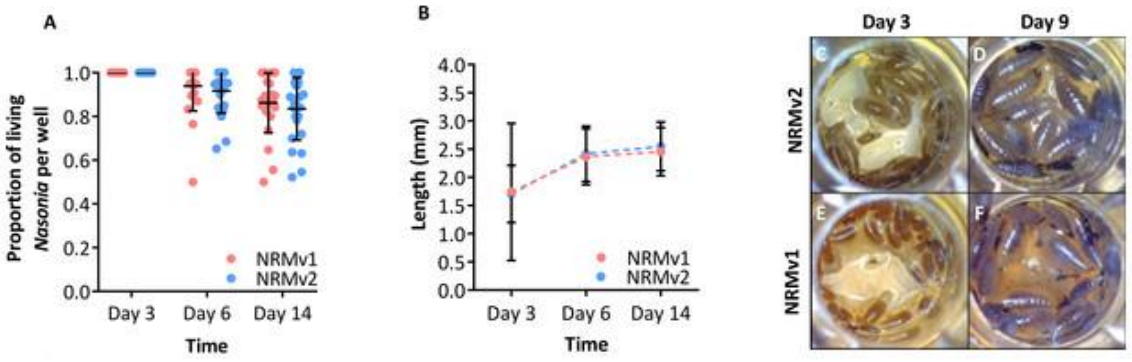

Figure IV-3. Comparison of *Nasonia* germ-free larval development on NRMv1 and NRMv2. (A) The number of living *Nasonia vitripennis* in transwells on days 3, 6, and 14. There are no statistically significant differences in larval survival on NRMv1 and NRMv2. (B) Equivalent larval lengths measured from anterior to posterior end in mm. (C–F) Visual comparison of larvae reared on NRMv1 and NRMv2 on days 6 and 9. Vertical bars with caps represent standard deviation from the mean.

NRMv1 yielded low adult survival compared to conventional rearing (Brucker and Bordenstein 2012b). To investigate if using NRMv2 improves larval to adult survival, both the number of transwells producing adults and the average number of adults produced per transwell were compared between NRMv1 and NRMv2. The number of transwells that produced at least a single adult did not differ between NRMv1 (79% productive; N = 24) and NRMv2 (88% productive; N = 24; Figure IV-4A; Fisher's exact test $p = 0.7$). However, and importantly, NRMv2 yielded a higher proportion of adults than NRMv1 (Figure IV-4B; MWU $p = 0.001$), accounting for a 52% increase in larval to adult survival. Finally, to ensure that adults produced in the *in vitro* system are similar in size to conventional adults, the head width of adult males produced on NRMv2 (N = 16) was compared to conventionally reared (N = 16) adult males, and there was no significant difference (Figure IV-4C; MWU $p = 0.72$).

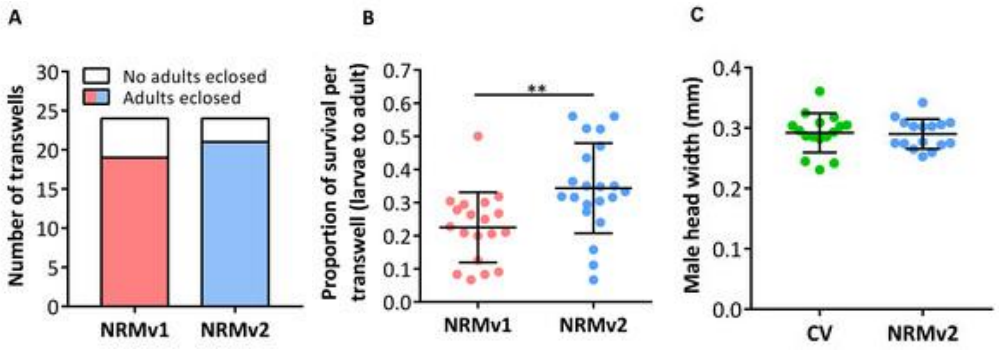

Figure IV-4. Survival and size of *Nasonia* germ-free adult males. (A) Comparison of the number of transwells producing adults between NRMv1 and NRMv2. (B) Proportion of larval to adult survival in each transwell is determined as follows: (the number of larvae on day 3 – the number of larvae and pupae remaining on day 20) / the number of larvae on day 3. (C) Adult head widths from germ-free males reared in NRMv2 and males rearer conventionally. Larval to adult survival was statistically different between the two media (Mann-Whitney U, P-value = 0.001). All other measures were not significant with $\alpha = 0.05$. Vertical bars with caps represent standard deviation of the mean.

Discussion

The previously established *Nasonia in vitro* germ-free rearing protocol (Brucker and Bordenstein 2012b), which involved sterilizing embryos and feeding the larvae NRMv1, was crucial for conducting experiments on *Nasonia*-microbiota interactions (Brucker and Bordenstein 2013). However, this initial version of the germ-free rearing system contained highly artificial elements such as bleach rinsing, FBS, and antibiotics (Figure IV-1; NRMv2). Following removal of these elements, we show that the alterations to the NRM did not influence larval and pupal survival to day 14 in replicate experiments (Figure IV-2; Figure IV-3A) or larval growth (Figure IV-3B), but importantly resulted in a 52% increase in larval to adult survival (Figure IV-4B). Moreover, the size of adult males produced on NRMv2 and in vivo do not differ (Figure IV-4C), suggesting that both *in vitro* and *in vivo* rearing produce morphologically similar adults.

Aside from making the *Nasonia in vitro* system more biologically relevant, the new media has multiple experimental implications. For example, antibiotics are a confounding variable with unknown consequences to *Nasonia* biology, and they can hinder inoculation capabilities of the system by causing bacterial communities introduced to rapidly shift in composition. Thus, removal of antibiotics in NRMv2 makes it easier to derive conclusions and may provide more flexibility for inoculations *in vitro*, namely introduction of full microbial communities derived from *Nasonia* species. This new system permits the introduction of both autochthonous and allochthonous microbial communities, enabling investigations of the functional relevance of host-specific

microbial communities or microbial species. For example, the *Nasonia* microbiota exhibits "phylosymbiosis," a pattern in which microbial community relationships parallel the phylogenetic relationships of the host species (Brucker and Bordenstein 2012a; Brucker and Bordenstein 2013). Transplanting communities between species will test the functional relevance of phylosymbiosis.

Furthermore, improved survival of larvae to adults on NRMv2 makes obtaining sample sizes of adults and the measurement of adult phenomes (e.g., physiology, anatomy, and behavior) more feasible. In this context, NRMv2 permits improved exploration of *Nasonia* adult-microbiota interactions. For example, there are many examples of microbe-mediated signals used in mate-choice, species recognition, and kin recognition (Reviewed in Shropshire & Bordenstein 2016). *Nasonia* species produce several different signals including cuticular hydrocarbons (Buellesbach et al. 2013), abdominal sex pheromones (Diao et al. 2016), and cephalic pheromones housed in an oral gland (Miko and Deans 2014; Ruther and Hammerl 2014). This *in vitro* rearing system allows for the exploration of the interaction of microbes with host signals to test what role these complex interactions may have in adult behavior, insect communication, and reproductive isolation.

Parasitoid wasps are also difficult to study developmentally because the fly host's puparium obstructs visualization of the *Nasonia* larvae and pupae, preventing multiple measures of a single individual over time. *In vitro* rearing of *Nasonia* allows for observations of single individuals over developmental time and for strict control of larval diet, bacterial exposure, and *Nasonia* density. Using this system, one may test how these variables influence metamorphosis (Johnston and Rolff 2015), wing and body size (Rivers and Losinger 2014), craniofacial anomalies (Werren et al. 2015), and many other physiological traits.

Conclusion

In summary, we streamlined and improved upon the *Nasonia in vitro* rearing system while removing antibiotics and other factors from the equation. These improvements to the methodology allow for a technique that minimizes the confounding effects antibiotics and exogenous proteins and nutrients may have on *Nasonia* development and behavior. The NRMv2 methodology permits the examination of the *Nasonia* lifecycle under gnotobiotic conditions, which opens the door to multidisciplinary studies of host-microbiota interactions and add to *Nasonia*'s utility as a model system.

CHAPTER V. A FUNCTIONAL ASSOCIATION OF PHYLOSYMBIOSIS WITHIN THE *NASONIA* WASP CLADE

Abstract

To interface the ecology of microbiota assembly with the evolution of their host, phylosymbiosis was proposed to describe the pattern when ecological relatedness of the host's microbiota composition recapitulates the phylogenetic relationships of the host species. This pattern is frequently observable under controlled rearing conditions in a variety of vertebrate and invertebrate species. However, it is currently unclear if this pattern is consequential to host fitness, with a positive result having implications for selection on host-gut microbiota interactions. In order to determine the functionality of this relationship in an evolutionary model, we conducted intra- and interspecific gut microbiota transplantations between three closely related parasitoid wasp *Nasonia spp.*, *N. vitripennis*, *N. giraulti*, and *N. longicornis*. Wasp hosts were reared germ-free, transplanted with intraspecific (autochthonous) or interspecific (allochthonous) gut microbiota, and assessed during development. Metrics of development included: larval length, pupation, and adult reproductive capacity. We report three key findings. First, larval growth was significantly delayed when host species were reared with a sibling species' interspecific gut microbiota versus their own gut microbiota. Second, there were significant decreases in pupation when host species were reared with sibling species' interspecific gut microbiota. Third, interspecific gut microbiota rearing did not significantly influence the host species' adult reproductive capacity including male fertility and longevity. Overall, these microbiota transplantation studies in a controlled environment specify, for the first time, that phylosymbiosis among closely related species is functionally driven and affects host development. The results are consistent with selection acting on adaptive host-microbiota interactions.

Introduction

To understand animal-microbe interactions means to appreciate the importance of microbial roles in nearly all aspects of animal development, immunology, digestion, and behavior (Eisthen and Theis 2016; McFall-Ngai 2013). While there continues to be debate over the relative importance of environmental factors vs. host genetics in the formation of a host-associated

microbiota (Margulis 1993; Rosenberg et al. 2007), many researchers agree on the term "holobiont" to define an animal or plant and its associated microbiota as a single entity. Some researchers take the concept a step further in support of a hologenome theory of evolution, which groups the genetic content of the host and its microbiota into one unit upon which selection operates. This theory is based on several tenets including: (1) host-associated microbial communities are not acquired randomly, (2) host-microbiota interactions can have fitness consequences for the holobiont, (3) the association of hosts with their microbiotas can be transgenerational, and (4) genetic variation of the holobiont can occur through changes in host genomes or genomes of microbiota members (Bordenstein and Theis 2015; Theis et al. 2016; Rosenberg and Rosenberg 2018; Theis 2018). However, this evolutionary hypothesis has created some controversy and been argued to be "based on overly restrictive assumptions" when considering selection processes to operate on the entire holobiont (Moran and Sloan 2015; Douglas and Werren 2016).

As discussed in CHAPTER III, the concept of phylosymbiosis provides an observable pattern that may support the hologenome theory; however, it does not presume the holobiont acts as a unit of selection or that the microbiota remains a stable community within the host. Phylosymbiosis refers to an eco-evolutionary pattern in which evolutionary changes in the host genome associate with ecological changes in the microbiota. It was shown that there is a functional eco-evolutionary basis for phylosymbiosis, at least under lab-controlled conditions for *Peromyscus* deer mice and *Nasonia* wasps. Since the publication of CHAPTER III, the pattern of phylosymbiosis has also been observed in pikas (Kohl et al. 2018a), woodrats and other rodents (Kohl et al. 2018b), and among the skin communities of 38 different mammalian species (Ross et al. 2018). However, there have only been a few studies which explore the functional outcomes of a phylosymbiosis pattern. To emphasize the importance of evolutionary changes in the host brought about by a phylosymbiotic pattern, the functional outcomes of the host need to be further studied through transplantation experiments of autochthonous and allochthonous microbiotas. It was previously shown that the colonization of a human gut microbiota in mice resulted in immune response deficiencies and increased susceptibility to enteric pathogens when compared to conventionally-colonized mice (Chung et al. 2012). However, the mechanisms by which allochthonous microbiota transplants reduce host survival and functionality has yet to be explored

in much detail and may provide insight into how the microbiota has influenced host evolution in a phylosymbiotic framework.

While decreased survival outcomes in *Nasonia vitripennis* and *Nasonia giraulti* from allochthonous microbiota transplants was shown in CHAPTER III, the *Nasonia* physiology which resulted in these functional outcomes was not described. Considering that the majority of metabolic activity, growth and development occurs before adult eclosion, the effects of allochthonous transplantation must be observed throughout the *Nasonia* life cycle to determine which developmental stages are affected most by the transplantation. These microbiota transplants are heat-inactivated, which decreases the likelihood that the microbial communities are influencing the *Nasonia* by means of metabolic byproducts but does allow for the possibility of energetic *Nasonia* immune responses during an important period of growth and metamorphosis. The *Nasonia* larval microbiota is dominated by the major genera, *Proteus* and *Providencia*, which are considered commensals in lab reared *Nasonia* wasps. However, several different *Providencia* strains exhibit variable levels of host immunogencity in the larvae of other insect models such as *Drosophila melanogaster* (Galac and Lazzaro 2012; Duneau and Lazzaro 2018). This variability of *Drosophila* immune responses to different *Providencia* strains may provide a potential pathway by which *Nasonia* development is altered between different microbiota transplants.

In this study, the effects of allochthonous microbiota transplantation between three of the four *Nasonia spp.* previously reported in CHAPTER III were observed from initial embryo hatching throughout the entire life cycle. The influences of allochthonous microbiota transplants were analyzed through larval growth mesurements, pupation counts, and adult reproductive success.

Materials and methods

Nasonia strains and collections

Wolbachia uninfected *N. vitripennis* AsymCx, *N. giraulti* RV2x[u], and *N. longicornis* NLMN8510 mated females were hosted on *S. bullata* pupae and housed in glass culture tubes capped with cotton at 25 ± 2 °C in constant light, as previously described (Werren & Loehlin, 2009b). After 10–12 days, *S. bullata* puparіums were opened and either virgin *N. vitripennis* or *N. giraulti* female offspring were collected as black pupae. Upon adult eclosion, 200 individual virgin females were isolated and provided two *S. bullata* pupae for two days of hosting to increase the

egg deposition. As haplodiploids, *Nasonia* virgin females are fecund and lay all male (haploid) offspring. After the initial two days of hosting, females were provided with a new *S. bullata* pupae housed in a Styrofoam plug, allowing her to oviposit only on the anterior end of the host for easy embryo collection.

Germ-free rearing of Nasonia

N. vitripennis AsymCx or *N. giraulti* RV2x[u] embryos were extracted with a sterile probe from *S. bullata* pupae parasitized by virgin females after 12–24 hr. 20–25 embryos were placed on a 3 µm pore transwell polyester membrane (Costar; Corning Incorporated, Corning, NY, USA) and sterilized twice with 70 µL of 10% bleach solution and once with 70 µL of 70% ethanol solution. The embryos were then rinsed three times with 80 µl of sterile millipore water. After rinsing, the transwell insert was moved into a 24 well plate with 200 µl of NRM (prepared according to the NRMv2 protocol described in CHAPTER IV) in the basolateral compartment. All plates were stored in an autoclaved Tupperware box at 25 ± 2 °C in constant light conditions for the duration of the experiment. Under sterile laminar flow, transwells were moved to new wells with 200 µl of fresh NRM every day. After eight days, the transwells were drained of their media on a sterile Kimwipe and moved to a clean, dry 24-well plate and the 12 empty surrounding wells were filled with 1 mL of sterile millipore water and 65.7mM Tegosept solution to increase humidity and prevent fungal growth.

Heat-inactivated microbiota preparation

We tested the effects of allochthonous microbial communities on host survival by transplanting heat-inactivated microbiota from three donor *Nasonia* species (*N. vitripennis, N. giraulti*, and *N. longicornis*) into *N. vitripennis* or *N. giraulti* male recipients. Microbiota were purified from fourth instar larvae of each of the *Nasonia* donor species by homogenization of ~100 larvae in 200 µL of sterile 1x PBS. The larval homogenate was then centrifuged at 800 RPM for 3 minutes to pellet large cellular debris and the resulting supernatant was filtered through a 5 µm filter. The filtrate was centrifuged at 10,000 rpm for three minutes and the supernatant was removed. The pellet was resuspended in sterile 1x PBS. This centrifugation step was repeated and the pellet was resuspended in 200 µL 1x PBS. After the supension was plated on Tryptic soy agar to determine the rough microbiota concentration, it was heat-inactivated by placement in a 75^{o}C

water bath for one hour. After counting colonies on the Tryptic soy agar plates, the heat-inactivated suspension was diluted in sterile 1x PBS to achieve a concentration of 5 x 10^6 CFU of microbiota bacteria per milliliter. This procedure was performed independently for each of the donor microbial communities one day before transplantation.

Transplantation of the heat-inactivated Nasonia spp. microbiota

After the first 24 hrs of germ-free *Nasonia* rearing, the transwell inserts were randomly separated into four experimental groups, a PBS control and transplantation of heat-inactivated *N. vitripennis*, *N. giraulti*, and *N. longicornis* microbiotas. For the transwells in each group, 20 µL of this microbiota suspension was added directly to the transwell inserts daily during the eight transplantation days before *Nasonia* pupation. *Nasonia* rearing media was replaced daily just before the inoculations. On days 2-8 of transplantation, the transwell insert was drained on a sterile Kimwipe before the addition of the 20 µL of microbiota suspension. If there was any bacterial or fungal contamination in a transwell during the course of the *Nasonia* development, the transwell and its data were removed from the experiment.

Comparative analysis of Nasonia development

After the replacement of *Nasonia* rearing media and addition of heat-inactivated *Nasonia* microbiota, a picture was taken of each well under magnification using a microscope-attached AmScope MT1000 camera. Pictures of each transwell were taken from the first day of heat-inactivated microbiota transplantation to the first day of adult eclosion (~14-15 days). Starting on the second day of microbiota transplantation, larval length was determined using ImageJ software by measuring the anterior to posterior end of larvae for all larvae in the transwell. Normalized larval growth per transwell sample was calculated as the average larval length of *Nasonia* per transwell divided by the average larval length of the autochthonous microbiota treatment group for each treatment day. Larvae were identified as dead if they were visibly desiccated or malformed and were not included in the analysis.

On the last day of *Nasonia* pupation before adult eclosion (5 days after initial pupation begins), the proportion of pupated larvae was measured for each transwell. Normalized pupation per transwell sample was calculated as the percent pupated *Nasonia* per transwell divided by the average percent pupated of the autochthonous microbiota treatment group.

For each transwell, live larval counts were recorded on the third day after embryo deposition to be sure that all the embryos had hatched. Adult counts were determined by recording the number of remaining larvae and pupae in each transwell 20 days after embryo hatching (5-7 days after first adult eclosion) and subtracting that number from the larval counts previously recorded. Normalized adult survival per transwell sample was calculated as the percent survival of *Nasonia* from 3 days to 20 days after embryo hatching divided by the average percent survival of the autochthonous microbiota treatment group. Larvae and pupae were identified as dead if they were visibly desiccated or malformed. Larval growth, pupation, and adult survival between the autochthonous and allochthonous treatment groups were compared using a Kruskal Wallis test with a Dunn's multiple comparisons test.

Comparative analysis of adult reproductive capacity

After initial adult eclosion from each experimental group, adult males were collected from the transwells daily and mated with a conventional newly-eclosed (< 24 hrs) virgin female for 24 hrs. The mated female was then given two *S. bullata* pupae to parasitize. When the offspring pupae reached the black pupal development stage, males and females were counted and a sex ratio recorded. Adult male longevity was measured by moving the post-mated males to a cotton-plugged sterile glass tube and recording survival every 12 hours. Adults males which eclosed with deformities that may influencing mating were not used in the analysis.

Results

Allochthonous microbiota transplants alter Nasonia larval development

To determine the effect of microbiota transplants on *Nasonia* growth in the larval stage, I captured pictures of the treated larvae during each day of development before pupation and measured their length. Shown in Figure V-1, the growth curves of PBS buffer-treated *N. vitripennis* and *N. giraulti* larvae were used to observe the period of largest larval growth corresponding to specific larval instar stages. In the *N. vitripennis* lifecycle, the peak larval growth occurs during the 2^{nd} to 4^{th} day of larval development which coincides with the $2^{nd}/3^{rd}$ instar transition. During this stage of development, there was a 1.14 mm increase in larval length, particularly between the 2^{nd} to 3^{rd} day of development equating to a 75% of the total larval growth before pupation. In *N. giraulti* larvae, the same peak growth occurs at the $2^{nd}/3^{rd}$ instar transition with a 1.39 mm increase

in length representing 90% of the total larval growth. However, the slightly delayed growth in *N. girault*i resulted in the most growth from the 3rd to 4th day of development, which is consistent with slower *N. girault*i growth in conventionally-reared *Nasonia*.

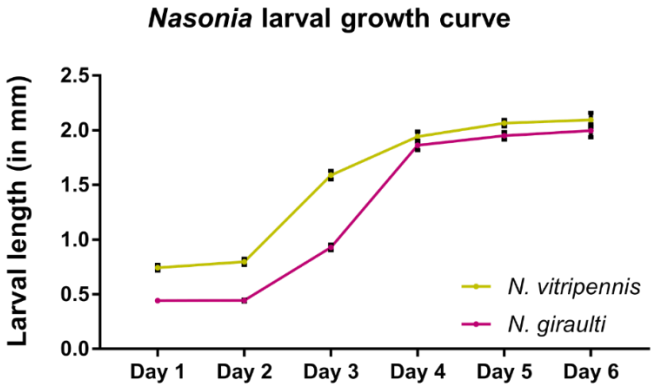

Figure V-1. Peak larval growth occurs between the 2nd and 3rd instar 3-4 days after hatching. Starting one day after embryo deposition on the transwells, the average larval length of 1x PBS treated *Nasonia* is shown for the first six days of larval development. Days 1 & 2 represent the first two larval instars, Days 3 & 4 represent the 3rd larval instar after rapid growth, and Days 5-6 represent the 4th larval instar before gut contents are evacuated for pupation. The yellow line displays *N. vitripennis* larval growth while the red line represents *N. girault*i larval growth. Black bars at each developmental day indicate the larval length standard error of mean (N= 13-15).

With peak larval growth of *N. vitripennis* and *N. girault*i established in the germ-free rearing setup, the effects of allochthonous heat-inactivated microbiota transplants were observed at the beginning and end of this growth. On the 2nd day of larval growth after only one day of transplantion, there was no significant difference in larval length between the control and treatment groups for *N. girault*i recipients (Figure V-2B). However, there was already a significant difference in *N. vitripennis* normalized larval length from an autochthonous or intraspecific transplantation compared to the allochthonous treatment groups (Figure V-2A).

On the 4th day of larval development at the end of peak growth, *N. vitripennis*'s normalized larval length was significantly different ($p<0.001$ and $p<0.0001$) between the autochthonous and allochthonous transplants. Interestingly, the only significant difference in *N. girault*i normalized larval length was between the autochthonous transplant and the allochthonous transplant from the most distantly diverged donor species, *N. vitripennis*. While there was a slight decrease in normalized larval length with the allochthonous transplant from a more recently diverged donor species, *N. longicornis*, this difference was not significant.

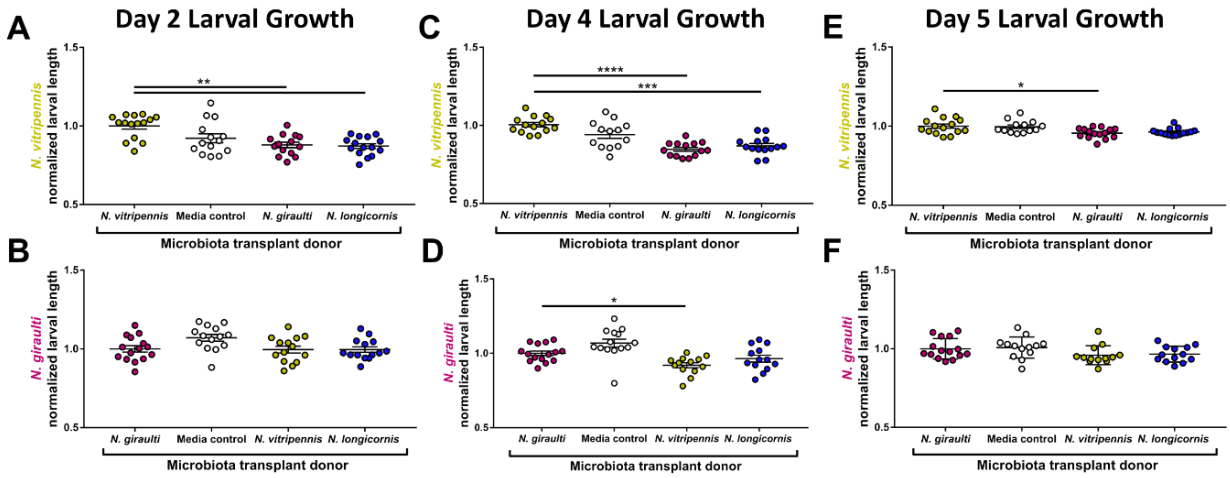

Figure V-2. Allochthonous microbiota transplants delay larval development during L2/L3 instar stage transition. Normalized larval length for *N. vitripennis* and *N. girault* germ-free recipients of heat-inactivated microbiota transplants on (A-B) the 2nd day of larval growth before the 2nd-3rd instar transition, (C-D) the 4th day at peak larval growth, and (E-F) the 5th day of larval growth just before pupation. X-axis titles represent the different microbiota transplant donor experimental groups. *p < 0.05, **p < 0.01, ***p < 0.001 and ****p < 0.0001, Kruskal Wallis test with Dunn's multiple correction. All error bars represent mean ± SEM (N=13-15).

To determine whether these larval length differences persisted outside of the peak larval growth, the effects of the microbiota transplants were observed on the 5th day of larval development. The difference in normalized larval length was greatly diminished in the autochthonous and allochthonous microbiota transplants into *N. vitripennis* larvae with only a slight significant difference between the autochthonous transplant and the allochthonous transplant from a *N. girault* donor ($p<0.05$). In *N. girault* larvae, there were no significant differences in normalized larval length on the 5th day of development. These differences in larval length resulted in a significant difference in the survival of late stage *N. vitripennis* larvae between the autochthonous transplant and the allochthonous transplant from an *N. girault* donor measured on the last day of larval development, which was not observed in *N. girault* recipients (data not shown).

Nasonia pupation is impacted by allochthonous microbiota transplants

In both the *N. vitripennis* and *N. girault* lifecycle, pupation and metamorphosis occurs over a 5-day window before the start of adult eclosion in the germ-free rearing methodology. It is important to note that at this stage in development, the *Nasonia* do not receive any more microbiota

transplants. On the 5th day of pupation for both *Nasonia sp.* recipients, the proportion of pupae in each transwell was normalized across the different treatment groups in comparison to the autochthonous microbiota transplant. For *N. vitripennis* pupae, the first eight days of transplantation during larval development resulted in significant decreases in larval pupation in the allochthonous microbiota treatment groups compared to the autochthonous treatment group, which was not observed in the buffer control group (Figure V-3A). For *N. giraulti* pupae, there was a significant decrease in larval pupation, but only between the autochthonous transplant group and the allochthonous transplant group with the more distantly diverged *N. vitripennis* donors (Figure V-3B). While there was a large drop in pupation of the allochthonous transplant group from *N. longicornis* donors, this decrease was not significant.

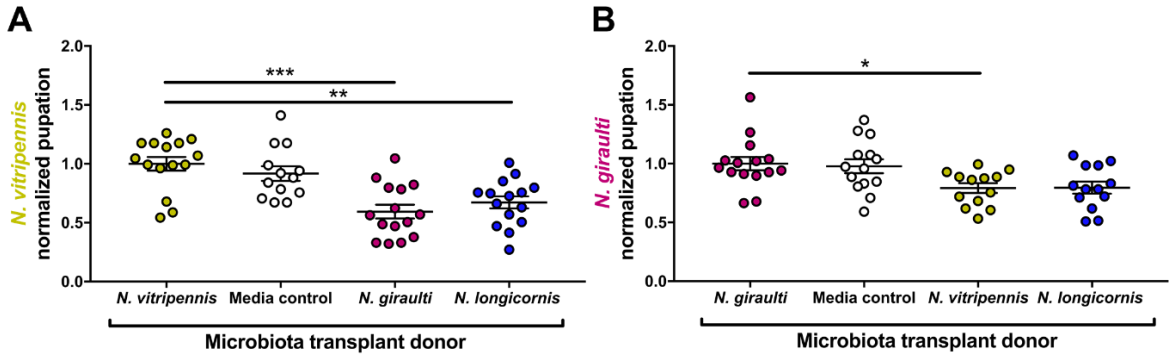

Figure V-3. Developmental delays from allochthonous transplants result in decreased overall pupation. Normalized proportion of pupated larvae on the last day of pupation before adult eclosion for (A) *N. vitripennis* and (B) *N. giraulti* germ-free recipients of heat-inactivated microbiota transplants. *p < 0.05, **p < 0.01, and ***p < 0.001, Kruskal Wallis test with Dunn's multiple correction. All error bars represent mean ± SEM (N=13-15).

Adult reproductive capacity is not altered by microbiota transplantation

Utilizing the more pronounced changes in larval growth and pupation from *N. vitripennis* wasps, adult males were moved to sterile mating chambers within 24 hours after eclosion. The males from the different treatment groups were collected individually and mated to conventional *N. vitripennis* females. The reproductive capacity of these *Nasonia* males was measured by observing their fertility and longevity after mating. Male fertility was observed by analyzing the female/male ratio for the resulting offspring since in *Nasonia* only fertilized embryos are female. Male longevity was recorded as the amount of time in hours the males survived after mating. Considering a typical conventional *Nasonia* female/male sex ratio of ~0.9, there was no effect of the different microbiota transplants on male fertility (Figure V-4A). There was a slight decrease in

the longevity of the allochthonous transplant from an *N. giraulti* donor, but this difference was not significant (Figure V-4B).

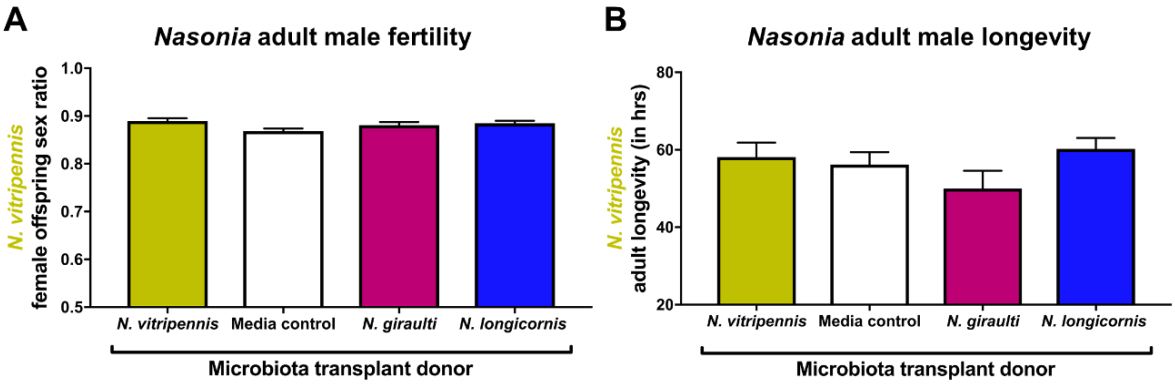

Figure V-4. Adult male reproductive capacity is not affected by allochthonous transplantation. (A) Adult male fertility is measured based on the female offspring sex ratio, which is normally maintained at ~0.9 in conventional *N. vitripennis* rearing (Whiting 1967). Because of *Nasonia*'s haplodiploidy, a drop in this ratio represents a decrease in fertility. (B) Adult male longevity is measured in the hours of *Nasonia* survival after mating with a conventional female, checked in 12-hour increments. Statistics were performed using the Kruskal Wallis test with Dunn's multiple correction. All error bars represent mean ± SEM (N=20-45).

Discussion

Previously, a host evolutionary component to the phylosymbiosis concept was demonstrated with transplantation of microbial communities from more evolutionarily distant hosts creating pronounced reductions in *Nasonia* adult survival (CHAPTER III). This result supports the idea that, within the *Nasonia* clade, three of the four wasp species have evolved specifically with their own gut microbiota, diverging away from interactions with gut microbiotas from closely-related sister species. However, the specific processes that drive the adaptations of particular *Nasonia* wasp species to their gut microbiota was still poorly defined. Were *Nasonia* wasps adapting to nutrition benefits conferred by the microbiota, a microbial signaling pathway beneficial to metamorphosis, or an immune tolerizing pathway?

Here, we report that the detrimental impact of the allochthonous microbiota transplants begins early in larval development. After one day of treatment with the heat-inactivated allochthonous microbiota, growth delays were evident in *N. vitripennis* wasps during the point in larval development when the greatest growth occurs in control wasps. Interestingly, in late larval development, the effect of the transplants was reduced as larval size equilibrated across the different treatment groups going into the 4th larval instar, although there was a significant decrease

in larval survival of the *N. vitripennis* recipients with the allochthonous transplant from the *N. giraulti* donor. Without continued transplants past the larval development stage, *N. vitripennis* larvae were still significantly less likely to undergo pupation if they received allochthonous transplants as larvae. Conversely, allochthonous microbiota transplantation had only a minor detrimental impact to larvae and pupae from the more recently diverged species in the *Nasonia* clade, *N. giraulti*. The significant reductions in development and pupation only occurred with transplants from their more distantly diverged sister species, *N. vitripennis* (~ 1 mya), but not from the more closely related species, *N. longicornis* (~400 kya). This disparity in *N. giraulti* development between the microbiota donors could shed light into the evolutionary timescale in which *Nasonia* wasps begin to adapt to their microbiota.

Because the *Nasonia* wasps were transplanted with a normalized concentration of heat-inactivated microbiota, there is little chance that the negative effects from an allochthonous microbiota transplant resulted from reduced nutrition conferred by the heat-inactivated microbiota. This conclusion is also validated since the buffer-treated larvae remained microbe-free and showed no significant decreases in growth or pupation. While microbial signaling to the host may be a possible mechanism for the growth delays, decreased pupation, and decreased larval survival from allochthonous microbiota transplants, we hypothesize that greater immune tolerance to autochthonous vs. allochthonous microbiota transplants caused *Nasonia spp.* to adapt to their species microbial community. During larval development, the largest effects of the allochthonous transplants occurred during the time when most of the larval energy supply is being utilized on growth and storage. Any shunting of that energy flow into an activated immune response would stunt growth, which was seen in Figure V-2. It has previously been studied in *Drosophila* that introduction of pathogenic *Providencia spp.* and other pathogens can result in delayed larval growth and survival (Olcott et al. 2010; Galac and Lazzaro 2012). Moreover, in *Drosophila*, larvae that are unable to achieve adequate stores of lipids and other nutrients will be less likely to complete an energy-costly pupation (Merkley et al. 2011; Arrese and Soulages 2010). However, additional experimentation is necessary to compare immune gene expression of key antibacterial pathways such as Toll and IMD to show that allochthonous microbiota transplants upregulate an immune response during larval development.

Because of the limiting nature of the heat-inactivated transplant model, it is still possible that other mechanisms play a role in the adaptation of a wasp host to its microbiota. While there

was no significant impact to adult reproductive capacity from the heat-inactivated transplants, it is known that the microbiota has a role in adult behavior and mating (Shropshire and Bordenstein 2016). While the heat-inactivated transplant methodology has highlighted a potential for immune tolerization of the host towards its microbiota, there may be other host adaptations at work that can only be observed using live bacterial communities. Unfortunately, the current germ-free rearing technique for *Nasonia* make stable microbiota transplantation difficult to maintain. Because antibiotics and exogenous FBS were removed from the methodology to maintain a more natural system, the *Proteus spp.* and *Providencia spp.* have ample nutrients and little resistance in the media to overproliferate. With both bacteria, the transwell insert begins to overgrow within the first 8 hours after transplantation. The issue lies with the media remaining as a stagnant pool within the transwell during *Nasonia* development. One possibility to keep the transplanted bacteria in check from overgrowth would be to create a dynamic rearing system using a microfluidic set up to flow the *Nasonia* rearing media through larval growth chambers. This method of germ-free *Nasonia* rearing is currently being tested at the Brucker lab and could be available for public use in the near future (personal communication).

Conclusion

Overall, we have provided a more detailed approach to determining the mechanisms that cause the functional effects of phylosymbiosis in *Nasonia* wasps. This study suggests that potential host immune responses interacting with the heat-inactivated microbiota transplants in the larval stage influence the resulting decreased development and survival of *Nasonia*. However, further studies utilizing live microbiota transplantations will be necessary to probe the host-microbiota interactions that could not be interrogated here such as developmental signaling, nutrition and digestion, and behavioral processes. These transplantation studies in *Nasonia* wasps and other animals with phylosymbiotic structuring will help to elucidate the mechanisms by which animals adapt and evolve to their respective gut microbial communities.

CHAPTER VI. CONCLUSIONS AND FUTURE DIRECTIONS

Nasonia wasps act as a promising model to interrogate the influence of host-microbe interactions within an eco-evolutionary framework because of their recent evolutionary divergence and experimental tractability. In the previous chapters, *Nasonia* interactions with their resident endosymbiont, *Wolbachia* and microbiota communities had an impact on host evolution. Within this thesis, I demonstrate how a single *Wolbachia* strain interacts with *Nasonia* wasps to influence host genome evolution through host regulation of *Wolbachia* titers. I also describe the eco-evolutionary concept of phylosymbiosis between hosts and their gut microbiota and present how a *Nasonia* wasp species may adapt to its specific microbial community following a pattern of phylosymbiosis. However, future research must be performed to answer remaining mechanisitic questions about these *Nasonia*-*Wolbachia* and *Nasonia*-microbiota interactions to determine the specific biological pathways by which these evolutionary processes emerge. Some of these ongoing and future studies will be discussed in this final chapter.

Investigating the mechanisms by which Wds suppresses *Wolbachia* densities during maternal transmission

Induction of Wolbachia bacteriophage WOVitA

While no annotated domains were discovered in the Wds protein to elucidate potential functionality, I recently observed that *w*VitA lytic phage activity was heightened in *Nasonia* females that contain the *N. vitripennis Wds* gene (Figure VI-1). The *Wolbachia w*VitA strain has three prophage regions, and WOVitA1 actively produces lytic viral particles while the other two prophages do not contain a full complement of lytic machinery (Kent et al. 2011). Interestingly, the *Wolbachia w*VitA titer difference between *N. vitripennis* and *N. giraulti* described in CHAPTER II are not observed with the *Wolbachia w*VitB strain, which does not contain any lytic phages. With these findings, it is possible that the *Wds* gene suppresses *Wolbachia* densities during maternal transmission through induction of phage particles in the ovaries. Phage WO titers are significantly higher in adult female lines containing *Wds* (12.1, IntC3, 7.77). Additionally, viral purifications of each of these lines revealed phage WO particles as determined by presence of the phage WO capsid gene and absence of *Wolbachia* DNA as determined by PCR. If Wds is capable

of inducing lytic phage in *Nasonia* ovaries during oogenesis, then Wds may utilize *Wolbachia*'s bacteriophage to lyse and lower the titer of viable *Wolbachia* that can be transferred into the developing oocyte. This proposed phage induction hypothesis would support the recent and specific divergence of Wds in *N. vitripennis* compared to the rest of the *Nasonia* clade and closely related *Trichomalopsis sarcophagae* as bacteriophage lysis timing in a host is capable of rapid evolution (Wang 2006).

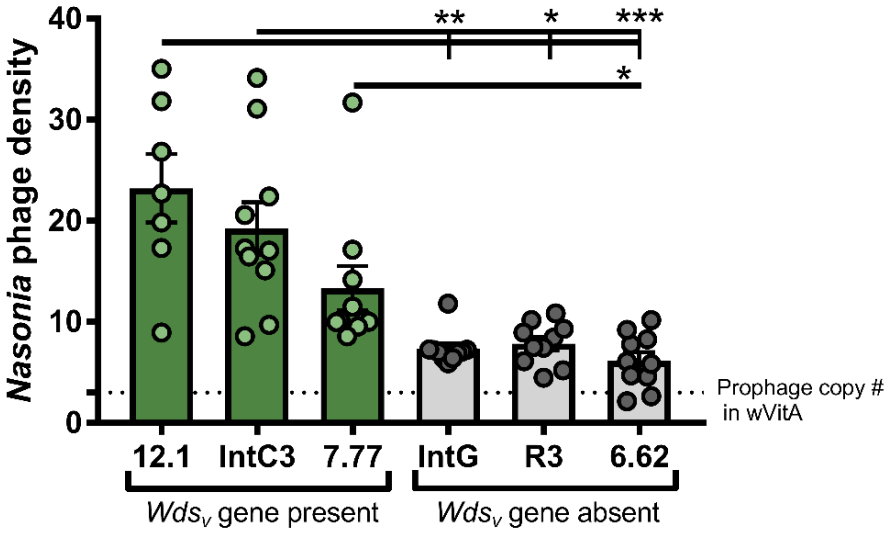

Figure VI-1. Phage WO density of *Nasonia* lines with the *N. vitripennis Wds* gene present and absent in *Nasonia* adult females. Phage densities are presented as WOVitA *orf7* copy number divided by *Wolbachia groEL* copy number. 12.1 represents a complete *N. vitripennis* genome while IntC3 and 7.77 indicate *N. vitripennis* introgressions into the *N. giraulti* genome containing the *Wds* gene. IntG represents a complete *N. giraulti* genome while R3 and 6.62 indicate *N. vitripennis* introgressions into the *N. giraulti* genome absent of the *Wds* gene. The dotted line represented the three prophages present in the *Wolbachia* genome. $^{*}p < 0.05$, $^{**}p < 0.01$ and $^{***}p < 0.001$, Kruskal Wallis test with post hoc Dunn's multiple comparisons test. All error bars represent mean ± SEM (N=10).

To link Wds to phage induction, *Wds* gene knockdown experiments need to be repeated in the 32-gene *N. vitripennis* introgression line so *Wds* knockdown efficiency can be correlated to phage WO and *Wolbachia* titers from *Nasonia* ovaries, in addition to the offspring embryo titers, using qPCR amplification. Localization of Wds within the *Nasonia* ovaries will provide further insight into its mechanism of *Wolbachia* density suppression. While phage induction is a hypothesized mechanism, future studies can determine whether Wds interacts directly or indirectly with *Wolbachia* in the ovaries. It may be possible that Wds induces lytic phages by directly interacting with *Wolbachia* or indirectly by producing a stressed environment for the *Wolbachia*

in the ovaries. Therefore, a Wds antibody will be made to visualize the role of Wds during oogenesis and determine possible mechanisms of phage WO induction and *Wolbachia* density suppression through mass spectrometry of bound ligands.

Cytoskeletal transport of wVitA into the developing oocyte

As cytoskeletal trafficking plays a large role in transferring *Wolbachia* between nurse cells and the oocyte (Ferree et al., 2005), the potential for Wds as a regulator of this pathway in *Nasonia* also needs to be further explored. To investigate the role of cytoskeletal transport during oogenesis in regulating *w*VitA densities, microtubule or actin depolymerizing drugs like colchicine and cytochalasin-D could be used to disrupt the cytoskeletal networks. The mechanisms of Wds in *Wolbachia* density suppression can then be sorted into interactions within the nurse cells or during and after transport into the oocyte based on visualization of nurse cell *Wolbachia* titers. These observations can be made by using the anti-hsp60 antibody which stains for *Wolbachia* (Serbus and Sullivan 2007).

Wds specificity in regulating Wolbachia titers

Changes in *Wolbachia* titer occurred only when *w*VitA was transferred from *N. vitripennis* to *N. giraulti*, but not through the transfer of *w*VitB (Chafee et al. 2011). With the discovery of Wds as a suppressor of *Wolbachia* titers, no study has yet observed whether Wds exhibits specificity for regulating *w*VitA titers while excluding other *Wolbachia* strains such as *w*VitB, *w*GirA, and *w*GirB. In Figure VI-2, a preliminary study indicated that *Wds* knockdown in *N. vitripennis* line 12.1 containing *w*VitA significantly increased embryonic *Wolbachia* titers while the *w*VitB-containing *N. vitripennis* line 4.9 did not.

This result may support the specificity of Wds for regulating only *w*VitA titers; however more studies are needed. Importantly, these two *N. vitripennis* lines were derived from a dual *w*VitA/*w*VitB-infected line R511, which can more clearly answer the question of Wds specificity if included in future experiments. *Wolbachia* strain specific primers for qPCR could be used to differentiate whether Wds will still suppress titers of only *w*VitA if both *Wolbachia* strains are present in the same host or if there is a synergistic effect in dual infection lines.

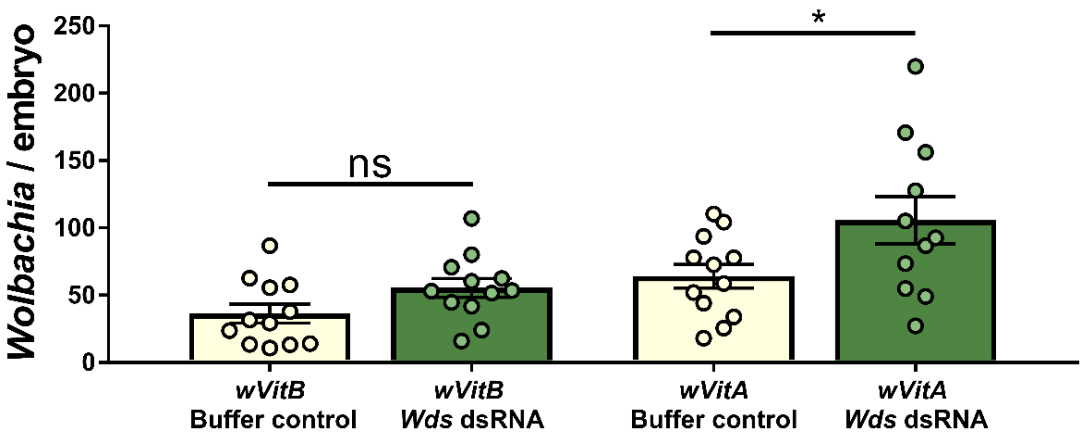

Figure VI-2. *Wdsv* knockdown increased embryonic *w*VitA but not *w*VitB *Wolbachia* titers. Number of *w*VitB and *w*VitA *Wolbachia* per embryo from *Nasonia vitripennis* 4.9 and 12.1 females, respectively, that were buffer injected or injected with dsRNA against Wds_v. $^*p < 0.05$, MWU test. All error bars represent mean ± SEM (N=12).

Predicting new candidate genes on chromosome 2

While the gene candidate *Wds* on chromosome 3 was validated for suppression of *Wolbachia* density, candidate genes in the chromosome 2 quantitative trait loci (QTL) described in CHAPTER II have yet to be fully explored. Iterative introgressions of the *N. vitripennis* chromosome 2 QTL into a *N. giraulti* background were previously performed to narrow down the genomic region associated with *Wolbachia* density suppression. However, these attempts to create heterozygous chromosome 2 introgression lines (assisted by undergraduate student Ananya Sharma) produced a 400-gene *N. vitripennis* introgression region with no significant *Wolbachia* density suppression. We also found that a hybrid incompatibility exists between the *N. vitripennis* introgression region and the *N. giraulti* genome resulting in behavioral sterility where all homozygous females and some heterozygous females failed to parasitize their *S. bullata* host. This sterily affected the stability of heterozygous lines and prevented generation of homozygous introgression lines. Because of these issues, the methodology from CHAPTER II can not be applied in the same fashion to study chromosome 2 introgression lines. Future experiments will need to introgress the flanking *N. vitripennis* genomic regions from the 400 gene region that lie within the chromosome 2 QTL region. By testing these flanking regions, we may determine the *N. vitripennis* genomic region associated with *Wolbachia* density suppression that bypasses any hybrid incompatibility regions causing behavioral sterility.

Exploring mechanisms for *Nasonia* adaptation to their microbiota

Immune response changes from microbiota transplantations

As stated in CHAPTER V, the altered larval development from allochthonous microbiota transplants is hypothesized to occur from the diverged *Nasonia spp.* adapting their immune response to their own specific gut microbial communities. In order to test this hypothesis, larvae from the different microbiota transplant groups need to be collected across different time points. The RNA expression of key immune response regulators such as *Toll* genes, *Imd*, *Pgrp* genes, serine protease genes, and antimicrobial peptides would then need to be measured through qRT-PCR. Because the effects of allochthonous transplants were observed as late in development as adult survival, the expression of these immune genes should be measured through late pupation. The four-day old larvae should be measured for immune response gene expression since this day coincides with the peak growth of *Nasonia* larvae. Depending on the gene expression results between the transplantation groups, we can also test whether chemical inhibitors of the immune response could prevent the larval growth lag, decreased pupation, and decreased adult survival observed from allochthonous transplantation.

Investigation of vertical transmission of Nasonia microbiota

While the microbiota community profiles of the *Nasonia spp.* and *S. bullata* were shown in CHAPTER I, it is difficult to pinpoint the mode of transmission for these bacteria beyond intracellular symbionts such as *Wolbachia*. It is still unknown whether the high abundance of *Proteus* and *Providencia* bacteria found in *Nasonia* larvae are vertically or horizontally transmitted. Understanding the mechanism by which these abundant microbes are aquired by the host would aid in determining how *Nasonia* may adapt to specific gut microbiota over time. Vertical transmission of these microbes would support the idea that a *Nasonia* species seeds a unique microbial community for their offspring that can be propagated across multiple generations. However, it has not been discounted that *Nasonia* larvae acquire their initial microbes through horizontal transmission by ingestion from their *S. bullata* host.

To better understand these transmission mechanisms, a recent postdoctoral researcher in the Bordenstein lab, Dr. Aram Mikaelyan, created a GFP-expressing *Proteus mirabilis* strain derived from a native *Nasonia* bacterial isolate. With this *Proteus* strain, we can observe the vertical transmission of a *Nasonia*-associated bacterium from mother to offspring. Until now, the

Proteus spp. from *S. bullata* pupae and *Nasonia* larvae have been too similar to compare by DNA sequencing technology. Instead, the GFP-expressing bacterial strain can be fed to *Nasonia* female adults for several days to accumulate within their body before they parasitize the *S. bullata* pupae. The resulting hatched larvae within the *S. bullata* pupae can then be tested through DNA amplification of the GFP gene or visualization to see if the GFP-expressing *Proteus* has colonized the larval gut. If the resulting larval offspring maintain the GFP-expressing *Proteus*, then a strong case can be built for an initial colonization of the larval gut by maternally-deposited bacteria. The transmission of other *Nasonia* derived bacteria could then be observed by cloning GFP into the other abundant *Nasonia* larval bacteria such as *Providenia*, and *Morganella* assuming they are genetically tractable.

Utilization of live microbiota communities in determining functional outcomes from microbiota transplantation

Adjusting the methodology for gnotobiotic rearing of Nasonia

As mentioned in CHAPTER V, the current methodology for *in vitro* rearing of germ-free *Nasonia* larvae cannot prevent overgrowth of live microbiota transplantation without the need for harsh sterilization procedures such as bleach or antibiotic treatment. Without these necessary procedures, the transwell setups result in bacterial overgrowth of the *Nasonia* rearing media within 8 hours that drastically reduce larval development and survival (personal observation). However, the need for stable transplantation of live allochthonous communities into *Nasonia* larvae is necessary to observe all of the physiological effects these gut microbial communities may have on a *Nasonia* larva during development. Only the introduction of live communities highlight how a *Nasonia* wasp species could adapt to particular microbiota communities by processes such as digestion, nutritional supplementation, developmental signaling, or mating behavior.

To circumvent the limitations of the current *in vitro* rearing method, a novel dynamic method involving microfluidics created in the Brucker lab (former Bordenstein postdoctoral researcher, currently at Harvard University) could be utilized to prevent the overgrowth of bacteria from live microbiota transplantation. In this methodology, a series of microfluidic chambers housing a single germ-free *Nasonia* larva are continuously supplied with a steady flow of *Nasonia* rearing media that exits through an outflow port, similar to a chemostat. With constant flowthrough of the *Nasonia* rearing media, there is a much lower chance for bacterial overgrowth to occur and

would allow us to sample the microbial community exiting the larval growth chamber. In this system, live microbiota transplantations could be added and passed through the larval growth chamber at specific times of development. This new microfluidic technology will be assessed for feasibility with microbiota transplantation by introducing GFP-expressing *Proteus* bacteria into the larval growth chamber and visualizing the dynamics of the bacteria in this system such as where the bacteria may pool and grow outside the larvae. It can then be validated whether bacteria will get ingested by the larvae at a particular flow rate.

Visualizing Nasonia acquisition and stabilization of its microbiota members

An important aspect to the phylosymbiosis concept is that microbial transmission does not need to occur vertically for the eco-evolutionary pattern to occur, but that the host may have evolved a preference for a particular gut microbiota. If the interaction between hosts and their gut microbial communities can drive adaptation and speciation, then we might expect that there would be close, stable associations between *Nasonia* and their gut microbiota within a particular niche in the digestive tract. A *Nasonia*-derived GFP-expressing *Proteus* bacterium could be used to visualize the bacteria's niche in the larval gut and to determine whether it closely interacts with the gut epithelium. We can then create GFP-expressing bacterial strains from *Nasonia*-derived *Providencia* and *Morganella* bacteria so the three major gut microbiota members of *Nasonia* larvae could be localized. Understanding the specific gut niches of these bacterial strains in different species of *Nasonia* larvae may help us understand how *Nasonia spp.* acquire their specific gut microbiota. As the *Nasonia* larvae undergoes pupation and adult eclosion, we can also observe the changes in the presence and localization of the GFP-expressing bacteria during metamorphosis. It could be determined whether the initial bacteria acquired by the *Nasonia* larvae are maintained within the wasps until adulthood or if newly eclosed wasps reacquire their gut microbiota that result in the observed phylosymbiotic pattern.

Concluding Remarks

Since the diversification of early animals, bacteria and other microbes have expanded host functions by influencing host nutrition, development, immune recognition, behavior, and more. To better understand the impact of these host-microbe interactions on the evolution of the *Nasonia* wasp, this dissertation described two different symbioses that occur in *Nasonia*. First, the

interaction of *Nasonia* with its endosymbiont *Wolbachia* was studied to identify the genetic basis by which *Nasonia* regulate their *Wolbachia* densities. Second, interactions between *Nasonia* and their gut microbiota were studied to understand how species-specific microbiota compositions are assembled. The research presented here: (1) determined a new function for a previously uncharacterized *Nasonia* gene that acts to regulate maternal *Wolbachia* transmission, (2) supported the pattern of phylosymbiosis through studies on the *Nasonia* clade and several other animal clades, and (3) added new insight into a potential mechanism for *Nasonia*'s adaptation to its gut microbiota.

While binary symbiotic relationships between animal hosts and individual microbial symbionts are well documented, in the case of arthropods and their *Wolbachia* endosymbiont, not much is known about how the host counteracts the effects of this reproductive parasite. Across diverse arthropod species, *Wolbachia* primarily utilize vertical transmission through the maternal germline for propagation in animal populations. Previous research into *Wolbachia* maternal transmission elucidated mechanisms that can influence *Wolbachia* densities such as embryonic axis determination with *gurken* or actin cytoskeletal transport with *profilin*. However, these studies did not consider the natural variation existing between different arthropod-*Wolbachia* interactions that can shed light on the evolution of these associations.

One component still missing from the study of this association is *Wolbachia*'s bacteriophage WO since bacteriophages can be a significant force of genomic evolution in bacteria. The fast rates of recombination in some phage WO regions and the ability to undergo the lytic cycle may be an understudied source of variation that drive rapid evolutionary change in *Wolbachia* strains and their associations with specific host species. The *Wolbachia* field needs to further study the role of bacteriophages in host-endosymbiont interactions, particularly with the recent knowledge that phage genomes contain genes with eukaryotic functions. Bacteriophages may also be influential in the regulation of many other host-microbe associations that warrants future research. Overall, *Wolbachia* maternal transmission acts as a targetable bottleneck in controlling *Wolbachia* densities and phenotypes in a wide variety of arthropods, so deciphering the mechanisms involved could prove useful in regulating *Wolbachia*'s effectiveness as a pest or disease vector control. The use of *Wolbachia* strains in mosquito vector control could also benefit from a better understanding of the mechanisms that control *Wolbachia* density, particularly since *Wolbachia*'s CI phenotype is dependent on maintaining the bacteria at specific densities.

Shifting from binary symbiotic relationships to interactions between animal hosts and their microbial communities, phylosymbiosis proposes a host-specific assembly of the microbiota in which microbiota compositional similarity reflects host evolutionary history. While phylosymbiosis was tested through lab-controlled studies in this dissertation, subsequent studies have observed phylosymbiosis in natural systems where environmental components may play a larger role in microbiota assembly. However, future studies are necessary to observe how common phylosymbiosis is among animals. There could be required animal features that cause certain animal taxa to show phylosymbiosis while others do not. For example, do variables such as habitat types, gut physiology, pH, or eusociality associate with the occurrence or breakdown of phylosymbiosis? Further pairing of lab and environmental studies could then reveal what changes in microbiota composition occur due to the aforementioned variables. These studies are necessary to understand the interplay of environment, diet, and genetics in guiding the assembly of a host-specific microbiota across diverse animal systems.

To understand the biological impact of phylosymbiosis, *Nasonia* microbiota transplantation assays demonstrated that there is reduced host performance when a germ-free recipient received a microbiota from a closely related species. This result supports a host adaptation to its microbiota, but future transplantation assays are needed to determine the host traits that are selected for or have undergone drift in response to a host-specific microbiota. While immunologic and metabolic pathways are likely targets, there may be other host processes that drive host-specific microbiota assembly. Another question is whether the host adapts to particular bacterial taxa or biochemical pathways found in the microbial community. Transplantation experiments that follow host colonization of different microbiota transplants would determine whether a host acquires shared bacterial taxa or functional pathways from these transplants. As the field begins to understand how host performance can be influenced by the microbiota, there will be direct implications in healthcare, particularly in utilizing microbiota profiles to predict and diagnose human health. For example, the combination of human and micriobiome variation can provide a more personalized approach to medicine and expand the potential targets available for drug intervention.

REFERENCES

Agler MT, Ruhe J, Kroll S, Morhenn C, Kim ST, Weigel D, et al (2016). Microbial hub taxa link host and abiotic factors to plant microbiome variation. *PLoS Biol*. 14:e1002352.

Alegado RA, Brown LW, Cao S, Dermenjian RK, Zuzow R, Fairclough SR, et al (2012). A bacterial sulfonolipid triggers multicellular development in the closest living relatives of animals. *eLife*. 1:e00013.

Alende N, Nielsen JE, Shields DC, and Khaldi N (2011). Evolution of the isoelectric point of mammalian proteins as a consequence of indels and adaptive evolution. *Proteins* 79, 1635-1648.

Andert J, Marten A, Brandl R, and Brune A (2010). Inter- and intraspecific comparison of the bacterial assemblages in the hindgut of humivorous scarab beetle larvae (*Pachnoda* spp.). *FEMS Microbiol. Ecol.* 74, 439–449.

Arrese EL and Soulages JL (2010). Insect fat body: energy, metabolism, and regulation. *Annu Rev Entomol.* 55:207-225.

Ashmead WH and Smith HH (1904). Classification of the Chalcid Flies: or the superfamily Chalcidoidea, with descriptions of new species in the Carnegie Museum, collected in South America by Herbert H. Smith. Memoirs of the Carnegie Museum. 1:311–318.

Baeder JM and King BH (2004). Associative learning of color by males of the parasitoid wasp *Nasonia vitripennis* (Hymenoptera: Pteromalidae) *Journal of Insect Behavior*. 17:201–213.

Bakula M (1969). The persistence of a microbial flora during postembryogenesis of *Drosophila melanogaster*. *J. Invertebr. Pathol.* 14, 365–374.

Baxter NT, Wan JJ, Schubert AM, Jenior ML, Myers P, and Schloss PD (2015). Intra- and interindividual variations mask interspecies variations in the microbiota of sympatric *Peromyscus* populations. *Appl Environ Microbiol*. 81:396-404.

Beeler SM, Wong GT, Zheng JM, Bush EC, Remnant, EJ, Oldroyd BP, et al (2014). Whole-genome DNA methylation profile of the jewel wasp (*Nasonia vitripennis*). *G3 (Bethesda)* 4, 383–388.

Bertossa RC, van Dijk J, Diao W, Saunders D, Beukeboom LW, and Beersma DG (2013). Circadian rhythms differ between sexes and closely related species of *Nasonia* wasps. *PLoS ONE* 8:e60167.

Beukeboom LW and Van den Assem J (2001). Courtship and mating behaviour of interspecific *Nasonia* hybrids (Hymenoptera, Pteromalidae): a grandfather effect. Behavioral *Genetics.* 31:167–177.

Beukeboom LW and van de Zande L (2010). Genetics of sex determination in the haplodiploid wasp *Nasonia vitripennis* (Hymenoptera: Chalcidoidea). *J. Genet.* 89, 333–339.

Bian, G., Zhou, G., Lu, P., and Xi, Z. (2013). Replacing a native *Wolbachia* with a novel strain results in an increase in endosymbiont load and resistance to dengue virus in a mosquito vector. *PLoS Negl Trop Dis* 7, e2250.

Blaser MJ (2014). The microbiome revolution. *J. Clin. Invest.* 124, 4162–4165.

Blaul B and Ruther J (2012). Body size influences male pheromone signals but not the outcome of mating contests in *Nasonia vitripennis*. *Animal Behaviour*. 84:1557–1563.

Blekhman R, Goodrich JK, Huang K, Sun Q, Bukowski R, Bell JT, et al (2015). Host genetic variation impacts microbiome composition across human body sites. Genome Biol. 16:191.

Bogdanowicz D, Giaro K, and Wróbel B (2012). TreeCmp: comparison of trees in polynomial time. *Evol Bioinform Online*. 8:475.

Bogdanowicz D and Giaro K (2013). On a matching distance between rooted phylogenetic trees. *Int J Appl Math Comp Sci*. 23:669-84.

Boot R, Koopman JP, Kruijt BC, Lammers RM, Kennis HM, Lankhorst A, et al (1985). The 'normalization' of germ-free rabbits with host-specific caecal microflora. *Lab Anim*. 19:344-52.

Bordenstein SR and Werren JH (1998). Effects of A and B *Wolbachia* and host genotype on interspecies cytoplasmic incompatibility in *Nasonia*. *Genetics* 148, 1833–1844.

Bordenstein SR, O'Hara FP, and Werren JH (2001). *Wolbachia*-induced incompatibility precedes other hybrid incompatibilities in *Nasonia*. *Nature*. 409:707-710.

Bordenstein SR, Uy JJ, and Werren JH (2003). Host genotype determines cytoplasmic incompatibility type in the haplodiploid genus *Nasonia*. *Genetics* 164, 223–233.

Bordenstein SR and Wernegreen JJ (2004). Bacteriophage flux in endosymbionts (*Wolbachia*): infection frequency, lateral transfer, and recombination rates. *Mol. Biol. Evol.* 21, 1981–1991.

Bordenstein SR, Marshall ML, Fry AJ, Kim U, and Wernegreen JJ (2006). The tripartite associations between bacteriophage, *Wolbachia*, and arthropods. *PLoS Pathog*. 2, e43.

Bordenstein SR and Werren JH (2007). Bidirectional incompatibility among divergent *Wolbachia* and incompatibility level differences among closely related *Wolbachia* in *Nasonia*. *Heredity*. 99:278–287.

Bordenstein SR and Bordenstein SR (2011). Temperature affects the tripartite interactions between bacteriophage WO, *Wolbachia*, and cytoplasmic incompatibility. *PLoS One* 6, e29106.

Bordenstein SR and Theis KR (2015). Host biology in light of the microbiome: ten principles of holobionts and hologenomes. *PLoS Biol*. 13:e1002226.

Bordenstein SR and Bordenstein SR (2016). Eukaryotic association module in phage WO genomes from *Wolbachia*. *bioRxiv*.

Braquart-Varnier C, Lachat M, Herbinière J, Johnson M, Caubet Y, Bouchon D, et al (2008). *Wolbachia* mediate variation of host immunocompetence. *PLoS ONE* 3:e3286.

Breeuwer JA and Werren JH (1990). Microorganisms associated with chromosome destruction and reproductive isolation between two insect species. *Nature* 346, 558–560.

Breeuwer JA, Stouthamer R, Barns SM, Pelletier DA, Weisburg WG, and Werren JH (1992). Phylogeny of cytoplasmic incompatibility microorganisms in the parasitoid wasp genus *Nasonia* (Hymenoptera: Pteromalidae) based on 16S ribosomal DNA sequences. *Insect Mol. Biol.* 1, 25–36.

Breeuwer JA and Werren JH (1993a). Cytoplasmic incompatibility and bacterial density in *Nasonia vitripennis*. *Genetics* 135, 565–574.

Breeuwer JA and Werren JH (1993b). Effect of genotype on cytoplasmic incompatibility in two species of *Nasonia*. *Heredity* 70, 428–436.

Breeuwer JA and Werren JH (1995). Hybrid breakdown between two haplodiploid species: the role of nuclear and cytoplasmic genes. *Evolution* 49, 705–717.

Broman KW, Wu H, Sen S, and Churchill GA (2003). R/qtl: QTL mapping in experimental crosses. *Bioinformatics* 19, 889-890.

Brooks AW. Data Availability: Dryad Digital Repository. GitHub.

Brownlie JC, Cass BN, Riegler M, Witsenburg JJ, Iturbe-Ormaetxe I, McGraw EA, et al (2009). Evidence for metabolic provisioning by a common invertebrate endosymbiont, *Wolbachia pipientis*, during periods of nutritional stress. *PLoS Pathog.* 5:e1000368.

Brucker RM, Bordenstein SR (2012a). The roles of host evolutionary relationships (genus: *Nasonia*) and development in structuring microbial communities. *Evol.* 66:349-62.

Brucker RM and Bordenstein SR (2012b). *In vitro* cultivation of the hymenoptera genetic model, *Nasonia*. *PLoS ONE*. 7:e2316.

Brucker RM and Bordenstein SR (2012c). Speciation by symbiosis. *Trends in Ecology & Evolution*. 27:443–451.

Brucker RM and Bordenstein SR (2013). The hologenomic basis of speciation: gut bacteria cause hybrid lethality in the genus *Nasonia*. *Science*. 341:667–669.

Buchner P (1965). *Endosymbiosis of Animals with Plant Microorganisms.* New York, NY: Interscience Publishers.

Buellesbach J, Gadau J, Beukeboom LW, Echinger F, Raychoudhury R, Werren JH, and Schmitt T (2013). Cuticular hydrocarbon divergence in the jewel wasp *Nasonia*: evolutionary shifts in chemical communication channels? *Journal of Evolutionary Biology*. 26:2467–2478.

Burns AR, Stephens WZ, Stagaman K, Wong S, Rawls JF, Guillemin K, et al (2015). Contribution of neutral processes to the assembly of gut microbial communities in the zebrafish over host development. *ISME Journal*. 10:655-64.

Calderone RA and Fonzi WA (2001). Virulence factors of Candida albicans. *Trends Microbiol* 9, 327-335.

Campbell BC, Steffen-Campbell JD, and Werren JH (1993). Phylogeny of the Nasonia species complex (Hymenoptera: Pteromalidae) inferred from an internal transcribed spacer (ITS2) and 28S rDNA sequences. *Insect Mol Biol* 2, 225-237.

Candela M, Perna F, Carnevali P, Vitali B, Ciati R, Gionchetti P, Rizzello F, Campieri M, and Brigidi P (2008). Interaction of probiotic Lactobacillus and Bifidobacterium strains with human intestinal epithelial cells: adhesion properties, competition against enteropathogens and modulation of IL-8 production. *Int J Food Microbiol* 125, 286-292.

Caporaso JG, Kuczynski J, Stombaugh J, Bittinger K, Bushman FD, Costello EK, et al (2010). QIIME allows analysis of high-throughput community sequencing data. Nat Method. 7:335-6.

Caragata EP, Rances E, O'Neill SL, and McGraw EA (2014). Competition for amino acids between *Wolbachia* and the mosquito host, Aedes aegypti. *Microb Ecol* 67, 205-218.

Cariveau DP, Elijah Powell J, Koch H, Winfree R, and Moran NA (2014). Variation in gut microbial communities and its association with pathogen infection in wild bumble bees (Bombus). *ISME J.* 8, 2369–2379.

Carmody RN, Gerber GK, Luevano JM, Gatti DM, Somes L, Svenson KL, et al (2015). Diet dominates host genotype in shaping the murine gut microbiota. Cell Host & Microbe. 17:72-84.

Chafee ME, Funk DJ, Harrison RG, and Bordenstein SR (2010). Lateral phage transfer in obligate intracellular bacteria (*Wolbachia*): verification from natural populations. *Mol. Biol. Evol.* 27, 501–505.

Chafee ME, Zecher CN, Gourley ML, Schmidt VT, Chen JH, Bordenstein SR, and Clark ME (2011). Decoupling of host-symbiont-phage coadaptations following transfer between insect species. *Genetics* 187, 203-215.

Chandler JA, Lang JM, Bhatnagar S, Eisen JA, Kopp A (2011). Bacterial communities of diverse Drosophila species: ecological context of a host-microbe model system. PLoS Genet. 7:e1002272.

Chaston JM, Dobson AJ, Newell PD, Douglas AE (2016). Host genetic control of the microbiota mediates the *Drosophila* nutritional phenotypes. Appl Environ Microbiol. 82:671-9.

Chu H and Mazmanian SK (2013). Innate immune recognition of the microbiota promotes host-microbial symbiosis. *Nat. Immunol.* 14, 668–675.

Chung H, Pamp SJ, Hill JA, Surana NK, Edelman SM, Troy EB, Reading NC, Villablanca EJ, Wang S, Mora JR, Umesaki Y, Mathis D, Benoist C, Relman DA, and Kasper DL (2012). Gut immune maturation depends on colonization with a host-specific microbiota. *Cell*. 149(7):1578-93.

Clark AG, Eisen MB, Smith DR, Bergman CM, Oliver B, Markow TA, et al (2007). Evolution of genes and genomes on the *Drosophila* phylogeny. Nature. 450:203-18.

Clark ME, O'Hara FP, Chawla A, Werren JH (2010). Behavioral and spermatogenic hybrid male breakdown in *Nasonia*. Heredity.104:289–301.

Cline MS, Smoot M, Cerami E, Kuchinsky A, Landys N, Workman C, et al (2007). Integration of biological networks and gene expression data using Cytoscape. Nat Protoc. 2:2366-82.

Colman DR, Toolson EC, and Takacs-Vesbach CD (2012). Do diet and taxonomy influence insect gut bacterial communities? *Mol. Ecol.* 21, 5124–5137.

Corby-Harris V, Maes P, and Anderson KE (2014). The bacterial communities associated with honey bee (*Apis mellifera*) foragers. *PLoS ONE* 9:e95056.

Costello EK, Stagaman K, Dethlefsen L, Bohannan BJM, Relman DA (2012). The application of ecological theory toward an understanding of the human microbiome. Science. 336:1255-1262.

Danneels EL, Gerlo S, Heyninck K, Van Craenenbroeck K, De Bosscher K, Haegeman G, et al (2014). How the venom from the ectoparasitoid Wasp *Nasonia* vitripennis exhibits anti-inflammatory properties on mammalian cell lines. *PLoS ONE* 9:e96825.

Darling DC and Werren JH (1990). Biosystematics of *Nasonia* (Hymenoptera: Pteromalidae): two new species reared from birds' nests in North America. *Ann. Entomol. Soc. Am.* 83, 352–370.

Darriba D, Taboada GL, Doallo R, Posada D (2012). jModelTest 2: more models, new heuristics and parallel computing. *Nat Method*. 9:772.

Davenport ER (2016). Elucidating the role of the host genome in shaping microbiome composition. *Gut Microbes*. 7:178-84.

David LA, Materna AC, Friedman J, Campos-Baptista MI, Blackburn MC, Perrotta A, et al (2014). Host lifestyle affects human microbiota on daily timescales. *Genome Biol.* 15:R89.

Davies NJ and Tauber E (2015). WaspAtlas: a *Nasonia vitripennis* gene database and analysis platform. *Database* (Oxford) pii: bav103.

Dedeine F, Vavre F, Shoemaker DD, and Bouletreau M (2004). Intra-individual coexistence of a *Wolbachia* strain required for host oogenesis with two strains inducing cytoplasmic incompatibility in the wasp *Asobara tabida*. *Evolution* 58, 2167–2174.

Desjardins CA, Perfectti F, Bartos JD, Enders LS, and Werren JH (2010). The genetic basis of interspecies host preference differences in the model parasitoid *Nasonia*. *Heredity (Edinb.)* 104, 270–277.

Desjardins CA, Gadau J, Lopez JA, Niehuis O, Avery AR, Loehlin DW, Richards S, Colbourne JK, and Werren JH (2013). Fine-scale mapping of the Nasonia genome to chromosomes using a high-density genotyping microarray. *G3* 3, 205-215.

Diao W, Mousset M, Horsburgh GJ, Vermeulen CJ, Johannes F, Van de Zande L, Ritchie MG, Schmitt T, and Beukeboom LW (2016). Quantitative trait locus analysis of mating behavior and male sex pheromones in *Nasonia* wasps. *G3* 6:1549–1562.

Dietrich C, Köhler T, and Brune A (2014). The cockroach origin of the termite gut microbiota: patterns in bacterial community structure reflect major evolutionary events. *Appl Environ Microbiol*. 80:2261-9.

Dittmer J, Beltran-Bech S, Lesobre J, Raimond M, Johnson M, and Bouchon D (2014). Host tissues as microhabitats for *Wolbachia* and quantitative insights into the bacterial community in terrestrial isopods. *Mol. Ecol.* 23, 2619–2635.

Dittmer J, Lesobre J, Moumen B, and Bouchon D (2016) Host origin and tissue microhabitat shaping the microbiota of the terrestrial isopod *Armadillidium vulgare*. *FEMS Microbiol. Ecol.* 92:fiw063.

Dong Y, Manfredini F, and Dimopoulos G (2009). Implication of the mosquito midgut microbiota in the defense against malaria parasites. *PLoS Pathog.* 5:e1000423.

Douglas AE (2010). *The Symbiotic Habit.* Princeton, NJ: Princeton University Press.

Douglas AE (2015). Multiorganismal insects: diversity and function of resident microorganisms. *Annu. Rev. Entomol.* 60, 17–34.

Douglas AE and Werren JH (2016). Holes in the hologenome: why host-microbe symbioses are not holobionts. *MBio* 7:e02099.

Drapeau MD, Werren JH (1999). Differences in mating behaviour and sex ratio between three sibling species of *Nasonia*. *Evolutionary Ecology Research*. 1:223–234.

Duneau DF and Lazzaro BP (2018). Persistence of an extracellular systemic infection across metamorphosis in a holometabolous insect. *Bio Lett.* 14(2). pii: 20170771.

Duron O, Bouchon D, Boutin S, Bellamy L, Zhou L, Engelstädter J, et al (2008). The diversity of reproductive parasites among arthropods: *Wolbachia* do not walk alone. *BMC Biol.* 6:27.

Duron O, Wilkes TE, and Hurst GD (2010). Interspecific transmission of a male-killing bacterium on an ecological timescale. *Ecol. Lett.* 13, 1139–1148.

Dyer KA, Minhas MS, and Jaenike J (2005). Expression and modulation of embryonic male-killing in Drosophila innubila: opportunities for multilevel selection. *Evolution* 59, 838-848.

Easson CG, Thacker RW (2014). Phylogenetic signal in the community structure of host-specific microbiomes of tropical marine sponges. *Front Microbiol*. 5:532.

Edgar RC (2004). MUSCLE: multiple sequence alignment with high accuracy and high throughput. *Nucl Acid Res*. 32:1792-7.

Edgar RC (2010). Search and clustering orders of magnitude faster than BLAST. *Bioinformatics* 26:2460-1.

Edgar RC, Haas BJ, Clemente JC, Quince C, Knight R (2011). UCHIME improves sensitivity and speed of chimera detection. *Bioinformatics* 27:2194-200.

Eisthen HL and Theis KR (2016). Animal-microbe interactions and the evolution of nervous systems. *Philos Trans R Soc Lond B Biol Sci. 371*.

Ellison CK, Niehuis O, and Gadau J (2008). Hybrid breakdown and mitochondrial dysfunction in hybrids of *Nasonia* parasitoid wasps. *J. Evol. Biol.* 21, 1844–1851.

Emerson KJ and Glaser RL (2017). Cytonuclear epistatis controls the density of symbiont *Wolbachia pipientis* in nongonadal tissues of mosquito *Culex quinquefasciatus*. *G3 (Bethesda)*. 7(8):2627-2635.

Erdmann GR, Bromel M, Gassner G, Freeman TP, and Fischer A (1984). Antibacterial activity demonstrated by culture filtrates of Proteus mirabilis isolated from screwworm (*Cochliomyia hominivorax*) (*Diptera*: *Calliphoridae*) larvae. *J. Med. Entomol.* 21, 159–164.

Everard A, Lazarevic V, Gaïa N, Johansson M, Ståhlman M, Backhed F, et al (2014). Microbiome of prebiotic-treated mice reveals novel targets involved in host response during obesity. *ISME Journal* 8:2116-30.

Federici BA and Bigot Y (2003). Origin and evolution of polydnaviruses by symbiogenesis of insect DNA viruses in endoparasitic wasps. *J. Insect Physiol.* 49, 419–432.

Ferrari J, Darby AC, Daniell TJ, Godfray HCJ, and Douglas AE (2004). Linking the bacterial community in pea aphids with host-plant use and natural enemy resistance. *Ecol. Entomol.* 29, 60–65.

Ferree PM, Frydman HM, Li JM, Cao J, Wieschaus E, and Sullivan W (2005). *Wolbachia* utilizes host microtubules and Dynein for anterior localization in the Drosophila oocyte. *PLoS Pathog.* 1, e14.

Ferree PM, Avery A, Azpurua J, Wilkes T, and Werren JH (2008). A bacterium targets maternally inherited centrosomes to kill males in *Nasonia*. *Current Biology* 18:1409–1414.

Fisher CK and Mehta P (2014). Identifying keystone species in the human gut microbiome from metagenomic timeseries using sparse linear regression. *PLoS One* 9:e102451.

Fleury F, Vavre F, Ris N, Fouillet P, and Bouletreau M (2000). Physiological cost induced by the maternally-transmitted endosymbiont *Wolbachia* in the Drosophila parasitoid Leptopilina heterotoma. *Parasitology* 121 Pt 5, 493-500.

Franzenburg S, Walter J, Künzel S, Wang J, Baines JF, Bosch TC, et al (2013). Distinct antimicrobial peptide expression determines host species-specific bacterial associations. *Proc Natl Acad Sci*. 110:E3730-8.

Fraune S and Bosch TCG (2007). Long-term maitenance of species-specific bacterial microbiota in the basal metazoan *Hydra*. *Proc Natl Acad Sci*. 104:13146-51.

Fukuda S, Toh H, Hase K, Oshima K, Nakanishi Y, Yoshimura K, Tobe T, Clarke JM, Topping DL, Suzuki T, et al. (2011). Bifidobacteria can protect from enteropathogenic infection through production of acetate. *Nature* 469, 543-547.

Funkhouser LJ and Bordenstein SR (2013). Mom knows best: the universality of maternal microbial transmission. *PLoS Biol*. 11, e1001631.

Funkhouser-Jones LJ, van Opstal EJ, Sharma A, and Bordenstein SR (2018). The maternal effect gene *Wds* controls *Wolbachia* titer in *Nasonia*. *Current Biology* 28(11):1692-1702.

Futahashi R, Tanaka K, Tanahashi M, Nikoh N, Kikuchi Y, Lee BL, et al (2013). Gene expression in gut symbiotic organ of stinkbug affected by extracellular bacterial symbiont. *PLoS ONE* 8:e64557.

Gadau J, Page RE, and Werren JH (2002). The genetic basis of the interspecific differences in wing size in Nasonia (Hymenoptera; Pteromalidae): major quantitative trait loci and epistasis. *Genetics* 161, 673-684.

Galac MR and Lazzaro BP (2012). Comparative genomics of bacteria in the genus *Providencia* isolated from wild *Drosophila melanogaster*. *BMC Genomics* 13:612.

Gatschenberger H, Azzami K, Tautz J, and Beier H (2013). Antibacterial immune competence of honey bees (*Apis mellifera*) is adapted to different life stages and environmental risks. *PLoS ONE* 8:e66415.

Gaukler SM, Ruff JS, Galland T, Underwood TK, Kandaris KA, Liu NM, et al (2016). Quantification of cerivastatin toxicity supports organismal performance assays as an effective tool during pharmaceutical safety assessment. *Evol Appl*. 5:685-96.

Gavotte L, Vavre F, Henri H, Ravallec M, Stouthamer R, and Boulétreau M (2004). Diversity, distribution and specificity of WO phage infection in *Wolbachia* of four insect species. *Insect Mol. Biol.* 13, 147–153.

Gavotte L, Henri H, Stouthamer R, Charif D, Charlat S, Boulétreau M, et al (2007). A Survey of the bacteriophage WO in the endosymbiotic bacteria *Wolbachia*. *Mol. Biol. Evol.* 24, 427–435.

Gibson JD, Niehuis O, Peirson BR, Cash EI, and Gadau J (2013). Genetic and developmental basis of F2 hybrid breakdown in *Nasonia* parasitoid wasps. *Evolution* 67, 2124–2132.

Gilbert SF, Sapp J, and Tauber AI (2012). A symbiotic view of life: we have never been individuals. *Q. Rev. Biol.* 87, 325–341.

Goodrich JK, Waters JL, Poole AC, Sutter JL, Koren O, Blekhman R, et al (2014). Human genetics shape the gut microbiome. *Cell* 159:789-99.

Guindon S, Dufayard JF, Lefort V, Anisimova M, Hordijk W, and Gascuel O (2010). New algorithms and methods to estimate maximum-likelihood phylogenies: assessing the performance of PhyML 3.0. *Syst Biol* 59, 307-321.

Hansen AK and Moran NA (2011). Aphid genome expression reveals host-symbiont cooperation in the production of amino acids. *Proc. Natl. Acad. Sci. U.S.A.* 108, 2849–2854.

He S, Ivanova N, Kirton E, Allgaier M, Bergin C, Scheffrahn RH, et al (2013). Comparative metagenomic and metatranscriptomic analysis of hindgut paunch microbiota in wood- and dung-feeding higher termites. *PLoS ONE* 8:e61126.

Heath BD, Butcher RD, Whitfield WG, and Hubbard SF (1999). Horizontal transfer of *Wolbachia*between phylogenetically distant insect species by a naturally occurring mechanism. *Curr. Biol.* 9, 313–316.

Hilgenboecker K, Hammerstein P, Schlattmann P, Telschow A, and Werren JH (2008). How many species are infected with *Wolbachia*? - A statistical analysis of current data. *FEMS Microbiol. Lett.* 281, 215–220.

Hird SM, Sánchez C, Carstens BC, Brumfield RT (2015). Comparative gut microbiota of 59 Neotropical bird species. Front Microbiol. 6:1403.

Honn KV, Singly JA, and Chavin W (1975). Fetal Bovine Serum: a multivariate standard. *Proceedings of the Socieity for Experimental Biology and Medicine* 149:344–347.

Hooper LV and Gordon JI (2001). Glycans as legislators of host-microbial interactions: spanning the spectrum from symbiosis to pathogenicity. *Glycobiol.* 11:1-10.

Huelsenbeck, J.P., and Ronquist, F. (2001). MRBAYES: Bayesian inference of phylogenetic trees. *Bioinformatics* 17, 754-755.

Huger AM, Skinner SW, and Werren JH (1985). Bacterial infections associated with the son-killer trait in the parasitoid wasp *Nasonia* (=Mormoniella) vitripennis (Hymenoptera: Pteromalidae). *J. Invertebr. Pathol.* 46, 272–280.

Hughes GL, Dodson BL, Johnson RM, Murdock CC, Tsujimoto H, Suzuki Y, et al (2014). Native microbiome impedes vertical transmission of *Wolbachia* in Anopheles mosquitoes. *Proc. Natl. Acad. Sci. U.S.A.* 111, 12498–12503.

Huigens ME, de Almeida RP, Boons PA, Luck RF, and Stouthamer R (2004). Natural interspecific and intraspecific horizontal transfer of parthenogenesis-inducing *Wolbachia* in Trichogramma wasps. *Proc. Biol. Sci.* 271, 509–515.

Husnik F, Nikoh N, Koga R, Ross L, Duncan RP, Fujie M, et al (2013). Horizontal gene transfer from diverse bacteria to an insect genome enables a tripartite nested mealybug symbiosis. *Cell* 153, 1567–1578.

Ishmael N, Dunning Hotopp JC, Ioannidis P, Biber S, Sakamoto J, and Siozios S, et al (2009). Extensive genomic diversity of closely related *Wolbachia* strains. *Microbiology* 155, 2211–2222.

Ivanov, II, Frutos Rde, L., Manel, N., Yoshinaga, K., Rifkin, D.B., Sartor, R.B., Finlay, B.B., and Littman, D.R. (2008). Specific microbiota direct the differentiation of IL-17-producing T-helper cells in the mucosa of the small intestine. *Cell Host Microbe* 4, 337-349.

Jaenike J (2009). Coupled population dynamics of endosymbionts within and between hosts. *Oikos* 118, 353-362.

Johnston PR and Rolff J (2015). Host and symbiont jointly control gut microbiota during complete metamorphosis. *PLoS Pathology*.11:e2316.

Kambris Z, Blagborough AM, Pinto SB, Blagrove MS, Godfray HC, Sinden RE, et al (2010). *Wolbachia* stimulates immune gene expression and inhibits Plasmodium development in *Anopheles gambiae*. *PLoS Pathog.* 6:e1001143.

Kashyap PC, Macobal A, Ursell LK, Smits SA, Sonnenburg ED, Costello EK, et al (2013). Genetically dictated change in host mucus carbohydrate landscape exerts a diet-dependent effect on the gut microbiota. *Proc Natl Acad Sci*. 110:17059-64.

Kellner K, Ishak HD, Linksvayer TA, and Mueller UG (2015). Bacterial community composition and diversity in an ancestral ant fungus symbiosis. *FEMS Microbiol. Ecol.* 91:fiv073.

Kent BN and Bordenstein SR (2010). Phage WO of *Wolbachia*: lambda of the endosymbiont world. *Trends Microbiol.* 18, 173–181.

Kent BN, Salichos L, Gibbons JG, Rokas A, Newton IL, Clark ME, et al (2011). Complete bacteriophage transfer in a bacterial endosymbiont (*Wolbachia*) determined by targeted genome capture. *Genome Biol. Evol.* 3, 209–218.

Kim JK, Kim NH, Jang HA, Kikuchi Y, Kim CH, Fukatsu T, et al (2013). Specific midgut region controlling the symbiont population in an insect-microbe gut symbiotic association. *Appl. Environ. Microbiol.* 79, 7229–7233.

Kirkness EF, Haas BJ, Sun W, Braig HR, Perotti MA, Clark JM, et al (2010). Genome sequences of the human body louse and its primary endosymbiont provide insights into the permanent parasitic lifestyle. *Proc. Natl. Acad. Sci. U.S.A.* 107, 12168–12173.

Koch H and Schmid-Hempel P (2012). Gut microbiota instead of host genotype drive the specificity in the interaction of a natural host-parasite system. *Ecol. Lett.* 15, 1095–1103.

Koehncke A, Telschow A, Werren JH, and Hammerstein P (2009). Life and death of an influential passenger: *Wolbachia* and the evolution of CI-modifiers by their hosts. *PLoS One* 4, e4425.

Koevoets T, Niehuis O, van de Zande L, and Beukeboom LW (2012). Hybrid incompatibilities in the parasitic wasp genus *Nasonia*: negative effects of hemizygosity and the identification of transmission ratio distortion loci. *Heredity (Edinb.)* 108, 302–311.

Koga R, Bennett GM, Cryan JR, and Moran NA (2013). Evolutionary replacement of obligate symbionts in an ancient and diverse insect lineage. *Environ. Microbiol.* 15, 2073–2081.

Kohl KD, Stengel A, and Dearing MD (2016). Inoculation of tannin-degrading bacteria into novel hosts increases performance on tannin-rich diets. *Environ Microbiol*. 6:1720-9

Kohl KD, Varner J, Wilkening JL, and Dearing MD (2018a). Gut microbial communities of American pikas (*Ochotona princeps*): evidence for phylosymbiosis and adaptations to novel diets. *J Anim Ecol.* 87(2):323-330.

Kohl KD, Dearing MD, and Bordenstein SR (2018b). Microbial communities exhibit host species distinguishability and phylosymbiosis along the length of the gastrointestinal tract. *Mol Ecol.* 27(8):1874-1883.

Kondo N, Shimada M, and Fukatsu T (2005). Infection density of *Wolbachia* endosymbiont affected by co-infection and host genotype. *Biol Lett* 1, 488-491.

Kremer N, Voronin D, Charif D, Mavingui P, Mollereau B, and Vavre F (2009). *Wolbachia* interferes with ferritin expression and iron metabolism in insects. *PLoS Pathog.* 5:e1000630.

Kremer N, Charif D, Henri H, Gavory F, Wincker P, Mavingui P, et al (2012). Influence of *Wolbachia* on host gene expression in an obligatory symbiosis. *BMC Microbiol.* 12(Suppl. 1):S7.

Kumar S, Stecher G, and Tamura K (2016). MEGA7: Molecular Evolutionary Genetics Analysis Version 7.0 for Bigger Datasets. *Mol Biol Evol* 33, 1870-1874.

Lander ES and Botstein D (1989). Mapping mendelian factors underlying quantitative traits using RFLP linkage maps. *Genetics* 121, 185-199.

Leal WS (1998). Chemical ecology of phytophagous scarab beetles. *Annu. Rev. Entomol.* 43, 39–61.

Le Clec'h W, Braquart-Varnier C, Raimond M, Ferdy JB, Bouchon D, and Sicard M (2012). High virulence of *Wolbachia* after host switching: when autophagy hurts. *PLoS Pathog.* 8, e1002844.

Lee KA, Kim SH, Kim EK, Ha EM, You H, Ki B, et al (2013). Bacterial-derived uracil as a modulator of mucosal immunity and gut-microbe homeostasis in *Drosophila*. *Cell* 153, 797–811.

Lepage DP, Metcalf JA, Bordenstein SR, On J, Perlmutter JI, Shropshire JD, Layton EM, Funkhouser-Jones LJ, Beckmann JF, and Bordenstein SR (2017). Prophage WO genes recapitulate and enhance *Wolbachia*-induced cytoplasmic incompatibility. *Nature* 543(7644):243-247.

Letunic I and Bork P (2017). 20 years of the SMART protein domain annotation resource. *Nucleic Acids Res*. 46(D1):D493-D496.

Ley RE, Turnbaugh PJ, Klein S, and Gordon JI (2006). Microbial ecology: human gut microbes associated with obesity. *Nature* 444, 1022-1023.

Ley RE, Hamady M, Lozupone C, Turnbaugh PJ, Ramey RR, Bircher JS, et al (2008). Evolution of mammals and their gut microbes. *Science.* 320:1647-51.

Liang H, Zhou W, and Landweber LF (2006). SWAKK: a web server for detecting positive selection in proteins using a sliding window substitution rate analysis. *Nucleic Acids Res* 34, W382-384.

Liang X, Bushman FD, FitzGerald GA (2015). Rhythmicity of the intestinal microbiota is regulated by gender and the host circadian clock. *Proc Natl Acad Sci*. 112:10479-84.

Livak KJ and Schmittgen TD (2001). Analysis of relative gene expression data using real-time quantitative PCR and the 2(-Delta Delta C(T)) Method. *Methods* 25, 402-408.

Liu S, Pires da Cunha A, Rezende RM, Cialic R, Wei Z, Bry L, et al (2016). The host shapes the gut microbiota via fecal microRNA. *Cell Host & Microbe*. 19:32-43.

Lize A, McKay R, and Lewis Z (2014). Kin recognition in *Drosophila*: the importance of ecology and gut microbiota. *ISME J.* 8, 469–477.

Lo N, Casiraghi M, Salati E, Bazzocchi C, Bandi C (2002). How many *Wolbachia* supergroups exist? *Mol Biol Evol*. 19:341-6.

Lo N, Paraskevopoulos C, Bourtzis K, O'Neill SL, Werren JH, Bordenstein SR, et al (2007). Taxonomic status of the intracellular bacterium *Wolbachia* pipientis. *Int. J. Syst. Evol. Microbiol.* 57, 654–657.

Loehlin DW, Oliveira DC, Edwards R, Giebel JD, Clark ME, Cattani MV, van de Zande L, Verhulst EC, Beukeboom LW, Munoz-Torres M, et al (2010). Non-coding changes cause sex-specific wing size differences between closely related species of Nasonia. *PLoS Genet.* 6, e1000821.

Login FH, Balmand S, Vallier A, Vincent-Monegat C, Vigneron A, Weiss-Gayet M, Rochat D, and Heddi A (2011). Antimicrobial peptides keep insect endosymbionts under control. *Science* 334, 362-365.

Lozupone C, Knight R (2005). UniFrac: a new phylogenetic method for comparing microbial communities. *Appl Environ Microbiol*. 71:8228-35.

Luan JB, Chen W, Hasegawa DK, Simmons AM, Wintermantel WM, Ling KS, et al (2015). Metabolic coevolution in the bacterial symbiosis of whiteflies and related plant sap-feeding insects. *Genome Biol. Evol.* 7, 2635–2647.

Lynch JA, Brent AE, Leaf DS, Pultz MA, and Desplan C (2006). Localized maternal orthodenticle patterns anterior and posterior in the long germ wasp Nasonia. *Nature* 439, 728-732.

Lynch JA (2015). The expanding genetic toolbox of the wasp *Nasonia vitripennis* and its relatives. *Genetics.* 199:897–904.

Malo MS, Alam SN, Mostafa G, Zeller SJ, Johnson PV, Mohammad N, et al (2010). Intestinal alkaline phosphatase preserves the normal homeostasis of gut microbiota. Gut. 59:1476-84.

Manzano-Marin A, Oceguera-Figueroa A, Latorre A, Jimenez-Garcia LF, and Moya A (2015). Solving a bloody mess: B-Vitamin independent metabolic convergence among gammaproteobacterial obligate endosymbionts from blood-feeding arthropods and the leech Haementeria officinalis. *Genome Biol. Evol.* 7, 2871–2884.

Margulis L (1991). "Symbiogenesis and symbionticism," in *Symbiosis as a Source of Evolutionary Innovation: Speciation and Morphogenesis*, eds L. Margulis and R. Fester (Cambridge, MA: MIT Press), 1–14.

Margulis L (1993). Symbiosis in Cell Evolution (New York: W.H. Freeman).

Martinson VG, Danforth BN, Minckley RL, Rueppell O, Tingek S, and Moran NA (2011). A simple and distinctive microbiota associated with honey bees and bumble bees. *Mol. Ecol.* 20, 619–628.

Masson F, Vallier A, Vigneron A, Balmand S, Vincent-Monégat C, Zaidman-Rémy A, et al (2015). Systemic infection generates a local-like immune response of the bacteriome organ in insect symbiosis. *J. Innate Immun.* 7, 290–301.

Masui S, Kamoda S, Sasaki T, and Ishikawa H (2000). Distribution and evolution of bacteriophage WO in *Wolbachia*, the endosymbiont causing sexual alterations in arthropods. *J. Mol. Evol.* 51, 491–497.

McCutcheon JP, McDonald BR, and Moran NA (2009). Convergent evolution of metabolic roles in bacterial co-symbionts of insects. *Proc. Natl. Acad. Sci. U.S.A.* 106, 15394–15399.

McCutcheon JP and Moran NA (2010). Functional convergence in reduced genomes of bacterial symbionts spanning 200 My of evolution. *Genome Biol. Evol.* 2, 708–718.

McCutcheon JP and von Dohlen CD (2011). An interdependent metabolic patchwork in the nested symbiosis of mealybugs. *Curr. Biol.* 21, 1366–1372.

McDonald D, Clemente JC, Kuczynski J, Rideout JR, Stombaugh J, Wendel D, et al (2010). The Biological Observation Matrix (BIOM) format or: how I learned to stop worrying and love the ome-ome. *GigaScience* 1:7.

McDonald D, Price MN, Goodrich JK, Nawrocki EP, DeSantis TZ, Probst A, et al (2012). An improved Greengenes taxonomy with explicit ranks for ecological and evolutionary analyses of bacteria and archaea. *ISME Journal* 6:610-8.

McFall-Ngai M, Hadfield MG, Bosch TCG, Carey HV, Domazet-Loso T, Douglas AE, et al (2013). Animals in a bacterial world, a new imperative for the life sciences. *Proc Natl Acad Sci*. 110:3229-36.

McGraw EA, Merritt DJ, Droller JN, and O'Neill SL (2002). *Wolbachia* density and virulence attenuation after transfer into a novel host. *Proc Natl Acad Sci* USA 99, 2918-2923.

McLoughlin K, Schluter J, Rakoff-Nahoum S, Smith AL, Foster KR (2016). Host selection of microbiota via differential adhesion. *Cell Host & Microbe* 4:550-9.

McMeniman CJ, Lane RV, Cass BN, Fong AW, Sidhu M, Wang YF, and O'Neill SL (2009). Stable introduction of a life-shortening *Wolbachia* infection into the mosquito Aedes aegypti. *Science* 323, 141-144.

McMurdie PJ and Holmes S (2013). phyloseq: an R package for reproducible interactive analysis and graphics of microbiome census data. *PLoS One* 8:e61217.

Meagher S, Penn D, Potts W (2000). Male-male competition magnifies inbreeding depression in wild house mice. *Proc Natl Acad Sci*. 97:3324-9.

Merkey AB, Wong CK, Hoshizaki DK, and Gibbs AG (2011). Energetics of metamorphosis in *Drosophila melanogaster*. *J Insect Physiol.* 57(10):1437-45.

Miko I and Deans A (2014). The mandibular gland in *Nasonia vitripennis* (Hymenoptera: Pteromalidae) *bioRxiv.*

Miller WJ, Ehrman L, and Schneider D (2010). Infectious speciation revisited: impact of symbiont-depletion on female fitness and mating behavior of *Drosophila paulistorum*. *PLoS Pathog. 6:e1001214.*

Millman KJ and Aivazis M (2011). Python for scientists and engineers. *Comp Sci Eng*. 13:9-12.

Min KT and Benzer S (1997). *Wolbachia*, normally a symbiont of Drosophila, can be virulent, causing degeneration and early death. *Proc Natl Acad Sci USA* 94, 10792-10796.

Mitchell J (2011). Streptococcus mitis: walking the line between commensalism and pathogenesis. *Mol Oral Microbiol* 26, 89-98.

Moeller AH, Li Y, Ngole EM, Ahuka-Mundeke S, Lonsdorf EV, Pusey AE, et al (2014). Rapid changes in the gut microbiome during human evolution. *Proc Natl Acad Sci.* 111:16431-5.

Moeller AH, Caro-Quintero A, Mjungu D, Georgiev AV, Lonsdorf EV, Muller MN, et al (2016). Cospeciation of gut microbiota with hominids. *Science* 016;353:380-2.

Montllor CB, Maxmen A, and Purcell AH (2002). Facultative bacterial endosymbionts benefit pea aphids *Acyrthosiphon pisum* under heat stress. *Ecol. Entomol.* 27, 189–195.

Moran NA (2007). Symbiosis as an adaptive process and source of phenotypic complexity. *Proc. Natl. Acad. Sci. U.S.A.* 104(Suppl. 1), 8627–8633.

Moran NA, McCutcheon JP, and Nakabachi A (2008). Genomics and evolution of heritable bacterial symbionts. *Annu. Rev. Genet.* 42, 165–190.

Moran NA and Sloan DB (2015). The hologenome concept: helpful or hollow? *PLoS Biol.* 13:e1002311.

Mouton L, Henri H, Bouletreau M, and Vavre F (2003). Strain-specific regulation of intracellular *Wolbachia* density in multiply infected insects. *Mol Ecol* 12, 3459-3465.

Mouton L, Dedeine F, Henri H, Boulétreau M, Profizi N, and Vavre F (2004). Virulence, multiple infections and regulation of symbiotic population in the *Wolbachia*-Asobara tabida symbiosis. *Genetics* 168, 181–189.

Muegge BD, Kuczynski J, Knights D, Clemente JC, González A, Fontana L, et al (2011). Diet drives convergence in gut microbiome functions across mammalian phylogeny and within humans. *Science* 332:970-4.

Munger JC and Karasov WH (1989). Sublethal parasites and host energy budgets: tapeworm infection in white-footed mice. *Ecology* 70:904-21.

Murfin KE, Lee M-M, Klassen JL, McDonald BR, Larget B, Forst S, et al (2015). *Xenorhabdus bovienii* strain diversity impacts coevolution and symbiotic maintenance with *Steinernema* spp. nematode hosts. mBio. 6:e00076-15.

Najarro MA, Sumethasorn M, Lamoureux A, and Turner TL (2015). Choosing mates based on the diet of your ancestors: replication of non-genetic assortative mating in *Drosophila melanogaster*. *PeerJ* 3:e1173.

Neafsey DE, Waterhouse RM, Abai MR, Aganezov SS, Alekseyev MA, Allen JE, et al (2015). Highly evolvable malaria vectors: the genomes of 16 *Anopheles* mosquitoes. *Science* 347:1258522.

Newell PD and Douglas AE (2014). Interspecies interactions determine the impact of the gut microbiota on nutrient allocation in *Drosophila melanogaster*. *Appl. Environ. Microbiol.* 80, 788–796.

Newton IL, Savytskyy O, and Sheehan KB (2015). *Wolbachia* utilize host actin for efficient maternal transmission in Drosophila melanogaster. *PLoS Pathog* 11, e1004798.

Newton IL and Sheehan KB (2015). Passage of *Wolbachia pipientis* through mutant *Drosophila melanogaster* induces phenotypic and genomic changes. *Appl Environ Microbiol.* 81(3):1032-7.

Niehuis O, Buellesbach J, Gibson JD, Pothmann D, Hanner C, Mutti NS, Judson AK, Gadau J, Ruther J, and Schmitt T (2013). Behavioural and genetic analyses of Nasonia shed light on the evolution of sex pheromones. *Nature* 494, 345-348.

Nielsen R, Bustamante C, Clark AG, Glanowski S, Sackton TB, Hubisz MJ, et al (2005). A scan for positively selected genes in the genomes of humans and chimpanzees. *PLoS Biol*. 3:e170.

Niehuis O, Judson AK, and Gadau J (2008). Cytonuclear genic incompatibilities cause increased mortality in male F2 hybrids of *Nasonia giraulti* and *N. vitripennis*. *Genetics* 178, 413–426.

Nishiguchi MK (2002). Host-symbiont recognition in the environmentally transmitted sepiolid squid-Vibrio mutualism. *Microb Ecol*. 44:10-8.

Noyes JS (2016) *Universal Chalcidoidea Database. World Wide Web Electronic Publication.* Available at: http://www.nhm.ac.uk/chalcidoids

Obbard DJ, Welch JJ, Kim K-W, and Jiggins FM (2009). Quantifying adaptive evolution in the *Drosophila* immune system. *PLoS Genet*. 5:e1000698.

Ochman H, Worobey M, Kuo CH, Ndjango JBN, Peeters M, Hahn BH, et al (2010). Evolutionary relationships of wild hominids recapitulated by gut microbial communities. PLoS Biol. 8:e1000546.

Olcott MH, Henkels MD, Rosen KL, Walker FL, Sneh B, Loper JE, and Taylor BJ (2010). Lethality and developmental delay in *Drosophila melanogaster* larvae after ingestion of selected *Pseudomonas fluorescens* strains. *PLoS One* 5(9):e12504.

Oliphant TE (2007). Python for scientific computing. *Comp Sci Eng*. 9:10-20.

Oliveira DC, Hunter WB, Ng J, Desjardins CA, Dang PM, and Werren JH (2010). Data mining cDNAs reveals three new single stranded RNA viruses in *Nasonia*(Hymenoptera: Pteromalidae). *Insect Mol. Biol.* 19(Suppl. 1), 99–107.

Oliver KM, Russell JA, Moran NA, and Hunter MS (2003). Facultative bacterial symbionts in aphids confer resistance to parasitic wasps. *Proc. Natl. Acad. Sci. USA.* 100, 1803–1807.

Oliver KM, Degnan PH, Hunter MS, and Moran NA (2009). Bacteriophages encode factors required for protection in a symbiotic mutualism. *Science* 325, 992–994.

O'Neill SL, Giordano R, Colbert AM, Karr TL, and Robertson HM (1992). 16S rRNA phylogenetic analysis of the bacterial endosymbionts associated with cytoplasmic incompatibility in insects. *Proc. Natl. Acad. Sci. USA.* 89, 2699–2702.

Org E, Parks BW, Joo JWL, Emert B, Schwartzman W, Kang EY, et al (2015). Genetic and environmental control of host-gut microbiota interactions. *Genome Res*. 25:1558-69.

Pan X, Zhou G, Wu J, Bian G, Lu P, Raikhel AS, et al (2012). *Wolbachia* induces reactive oxygen species (ROS)-dependent activation of the Toll pathway to control dengue virus in the mosquito *Aedes aegypti*. *Proc. Natl. Acad. Sci. USA.* 109, E23–E31.

Pantoja-Feliciano IG, Clemente JC, Costello EK, Perez ME, Blaser MJ, Knight R, et al (2013). Biphasic assembly of the murine intestinal microbiota during development. *ISME Journal*. 7:1112-5.

Paolucci S, van de Zande L, and Beukeboom LW (2013). Adaptive latitudinal cline of photoperiodic diapause induction in the parasitoid *Nasonia* vitripennis in Europe. *J. Evol. Biol.* 26, 705–718.

Parratt SR, Frost CL, Schenkel MA, Rice A, Hurst GD, and King KC (2016). Superparasitism drives heritable symbiont epidemiology and host sex ratio in a wasp. *PLoS Pathog.* 12:e1005629.

Patwardhan A, Ray S, and Roy A (2014). Molecular markers in phylogenetic studies - a review. *J Phylogen Evol Biol*. 2:131.

Perrot-Minnot MJ, Guo LR, and Werren JH (1996). Single and double infections with *Wolbachia* in the parasitic wasp Nasonia vitripennis: effects on compatibility. *Genetics* 143, 961-972.

Perrot-Minnot MJ, and Werren JH (1999). *Wolbachia* infection and incompatibility dynamics in experimental selection lines. *J Evol Biol* 12, 272-282.

Phillips CD, Phelan G, Dowd SE, McDonough MM, Ferguson AW, Hanson JD, et al (2012). Microbiome analysis among bats describes influences of host phylogeny, life history, physiology, and geography. *Mol Ecol*. 21:2617-27.

Platt RN, Amman BR, Keith MS, Thompson CW, Bradley RD (2015). What Is *Peromyscus*? Evidence from nuclear and mitochondrial DNA sequences suggests the need for a new classification. *J Mamm*. 96:708–19.

Price MN, Dehal PS, and Arkin AP (2010). FastTree 2--approximately maximum-likelihood trees for large alignments. *PLoS One*. 5:e9490.

Pultz MA, Westendorf L, Gale SD, Hawkins K, Lynch J, Pitt JN, Reeves NL, Yao JC, Small S, Desplan C, et al (2005). A major role for zygotic hunchback in patterning the Nasonia embryo. *Development* 132, 3705-3715.

Ramírez-Puebla ST, Servín-Garcidueñas LE, Ormeño-Orrillo E, Vera-Ponce de León A, Rosenblueth M, Delaye L, et al (2015). Species in *Wolbachia*? Proposal for the designation of ‘Candidatus *Wolbachia* bourtzisii’, ‘Candidatus *Wolbachia* onchocercicola’, ‘Candidatus *Wolbachia* blaxteri’ , ‘Candidatus *Wolbachia* brugii’, ‘Candidatus *Wolbachia*taylori’, ‘Candidatus *Wolbachia* collembolicola’ and ‘Candidatus *Wolbachia* multihospitum’ for the different species supergroups. *Syst. Appl. Microbiol.* 38:390-399.

Rawls JF, Mahowald MA, Ley RE, and Gordon JI (2006). Reciprocal gut microbiota transplants from zebrafish and mice to germ-free recipients reveal host habitat selection. *Cell* 127:423-33.

Raychoudhury R, Baldo L, Oliveira DC, and Werren JH (2009). Modes of acquisition of *Wolbachia*: horizontal transfer, hybrid introgression, and codivergence in the Nasonia species complex. *Evolution* 63, 165-183.

Raychoudhury R, Desjardins CA, Buellesbach J, Loehlin DW, Grillenberger BK, Beukeboom L, Schmitt T, and Werren JH (2010a). Behavioral and genetic characteristics of a new species of Nasonia. *Heredity* 104, 278-288.

Raychoudhury R, Grillenberger BK, Gadau J, Bijlsma R, van de Zande L, Werren JH, et al (2010b). Phylogeography of *Nasonia* vitripennis (Hymenoptera) indicates a mitochondrial-*Wolbachia* sweep in North America. *Heredity (Edinb.)* 104, 318–326.

Raychoudhury R and Werren JH (2012). Host genotype changes bidirectional to unidirectional cytoplasmic incompatibility in *Nasonia* longicornis. *Heredity* 108, 105–114.

Reumer BM, van Alphen JJ, and Kraaijeveld K (2012). Occasional males in parthenogenetic populations of *Asobara japonica* (Hymenoptera: Braconidae): low *Wolbachia* titer or incomplete coadaptation? *Heredity (Edinb)*. 108(3):341-6.

Ridley EV, Wong AC, Westmiller S, and Douglas AE (2012). Impact of the resident microbiota on the nutritional phenotype of *Drosophila melanogaster*. *PLoS ONE* 7:e36765.

Rio RV, Wu YN, Filardo G, and Aksoy S (2006). Dynamics of multiple symbiont density regulation during host development: tsetse fly and its microbial flora. *Proc Biol Sci.* 273, 805-814.

Rivers DB and Losinger M (2014). Development of the gregarious ectoparasitoid *Nasonia vitripennis* using five species of necrophagous flies as hosts and at various developmental temperatures. *Entomologia Experimentalis et Applicata*. 151:160–169.

Robinson DF and Foulds LR (1981). Comparison of phylogenetic trees. *Math Biosci*. 53:131-47.

Robinson, M.D., McCarthy, D.J., and Smyth, G.K. (2010). edgeR: a Bioconductor package for differential expression analysis of digital gene expression data. *Bioinformatics* 26, 139-140.

Rosenberg E, Koren O, Reshef L, Efrony R, and Zilber-Rosenberg I (2007). The role of microorganisms in coral health, disease and evolution. *Nat. Rev. Microbiol.* 5, 355–362.

Rosenberg MI, Brent AE, Payre F, and Desplan C (2014). Dual mode of embryonic development is highlighted by expression and function of *Nasonia* pair-rule genes. *Elife* 3:e01440.

Rosenberg E and Zilber-Rosenberg I (2018). The hologenome concept of evolution after 10 years. *Microbiome* 6(1):78.

Ross AA, Muller KM, Weese JS, and Neufeld JD (2018). Comprehensive skin microbiome analysis reveals the uniqueness of human skin and evidence for phlyosymbiosis within the class Mammalia. *Proc Natl Acad Sci USA.* 115(25):E5786-E5795.

Roth O, Sadd BM, Schmid-Hempel P, and Kurtz J (2009). Strain-specific priming of resistance in the red flour beetle, *Tribolium castaneum*. *Proc R Soc B.* 276:145-51.

Round JL, Lee SM, Li J, Tran G, Jabri B, Chatila TA, and Mazmanian SK (2011). The Toll-like receptor 2 pathway establishes colonization by a commensal of the human microbiota. *Science* 332, 974-977.

Rousset F, Bouchon D, Pintureau B, Juchault P, and Solignac M (1992). *Wolbachia* endosymbionts responsible for various alterations of sexuality in arthropods. *Proc. Biol. Sci.* 250: 91–98.

Russell DJ, Otu HH, and Sayood K (2008). Grammar-based distance in progressive multiple sequence alignment. *BMC Bioinformatics*. 9:306.

Ruther J and Hammerl T (2014). An oral male courtship pheromone terminates the response of *Nasonia vitripennis* females to the male-produced sex attractant. *Journal of Chemical Ecology*. 40:56–62.

Ryu JH, Kim SH, Lee HY, Bai JY, Nam YD, Bae JW, et al (2008). Innate immune homeostasis by the homeobox gene caudal and commensal-gut mutualism in *Drosophila*. *Science* 319, 777–782.

Sackton TB, Werren JH, and Clark AG (2013). Characterizing the infection-induced transcriptome of *Nasonia* vitripennis reveals a preponderance of taxonomically-restricted immune genes. *PLoS ONE* 8:e83984.

Sanders JG, Powell S, Kronauer DJC, Vasconcelos HL, Frederickson ME, and Pierce NE (2014). Stability and phylogenetic correlation in gut microbiota: lessons from ants and apes. *Mol Ecol*. 23:1268-83.

Schindelin J, Arganda-Carreras I, Frise E, Kaynig V, Longair M, Pietzsch T, Preibisch S, Rueden C, Saalfeld S, Schmid B, et al (2012). Fiji: an open-source platform for biological-image analysis. *Nat Methods* 9, 676-682.

Seedorf H, Griffin NW, Ridaura VK, Reyes A, Cheng J, Rey FE, et al (2014). Bacteria from diverse habitats colonize and compete in the mouse gut. *Cell* 159:253-66.

Serbus LR and Sullivan W (2007). A cellular basis for *Wolbachia* recruitment to the host germline. *PLoS Pathog* 3, e190.

Serbus LR, Casper-Lindley C, Landmann F, and Sullivan W (2008). The genetics and cell biology of *Wolbachia*-host interactions. *Annu Rev Genet*. 42, 683-707.

Serbus LR, Ferreccio A, Zhukova M, McMorris CL, Kiseleva E, and Sullivan W (2011). A feedback loop between *Wolbachia* and the Drosophila gurken mRNP complex influences *Wolbachia* titer. *J Cell Sci.* 124, 4299-4308.

Shannon CE (1948). A mathematical theory of communication. *Bell Syst Tech J*. 27:379-423.

Shapira M (2016). Gut microbiotas and host evolution: scaling up symbiosis. *Trends Ecol Evol*. 7:539-549.

Sharon G, Segal D, Ringo JM, Hefetz A, Zilber-Rosenberg I, and Rosenberg E (2010). Commensal bacteria play a role in mating preference of *Drosophila melanogaster*. *Proc. Natl. Acad. Sci. USA.* 107, 20051–20056.

Sharp KH, Eam B, Faulkner DJ, and Haygood MG (2007). Vertical transmission of diverse microbes in the tropical sponge *Corticium* sp. *Appl Environ Microbiol.* 73:622-9.

Shigenobu S and Stern DL (2013). Aphids evolved novel secreted proteins for symbiosis with bacterial endosymbiont. *Proc. Biol. Sci.* 280:20121952.

Shin SC, Kim S-H, You H, Kim B, Kim AC, Lee K-A, et al (2011). *Drosophila* microbiome modulates host developmental and metabolic homeostasis via insulin signaling. *Science* 334:670-4.

Shropshire JD, Opstal EJ, and Bordenstein SR (2016). An optimized approach to germ-free rearing in the jewel wasp *Nasonia*. *PeerJ*. 4:e2316.

Shropshire JD and Bordenstein SR (2016). Speciation by symbiosis: the microbiome and behavior. mBio. 7:e01785-15.

Sicard M, Dittmer J, Greve P, Bouchon D, and Braquart-Varnier C (2014). A host as an ecosystem: *Wolbachia* coping with environmental constraints. *Environ. Microbiol.* 16, 3583–3607.

Skinner SW (1985). Son-killer: a third extrachromosomal factor affecting the sex ratio in the parasitoid wasp, *Nasonia* (=Mormoniella) vitripennis. *Genetics* 109, 745–759.

Stamatakis A (2014). RAxML version 8: a tool for phylogenetic analysis and post-analysis of large phylogenies. *Bioinformatics* 30:1312-3.

Staubach F, Baines JF, Künzel S, Bik EM, and Petrov DA (2013). Host species and environmental effects on bacterial communities associated with Drosophila in the laboratory and in the natural environment. *PLoS One* 8:e70749.

Steiner S, Hermann N, and Ruther J (2006). Characterization of a female-produced courtship pheromone in the parasitoid *Nasonia vitripennis*. *Journal of Chemical Ecology* 32:1687–1702.

Steiper ME and Young NM (2006). Primate molecular divergence dates. *Mol Phylogenet Evol.* 41:384-94.

Stepphan SJ, Adkins RM, and Anderson J (2004). Phylogeny and divergence-date estimates of rapid radiations in muroid rodents based on multiple nuclear genes. *Syst Biol.* 53:533–53.

Storelli G, Defaye A, Erkosar B, Hols P, Royet J, and Leulier F (2011). *Lactobacillus plantarum* promotes *Drosophila* systemic growth by modulating hormonal signals through TOR-dependent nutrient sensing. *Cell Metab.* 14, 403–414.

Storelli G, Defaye A, Erkosar B, Hols P, Royet J, and Leulier F (2011). *Lactobacillus plantarum* promotes *Drosophila* systemic growth by modulating hormonal signals through TOR-dependent nutrient sensing. *Cell Metab.* 14, 403–414.

Suh E, Mercer DR, Fu Y, and Dobson SL (2009). Pathogenicity of life-shortening *Wolbachia* in Aedes albopictus after transfer from Drosophila melanogaster. *Appl Environ Microbiol.* 75, 7783-7788.

Taylor MJ and Hoerauf A (1999). *Wolbachia* bacteria of filarial nematodes. *Parasitol Today* 15, 437-442.

Theis KR, Dheilly NM, Klassen JL, Brucker RM, Baines JF, Bosch TCG, et al (2016). Getting the hologenome concept right: An eco-evolutionary framework for hosts and their microbiomes. *mSystems* 1:e00028-16.

Theis KR (2018). Hologenomics: systems-level host biology. *mSystems* 3(2). pii: e00164-17.

Tian C, Gao B, Fang Q, Ye G, and Zhu S (2010). Antimicrobial peptide-like genes in *Nasonia* vitripennis: a genomic perspective. *BMC Genomics* 11:187.

Tram U and Sullivan W (2002). Role of delayed nuclear envelope breakdown and mitosis in *Wolbachia*-induced cytoplasmic incompatibility. *Science* 296, 1124–1126.

Tsai Y-JJ, Barrows EM, Weiss MR, and Zeh D (2014). Pure self-assessment of size during male-male contests in the parasitoid wasp *Nasonia vitripennis*. *Ethology*. 120:816–824.

Tsuchida T, Koga R, and Fukatsu T (2004). Host plant specialization governed by facultative symbiont. *Science* 303:1989.

Turnbaugh PJ, Ley RE, Mahowald MA, Magrini V, Mardis ER, and Gordon JI (2006). An obesity-associated gut microbiome with increased capacity for energy harvest. *Nature* 444, 1027-1031.

van Opijnen T, Baudry E, Baldo L, Bartos J, and Werren JH (2005). Genetic variability in the three genomes of *Nasonia*: nuclear, mitochondrial and *Wolbachia*. *Insect Mol. Biol.* 14, 653–663.

van Opstal EJ and Bordenstein SR (2015). Rethinking heritability of the microbiome. *Science* 349:1172-3.

Varaldi J, Fouillet P, Ravallec M, López-Ferber M, Boulétreau M, Fleury F, et al (2003). Infectious behavior in a parasitoid. *Science* 302:1930.

Varaldi J, Bouletreau M, and Fleury F (2005). Cost induced by viral particles manipulating superparasitism behaviour in the parasitoid *Leptopilina boulardi*. *Parasitology* 131, 161–168.

Varaldi J, Ravallec M, Labrosse C, Lopez-Ferber M, Boulétreau M, and Fleury F (2006). Artifical transfer and morphological description of virus particles associated with superparasitism behaviour in a parasitoid wasp. *J. Insect Physiol.* 52, 1202–1212.

Vasanthakumar A, Handelsman J, Schloss PD, Bauer LS, and Raffa KF (2008). Gut microbiota of an invasive subcortical beetle, *Agrilus planipennis* Fairmaire, across various life stages. *Environ. Entomol.* 37, 1344–1353.

Vavre F, Fleury F, Lepetit D, Fouillet P, and Bouletreau M (1999). Phylogenetic evidence for horizontal transmission of *Wolbachia* in host-parasitoid associations. *Mol Biol Evol.* 16, 1711-1723.

Vavre F, Fleury F, Varaldi J, Fouillet P, and Bouletreau M (2000). Evidence for female mortality in *Wolbachia*-mediated cytoplasmic incompatibility in haplodiploid insects: epidemiologic and evolutionary consequences. *Evolution* 54, 191–200.

Vavre F, Mouton L, and Pannebakker BA (2009). Drosophila-parasitoid communities as model systems for host-*Wolbachia* interactions. *Adv. Parasitol.* 70, 299–331.

Vavre F and Kremer N (2014). Microbial impacts on insect evolutionary diversification: from patterns to mechanisms. *Curr Opin Insect Sci.* 4, 29–34.

Verhulst EC, Beukeboom LW, and van de Zande L (2010). Maternal control of haplodiploid sex determination in the wasp Nasonia. *Science* 328, 620-623.

Verhulst EC, Lynch JA, Bopp D, Beukeboom LW, and van de Zande L (2013). A new component of the *Nasonia* sex determining cascade is maternally silenced and regulates transformer expression. *PLoS ONE* 8:e2316.

Wang IN (2006). Lysis timing and bacteriophage fitness. *Genetics* 172(1):17-26.

Wang J, Wu Y, Yang G, and Aksoy S (2009). Interactions between mutualist *Wigglesworthia* and tsetse peptidoglycan recognition protein (PGRP-LB) influence trypanosome transmission. *Proc. Natl. Acad. Sci. USA.* 106, 12133–12138.

Wang J, Kalyan S, Steck N, Turner LM, Harr B, Künzel S, et al (2015). Analysis of intestinal microbiota in hybrid house mice reveals evolutionary divergence in a vertebrate hologenome. *Nat Comm.* 6:6440.

Wang X, Wheeler D, Avery A, Rago A, Choi JH, Colbourne JK, et al (2013). Function and evolution of DNA methylation in *Nasonia* vitripennis. *PLoS Genet.* 9:e1003872.

Weber JN and Hoekstra HE (2009). The evolution of burrowing behaviour in deer mice (genus *Peromyscus*). *Anim Behav*. 77:603-9.

Weinert LA, Araujo-Jnr EV, Ahmed MZ, and Welch JJ (2015). The incidence of bacterial endosymbionts in terrestrial arthropods. *Proc Biol Sci* 282, 20150249.

Werren JH, Skinner SW, and Huger AM (1986). Male-killing bacteria in a parasitic wasp. *Science* 231, 990–992.

Werren, JH, Zhang W, and Guo LR (1995). Evolution and phylogeny of *Wolbachia* - reproductive parasites of arthropods. *Proc R Soc Lond B Biol Sci.* 261, 55-63.

Werren JH, Baldo L, and Clark ME (2008). *Wolbachia*: master manipulators of invertebrate biology. *Nat Rev Microbiol.* 6, 741-751.

Werren JH and Loehlin DW (2009). The parasitoid wasp Nasonia: an emerging model system with haploid male genetics. *Cold Spring Harb Protoc* 2009, pdb emo134.

Werren JH, Loehlin DW, and Giebel JD (2009). Larval RNAi in *Nasonia* (parasitoid wasp). *Cold Spring Harb. Protoc.* 2009:pdb.prot5311.

Werren JH and Loehlin DW (2009a). Rearing *Sarcophaga bullata* fly hosts for *Nasonia* (parasitoid wasp). *Cold Spring Harb. Protoc*. (10):pdb.prot5308.

Werren & Loehlin Werren JH, and Loehlin DW (2009b). Strain maintenance of *Nasonia vitripennis* (parasitoid wasp). *Cold Spring Hab. Protoc*. (10):pdb.prot5307.

Werren JH, Richards S, Desjardins CA, Niehuis O, Gadau J, Colbourne JK, et al (2010). Functional and evolutionary insights from the genomes of three parasitoid *Nasonia* species. *Science* 327:343-8.

Werren JH, Cohen LB, Gadau J, Ponce R, Baudry E, and Lynch JA (2015). Dissection of the complex genetic basis of craniofacial anomalies using haploid genetics and interspecies hybrids in *Nasonia* wasps. *Dev Biol.* 415, 391-405.

White PM, Serbus LR, Debec A, Codina A, Bray W, Guichet A, Lokey RS, and Sullivan W (2017). Reliance of *Wolbachia* on High Rates of Host Proteolysis Revealed by a Genome-Wide RNAi Screen of *Drosophila* Cells. *Genetics* 205, 1473-1488.

Whiting AR (1967). The biology of the parasitic wasp *Mormoniella vitripennis* [=*Nasonia brevicornis*] (Walker). *The Quarterly Review of Biology* 42(3): 333-406.

Wilson AC, Ashton PD, Calevro F, Charles H, Colella S, Febvay G, et al (2010). Genomic insight into the amino acid relations of the pea aphid, Acyrthosiphon pisum, with its symbiotic bacterium *Buchnera aphidicola*. *Insect Mol. Biol.* 19(Suppl. 2), 249–258.

Wong ACN, Chaston JM, and Douglas AE (2013). The inconstant gut microbiota of *Drosophila* species revealed by 16S rRNA gene analysis. *ISME Journal* 7:1922-32.

Wong AC, Dobson AJ, and Douglas AE (2014). Gut microbiota dictates the metabolic response of *Drosophila* to diet. *J. Exp. Biol.* 217, 1894–1901.

Wu M, Sun LV, Vamathevan J, Riegler M, Deboy R, Brownlie JC, et al (2004). Phylogenomics of the reproductive parasite *Wolbachia* pipientis wMel: a streamlined genome overrun by mobile genetic elements. *PLoS Biol.* 2:E69.

Yatsunenko T, Rey FE, Manary MJ, Trehan I, Dominguez-Bello MG, Contreras M, et al (2012). Human gut microbiome viewed across age and geography. *Nature* 486:222-7.

Yoshiyama M and Kimura K (2009). Bacteria in the gut of Japanese honeybee, Apis cerana japonica, and their antagonistic effect against *Paenibacillus* larvae, the causal agent of American foulbrood. *J. Invertebr. Pathol.* 102, 91–96.

Yun JH, Roh SW, Whon TW, Jung MJ, Kim MS, Park DS, et al (2014). Insect gut bacterial diversity determined by environmental habitat, diet, developmental stage, and phylogeny of host. *Appl Environ Microbiol*. 80:5254-64.

Zhang C, Derrien M, Levenez F, Brazeilles R, Ballal S, Kim J, et al (2016). Ecological robustness of the gut microbiota in response to the ingestion of transient food-borne microbes. *ISME Journal* 10:2235-45.

Zilber-Rosenberg I and Rosenberg E (2008). Role of microorganisms in the evolution of animals and plants: the hologenome theory of evolution. *FEMS Microbiol. Rev.* 32, 723–735.

Zug R and Hammerstein P (2012). Still a host of hosts for *Wolbachia*: analysis of recent data suggests that 40% of terrestrial arthropod species are infected. *PLoS One* 7, e38544.

Zwier MV, Verhulst EC, Zwahlen RD, Beukeboom LW, Van de Zande L (2012). DNA methylation plays a crucial role during early *Nasonia* development. *Insect Molecular Biology* 21:129–138.

APPENDIX A. CHAPTER II SUPPLEMENTARY INFORMATION

Table A-1. Primers for *Nasonia* microsatellite markers. *cM locations based on genetic linkage map from (Desjardins et al. 2013). N/A = sequence is absent in *N. giraulti* so no PCR product is generated. Primers were used for quantitative trait loci mapping (QTL), fine mapping in segmental introgression lines (FM), or both.

Primer name	Chr	cM*	Primer Set (5' to 3')	Size *Nvit* (bp)	Size *Ngir* (bp)	Annealing Tm (°C)	Used For
MM1.12	1	31.4	F: GCGGTCCTGCTCCATTAACCGC R: CCAGACTCGCGCGGGTGTATTT	284	242	57	QTL
MM1.13	1	32.9	F: AGCTCCGAGAGCGCGAGTGA R: TCCCGTGCCGACGCATACAC	224	167	57	QTL
MM1.14	1	35.8	F: GCCGTCGAGAGACGAGCGAG R: GCGCGGCTGGAGGATGCTTT	219	266	57	QTL
MM1.L521	1	38.7	F: ACACGTCCCGATCCTTCTTTGAC R: GCGCCTCACTTGTTGTGCAT	118	160	54	QTL
MM1.16	1	40.9	F: ACGCGACTCCTTTCTCCGCA R: GCGGAAATCGAATGCGCGGC	233	199	56	QTL
MM1.17	1	43.8	F: TGCCTCGCGAGAGCGCAAAA R: ACTGCTCTCGTCAAGGCCGC	177	217	57	QTL
NvC1-21	1	46.7	F: GTAACAGTGAGATAAATGTG R: TAGCAACGATAGTCCACG	148	N/A	45	QTL
MM1.057	1	49.6	F: CTACCACATCTTTCGCCAGTTT R: TCGAGTGATTAGAGATCGACGTT	180	206	51	QTL
MM1.L3567	1	53.3	F: CGCTCTGTCTACCTGTCCCT R: CGGCCACAAAGCAAATAGGC	154	184	52	QTL
MM1.31	1	56.2	F: CGCATCATCAACCCCCGACCA R: TCCGCGGCATAACCACTTGCT	266	297	57	QTL
MM1.32	1	57.7	F: ACCGGGACGACTTGAGCGTA R: ACAATGGGCGAATTTTTCTGCCG	183	220	55	QTL
MM2.13	2	19	F: AAGACGAGAGCCGACGTTGC R: GGCCTGCACGAGTGTGTATAGGG	240	206	55	QTL
MM2.15	2	21.9	F: TGGCAGATGACTCACGGAAATTAACAG R: CAGTTTTAGATGAGTTTATGAACTGTGTC	87	154	52	QTL
MM2.17	2	24.8	F: CGCCGACGTCGTTGCTGCTT R: AGCTCCACAACGGCGGCATC	143	99	58	QTL
MM2.20	2	29.2	F: TCTCCGTTAATTTCCAGCGCGT R: TCTTCCAATCCACGGGAAAACTGGT	207	168	55	QTL
Nv-20	2	30.7	F: TGACGAAGTATCCGAGAAG R: TCGAAAAACGATATTGCTCG	105	87	48	QTL
MM2.26	2	32.9	F: GCATCGCGTATGCTAATCTGCCG R: GGCGGAGTGAGAGAGCGTTTCA	220	172	56	QTL

MM2.L5335	2	36.5	F: CGCACGCGGTAATTGGCTTT R: TGTCCACGGCTGCGATTTGT	202	168	54	QTL
MM2.28	2	38	F: ACGCTTACACGCTGGTGAATGAA R: ACACCGTAATGCAATTTCCCGCT	256	287	55	QTL
MM2.30	2	40.9	F: TGGATGCGAGCGCGGGTTAT R: CCCATCGCTGATCCACGTTCTT	135	172	55	QTL
MM2.L6870	2	43.8	F: GCTCTACACGGCGAAGGTCA R: CGCGCTTCTCTTTATGCCCG	140	191	54	QTL
MM2.33	2	46	F: ACGAAACTCTGTACTGTATACTCCGGT R: CGGCGAGTCCTCGAGAGCAG	204	250	55	QTL
MM2.36	2	49.6	F: GCCGTTGGAGAAATGTGCGGGA R: TCGCGTATATTTTCCGTAGTCACGC	178	139	55	QTL
MM2.39	2	52.6	F: ACCGTTACAAAGCGAGCGAGAAT R: GCCGCCGCATAGCTCGATGA	161	207	55	QTL
MM2.40	2	54.8	F: TCCGTTTATCGCGCTTCGGACG R: CATCGGGCTGACCTTGGCCG	179	211	57	QTL
MM2.L7336	2	57.7	F: CATTCATCGCTCGTGTGCGC R: ACACATCTCTCCGAACGGCG	118	85	54	QTL
MM2.44	2	60.6	F: TCGACGGAAGCGAGGACGAG R: CTGGGCCGCAACGGTAAGCA	203	172	56	QTL
MM2.49	2	68.6	F: ACTGTTGCAGATGATGATGGTAATTT R: TCTGAAACATGCAACAATCAGGT	146	92	51	QTL
MM3.14	3	17.5	F: CTCTCGAAGCCGCGCGTGAA R: AGCCAGCTTTGCTTTCGACCG	231	206	56	QTL
MM3.15	3	20.4	F: ACACACGTTGTGCGGGGGTG R: GGTCGAAAATTTCTGCGCAGCCT	106	152	56	QTL
MM3.17	3	23.4	F: TGCGCGATGGCTGCTGTGAT R: TCGAGCGCAATAAACGCCGC	126	170	57	QTL
MM3.19	3	26.3	F: GCGGAAATTCTCGCCCCTGC R: TCCCATCATCAAAACGAAAAAGTCGC	177	220	55	QTL, FM
MM3.22	3	29.2	F: TCTCCTCCTGCTTCGGCCCC R: TCGTTCATCGTTCGTCATCGCA	116	146	55	QTL, FM
MM3.L8514	3	32.1	F3: GCGGCGAGAAGAACAGAAGCGA R3: ACGTTGTCGCTGTTCTTCTTGCAGT	488	279	57	FM
MM3.23	3	32.9	F: TTGAAGGGCTCATGGTCGCA R: CGCGAAACAGCGCACACG	183	219	55	QTL, FM
MM3.L8610	3	34.3	F1: CGCGTATGCTTGATGTCGGC R1: AACACAGAGGAATATGCGGGA	172	129	51	FM
MM3.L8623	3	34.3	F: TTGGAGTTTCGCACAAGAGC R: CTACCGCCGAGAAAAGTGC	185	136	54	FM
MM3.L8651	3	35.0	F: AGATGAGAAGAAAGAGGAAGCCC R: ATGGCGATTTCTTCATGTCGC	164	117	54	FM
MM3.L8678	3	35.0	F: GCAGCCAGGGAGTGATATGCT R: AAAGGCCGACGACGAGAGAC	186	138	54	QTL, FM
MM3.L8716	3	36.5	F: TGCCCATCAAAGGTGAGAGG R: CGGACTCACTGTTTGCCCAG	237	208	54	FM
MM3.L8724	3	36.5	F: CCTCTGTCTGTGCTTTTACGG R: TTCCCGTAAACACGATTGCC	105	82	54	FM

MM3.L8756	3	36.5	F: CGCGTGTCGTGTGGACGTAA R: TCAAACATCCGCGAGAGTCGA	115	157	54	FM
MM3.L8780	3	37.2	F1: TTAACCGAATAGCACCGCCG R1: AAATCCCAGATCCCGCACTAG	185	140	51	FM
MM3.L8790	2	37.2	F1: ATTTACCGACGCGCAACAGC R1: AGGGCGGAGAGATTAGATTTCCC	159	195	53	FM
MM3.L8813	3	37.2	F: CCGAGTGTGGGAGGTTTGACA R: TGTCAGCCGAGAATAGGCCG	177	148	54	FM
MM3.L8850	3	37.2	F: TGGTTGAGAGATCCACGCGA R: TCCGCGTTTACAACCAACATGG	159	206	53	FM
NvC3-18	3	38	F: GCCCAAATCATGCTTTCG R: GTTGTTCTTAAATGTGTATTCC	104	N/A	48	QTL
MM3.29	3	39.4	F: GGCCGATTTTCTCGACAGACC R: GCGAGGGAGAGCGAACGTC	241	285	53	QTL, FM
MM3.L10131	3	40.2	F: TGATGCGTTCTCGCCTTTCC R: CGACCGCAGAGCAACGATCA	155	204	53	FM
MM3.L10212	3	41.6	F: CCTCCCAAATCACTTCCGCGT R: TCAGCGCAATCGTTACCCTT	108	135	52	QTL, FM
Nv184	3	44.5	F: GCGTCATCGATGCATTTCTT R: TCTCGGGAGAGATTCAGTACG	209	141	49	QTL
MM3.L10340	3	45.3	F: CGAAACACCATTCGCAACGAGT R: TGTCGCATCGAGAACTGCA	194	167	52	FM
MM3.29.7M	3	45.3	F: CCAGTTGGATAATTCTTGAGGTCTTTC R: ACTTTGCTTGGCCCGACGAT	148	118	52	FM
MM3.35	3	46.7	F: GTACGTGAACCGGAAGTGTTT R: GACGGCTGCTACCGGCTATA	111	161	51	QTL, FM
MM3.36	3	48.2	F: ATTCGCGCCGCGGCTAATGG R: TTCCATACGTGTGGCAGGCG	150	197	55	FM
MM3.37	3	50.4	F: ACAAGCTTCGCACACACCGCA R: CGGTCGAAGAAGCGTCGCACA	185	157	58	QTL, FM
MM3.L10502	3	54.8	F: GCGCGAAACGACGAGGAATT R: CGAGCGTCGTGTGCTCTTCT	63	94	54	QTL
MM3.41	3	58.4	F: ACCGTGGGTCCGTGCAAC R: GGTTTGTACTTCATCGTGAGGCAATCG	186	142	55	QTL, FM
MM3.L10553	3	63.5	F: GCGCTTAATTGCGTCGTGTT R: CCGGTGCGGTTTCTTCTCCT	196	234	52	QTL
MM3.43	3	65.7	F: CGGCTGTTTATATTCCTCACCTGACGC R: GCAGCGACGAATCAGGAAATGCG	138	158	57	QTL
MM3.45	3	69.4	F: CGATTATGCAAACGACGCGA R: TTCCGATCACGATTCTCTCCTT	222	168	51	QTL
MM3.L10661	3	73	F: CCCTCCGATTATAGATGCAAGTGTCA R: GGCAGTAGTGGCTCTCTTTGCT	159	181	54	QTL

Table A-2. Mapping statistics for RNA-seq of *Nasonia* ovaries. Nvit: *N. vitripennis* strain 12.1; IntG: *N. giraulti* strain IntG; IntC3: *N. giraulti* strain IntG introgressed with a chromosome 3 region from *N. vitripennis* strain 12.1. Analysis of the RNA-seq paired-end reads was performed on CLC Genomics Workbench 8.

Sample	# of Reads after QC	# of Mapped Paired Reads	% of Total Paired Reads Mapped	# of Mapped Intergenic Gene Reads	# of Mapped Gene Reads	# of Uniquely Mapped Gene Reads
Nvit-1	30,390,144	22,202,334	73.06	1,030,126	10,071,041	9,635,225
Nvit-2	34,665,838	25,567,636	73.75	1,253,382	11,530,436	11,022,442
Nvit-3	30,525,996	23,230,600	76.10	1,130,430	10,484,870	10,028,047
Nvit-4	26,369,828	19,186,084	72.76	1,046,799	8,546,243	8,152,609
IntC3-1	44,261,706	33,917,290	76.63	1,293,427	15,665,218	15,064,507
IntC3-2	49,692,100	35,712,884	71.84	1,658,981	16,197,461	15,517,397
IntC3-3	34,959,996	25,770,826	73.72	1,180,170	11,705,243	11,202,164
IntC3-4	42,765,380	30,299,978	70.85	1,327,688	13,822,301	13,261,676
IntG-1	36,821,016	27,095,510	73.59	1,051,834	12,495,921	12,020,977
IntG-2	35,451,744	26,505,936	74.77	1,114,883	12,138,085	11,647,781
IntG-3	40,863,430	31,432,456	76.92	1,234,399	14,481,829	13,913,515
IntG-4	38,523,210	25,325,636	65.74	1,744,894	10,917,924	10,470,342
IntG-5	38,697,378	27,021,558	69.83	1,201,004	12,309,775	11,765,553

Table A-3. Significant differentially expressed genes in R6-3 candidate region. Mean number of reads for each gene was calculated by dividing the total number of reads from all replicates that mapped to the gene by the number of replicates (N = 4-5 for each *Nasonia* strain). Positive fold change = upregulation in *N. vitripennis* 12.1 or introgression line IntC3, while negative fold change = upregulation in *N. giraulti* IntG. Fold change and p-values were calculated using EdgeR in CLC Genomics.

NCBI Gene ID	NCBI Annotated Gene Name	Mean Reads for Nvit	Mean Reads for IntC3	Mean Reads for IntG	Fold Change (Nvit/IntG)	p-value (FDR-corrected)	Fold Change (IntC3/ IntG)	p-value (FDR-corrected)
LOC100679092	Uncharacterized (*Wds*)	38.8	66.3	7.60	6.44	3.09E-10	7.42	2.07E-14
LOC100118928	Dentin Sialophosphoprotein-like	23.5	18	11.2	2.67	2.98E-3	1.40	1
LOC100118450	Abnormal long morphology protein 1-like	81.3	117	234	-2.26	2.29E-8	-2.30	5.32E-7
LOC100679834	Myb-like protein	147.5	380	546	-2.89	2.76E-5	-1.63	3.35E-3
LOC100114497	Girdin	640.5	1281	2508	-3.05	1.46E-40	-2.24	7.42E-19
LOC103317608	Interaptin-like	144	140	517	-2.82	3.48E-16	-4.25	1.28E-27
LOC100678491	Uncharacterized	26	46.3	152	-4.49	5.25E-15	-3.76	2.43E-13

Table A-4. Blastp homology to Wdsv protein sequence. BLASTp analysis performed on uncharacterized protein LOC100679092 (NCBI accession number XP_008213336.1) using the non-redundant protein sequences (nr) database.

BLASTp Result Organisms	Accession	BLASTp E-value	Query coverage	% identity	Reciprocal BLASTp E-value to LOC100679092
Hymenopterans					
Uncharacterized protein LOC100679092 [*Nasonia vitripennis*]	XP_008213336.1	1.00E-143	100%	100%	1.00E-143
hypothetical protein TSAR_005991 [Trichomalopsis sarcophagae]	OXU27029.1	3.00E-99	100%	95%	1.00E-101
Uncharacterized protein LOC106659966 [Trichogramma pretiosum	XP_014238261.1	4.00E-24	74%	42%	1.00E-21
Uncharacterized protein LOC106636480 [Copidosoma floridanum]	XP_014204363.1	5.00E-18	98%	35%	2.00E-17
Uncharacterized protein LOC106793189 [Polistes canadensis]	XP_014615392.1	2.00E-09	78%	29%	5.00E-07
Uncharacterized protein LOC100878703 [Megachile rotundata]	XP_003702181.1	6.00E-08	56%	32%	4.00E-05
Uncharacterized protein LOC107264954 isoform X2 [Cephus cinctus]	XP_015589287.1	5.00E-08	30%	55%	3.00E-08
Uncharacterized protein LOC107186552 [Dufourea novaeangliae]	XP_015429933.1	3.00E-07	56%	31%	2.00E-03
Uncharacterized protein LOC105276036 [Ooceraea biroi]	XP_011331664.1	4.00E-07	91%	31%	5.10E-02
Uncharacterized protein LOC108574276 [Habropoda laboriosa]	XP_017792325.1	2.00E-06	75%	26%	1.00E-03
Uncharacterized protein LOC100650078 [Bombus terrestris]	XP_003396525.1	2.00E-06	56%	31%	8.00E-05
Uncharacterized protein LOC107963970 [Apis mellifera]	XP_001121053.1	2.00E-05	56%	31%	1.00E-02
Uncharacterized protein LOC109860277 [Pseudomyrmex gracilis]	XP_020294850.1	3.00E-04	68%	28%	4.00E-03
Dipterans					
Uncharacterized protein LOC109418023 [Aedes albopictus]	XP_019547726.1	1.50E-02	32%	38%	1.60E+00
GL10758 [Drosophila persimilis]	XP_002015939.1	1.90E-02	32%	36%	8.90E-02
Uncharacterized protein Dpse_GA24472 [Drosophila pseudoobscura]	XP_002138301.1	7.60E-02	32%	34%	8.60E-02

Table A-5. Primers for *Nasonia* gene sequencing and allelic genotyping. cM locations based on genetic linkage map from (Desjardins et al. 2013).

Primer Name	Chr	cM*	Primer Set (5' to 3')	Annealing Temp (ºC)	Product Size (bp)
LOC100119494	3	35.0	F: CGCACTCGCACAACATTCCC R: GCCTTGCTCTTCTCCTTCTCCG	57	617
Mucin-5AC seq	3	35.0	F: TCGGCAAGAAGATGGGCGTC R: GCGTCGTTGTGGTGGTTGTG	57	747
LOC100679324	3	36.5	F: TATTGCCCCTCGCCCCATTG R: CTGGTTCATAGCGTTGTTTGACATC	56	715
LOC100119358	3	36.5	F: CATCATCGCCCTCGTCCTCTTC R: ACCGTCTGCGTCACTTCCTG	56	682
LOC100119295	3	36.5	F: CCAGGACCCAGACCAGGATTAG R: AACCCACTTCTACCAGCCCC	55	670
LOC100119259	3	36.5	F: TTGACCACACCGACAACAAC R: GCATTTCATAAGTTCCGCCAGAG	53	670
LOC100679834	3	36.5	F: GCCGATTACTGGACCGACAG R: GTTGGGGTTGCGGATAGTTCG	54	607
LOC103317434	3	36.5	F: ACGGGTATTTCAGCCTTCGCC R: ACAACTCACACCTTCCCACCG	57	723
Wds seq	3	36.5	F: GTTCCTGATACTGCTCGCCG R: ACTTTGCTTGGCCCGACGAT	55	250
LOC100118928	3	36.5	F: CGAGCGAAGCACCGAGTTAC R: GCAGGCGACAGTTCTCAACG	55	677
LOC100679277	3	36.5	F: TTCGGGTCTTTTGTTATTGCGAG R: TATCCTCCGTGTCCTCCGTG	53	616
LOC100118712	3	36.5	F: TAGACCACGAACGCAACCTCG R: GCTTCCCAAGAACCCATCCC	57	632
LOC100118529	3	36.5	F: GTCTCGGCGGGTTTTGATGG R: GCGTCCTTTGGTGGCTGTTG	55	685
LOC100118450	3	36.5	F: ATGGAAAAGGCATCGGTAAGCG R: GCAACTCAGAAATCGTCCTGCG	55	630
LOC100114497	3	36.5	F: ACGAGTCATCTTCTATGGTTTTGGC R: TGTGGCAGGCGTTTGAGTATC	54	375
LOC100678491	3	36.5	F: GGATCACAACCAAAAGTTCCTG R: GGTACGGCCTAAACACGG	54	540

Table A-6. Primers for dsRNA constructs and RT-qPCR of *Nasonia* genes

NCBI Gene ID	Gene Name	Name of Primer Set	Primer sequences (5' to 3')	Product Size (bp)
LOC100679092 (*Nasonia*)	Uncharacterized	Unchar RNAi	F: CGTTCCTGATACTGCTCGCC R: CCACCTGTTGCCTGTAGACG	438
		Unchar1 qPCR	F: ACCTACTGCTGACATCGTTCC R: AGCCCGTCTCTTGTTTCACG	165
LOC100679394 (*Nasonia*)	Mucin-5AC	Mucin5ac RNAi	F: TCGGCAAGAAGATGGGCGTC R: GCGTCGTTGTGGTGGTTGTG	627
		Mucin5ac qPCR	F: AAGGCTCGTGGAAGACTGCG R: TGGCGGCGTCCTGTTGTATC	145
malE (*E. coli*)	Maltose transporter subunit	MalE RNAi	F: ATTGCTGCTGACGGGGGTTAT R: ATGTTCGGCATGATTTCACCTTT	495
LOC100115795 (*Nasonia*)	60S Ribosomal protein L32	RP49 qPCR	F: CAAGCGTAACTGGAGGAAGC R: CTGCTAACTCCATGGGCAAT	221

APPENDIX B. CHAPTER III SUPPLEMENTARY INFORMATION

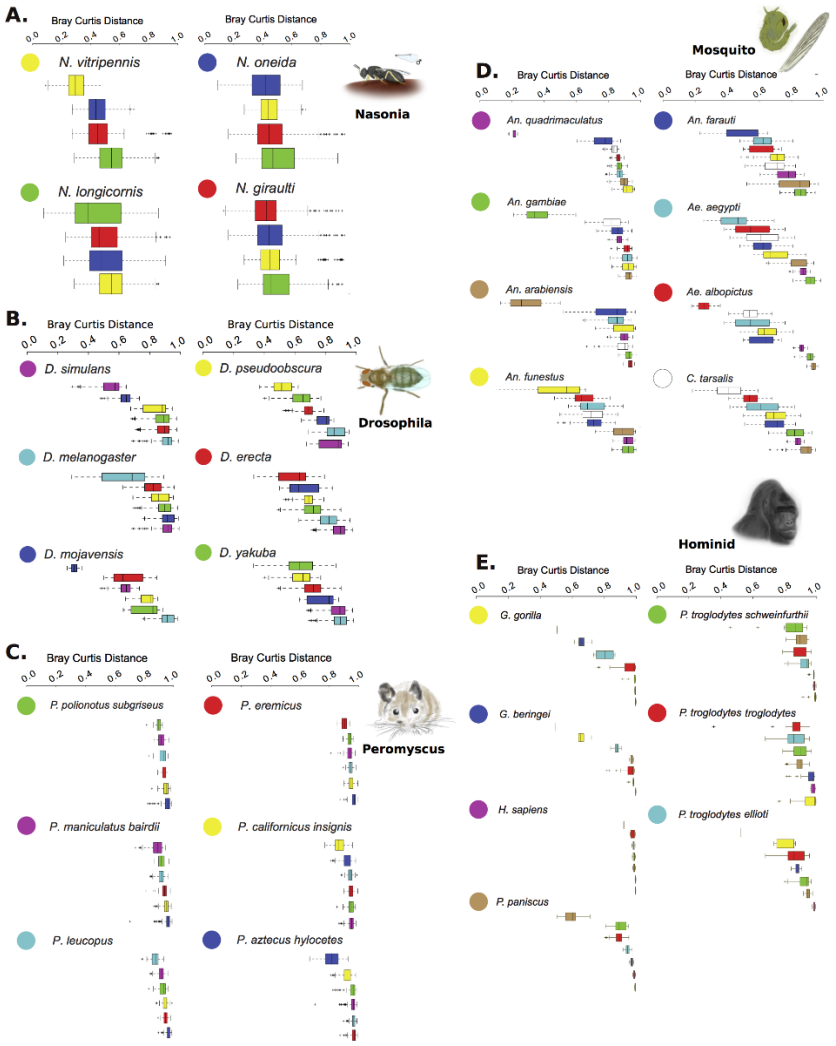

Figure B-1. Comparisons of intraspecific and interspecific Bray-Curtis distances for pairwise combinations of all species. Bray-Curtis beta diversity distances were computed for all pairs of individuals within each clade from 99 percent OTUs. Colored circles denote the named species, and colors within box-and-whisker plots denote to which species it is being compared. Boxes represent the 25th to 75thquartiles with the central line depicting the group median, and whiskers showing the 1.5 interquartile extent

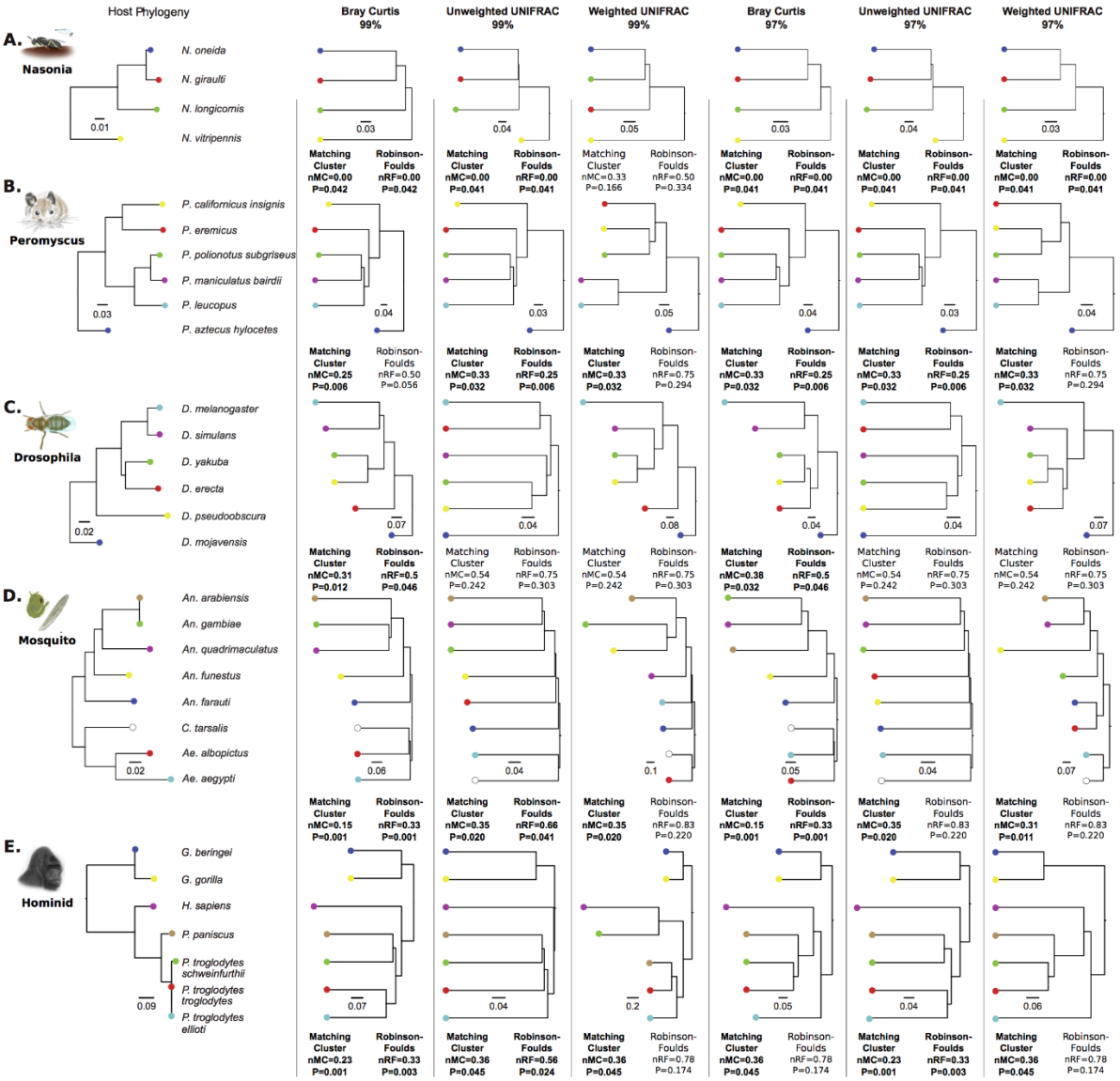

Figure B-2. Phylosymbiosis analysis for alternative beta-diversity metrics and OTU clustering cutoffs. The normalized Robinson-Foulds metric and the normalized Matching Cluster metric were used to evaluate the congruence between host phylogenies and microbiota dendrograms for Bray Curtis, Unweighted UniFrac, and Weighted UniFrac beta-diversity metrics at both 97 and 99 percent clustered OTUs.

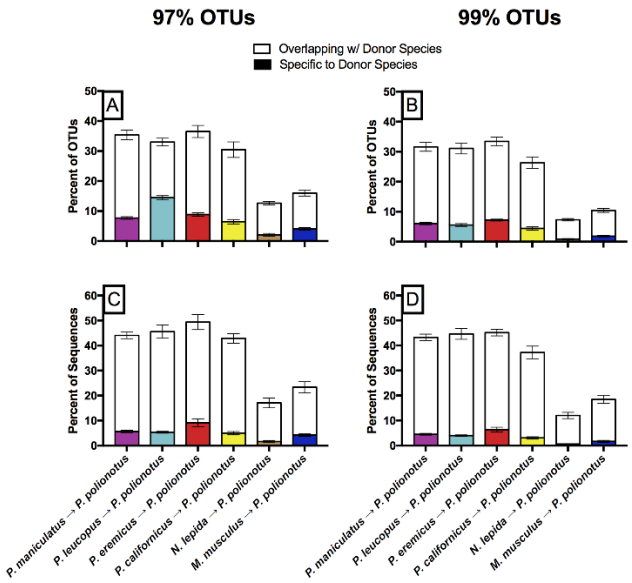

Figure B-3. Fine-resolution overlap between donor and recipient microbial communities. White bars represent shared OTUs between donor and recipients and thus the possible range of transfer. Colored bars represent the portion of shared OTUs that are donor-specific and thus transfer of unique OTUs between donor and recipients. Panels (A) and (B) depict the mean ± s.e.m. percentage of OTUs. Panels (C) and (D) show the mean ± s.e.m abundance of total sequences. These analyses were conducted with OTU-picking at both 97% and 99% sequence identities.

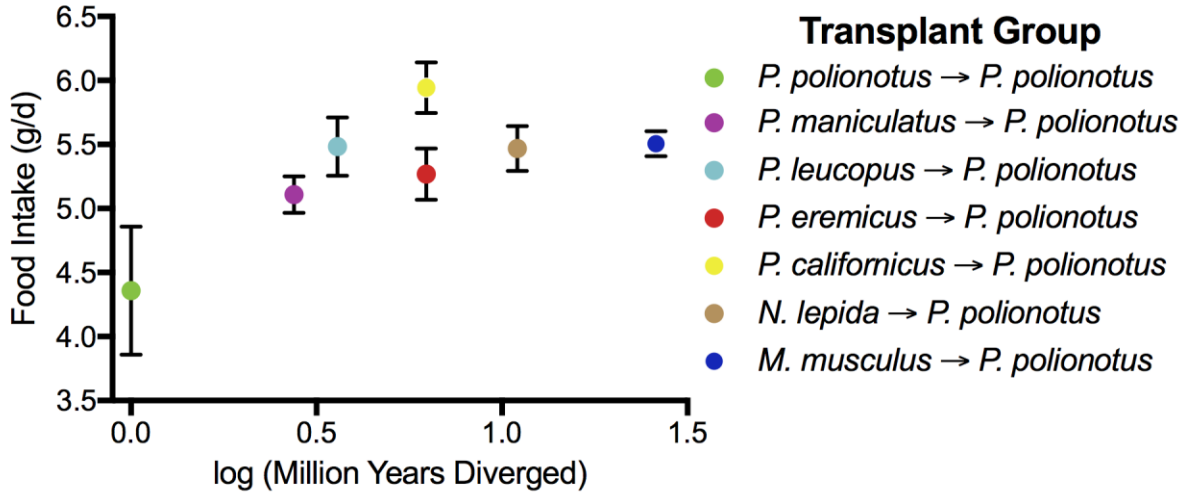

Figure B-4. Effects of allochthonous versus autochthonous microbial communities on the food intake of recipient mice. Divergence times between *P. polionotus* and donor species were determined from previously published phylogenies (Stepphan et al. 2004; Kohl et al. 2016). Points represent mean values ± s.e.m. for each group (n = 5–6 recipients per group).

APPENDIX C. RETHINKING HERITABILITY OF THE MICROBIOME

For almost a century, heritability has been routinely used to predict genetic influences on phenotypes such as intelligence, schizophrenia, alcoholism, and depression (Bouchard Jr and McGue 2003). However, there has been relatively little work on heritability of the human microbiome—defined here as the number and types of microorganisms and viruses present in or on the human body. This question has become increasingly more interesting as research reveals that humans and their microbial communities interact in complex and often beneficial networks. An underlying question is the degree to which environment versus human genotype influences the microbiome. A central goal of quantifying microbiome heritability is to discern genetic from environmental factors that structure the microbiome and to potentially identify functionally important microbial community members.

Twin-based studies provide one method for quantifying heritability (h^2) of microbial taxa. In such analyses, heritability is measured by comparing variation in microbial taxon abundances that is attributable to human genetics. This approach simplifies microbial abundances to continuously varying phenotypes, comparable to human height, weight, and eye color. In 2009 and 2012, studies of twins conducted in this manner concluded that there are no heritable gut microbial members (Turnbaugh et al. 2009), or low overall gut microbiome heritability (Yatsuneko et al. 2012), respectively. But in 2014, the largest twin cohort to date examined members of the gut microbiome and found that the bacterial family *Christensenellaceae* has the highest heritability ($h^2 = 0.39$), and associates closely with other heritable gut bacterial families (Goodrich et al. 2014). The groundbreaking discovery of a high heritability for members of the human microbiome raises specific questions about understanding the genetics of human-microbe symbioses: How should we interpret what heritability means for microbiome studies? Can microbiome heritability be viewed in a more comprehensive manner? Is h^2 the only term to measure and denote microbiome heritability?

Under a heritability analysis with standard statistical approaches [such as the Additive Genetics, Common Environment, Unique Environment (ACE) model], the abundance of each human-associated microbe is presented as a continuously varying, quantitative "trait" that is affected by host genetics—in other words, the host genome significantly dictates the abundance of a microbe. Although a suitable starting point, this host-centric interpretation of microbiome

heritability tends to consider the human-microbiome interaction as unidirectional, in which the host regulates colonization. This view, however, is only half of the story. The microbiome is a collection of different organisms with genotypes that interact with each other as well as with the host to achieve colonization. A more comprehensive view is advisable in which both the host and the microbiome play a role in heritability. This view, based on community genetics principles, requires that studies adopt a conceptual foundation of interspecies (genotype-by-genotype) interactions that drive the assembly of the host and microbial consortia. It also necessitates the use of a measure— "community heritability" (H^2_C)—that reflects genetic variation underlying interactions with the entire (or portions of the) community—in this case, the microbiome together with its human host.

Human-associated microbes contain distinct genetic, transcriptomic, metabolic, and proteomic features that can reciprocally influence their own colonization of specific human genotypes. These features span competitive nutrient acquisition, mechanisms to evade the host immune system, and niche construction, among others. Thus, heritable taxa such as *Christensenellaceae* may be "recruited" by the human genome to perform beneficial functions in the microbial community, but they also may encode traits that enable them to circumvent host defenses and colonize susceptible genotypes. For example, commensal bacteria tolerate or evade human immune responses by modifying surface components in their cell walls and outer membranes (Cullen et al. 2015). Other microbes proactively subvert the immune system by injecting effector proteins into host immune cells to kill them (Palmer and Brayton 2013). Microbes may alter the expression of genes involved in regulating immune, developmental, and metabolic functions (Lewis et al. 2011; Finlay and McFadden 2006; Broderick et al. 2014; Cox et al. 2014). Communities of microbes can also alter their human environment by forming internal biofilms. Biofilms can provide protection against the host immune response, afford stability in fluctuating environments, and promote the survival of a microbial community (Stoodley et al. 2004). Put simply, microbiome heritability can represent three outcomes: host control of the microbiome, host susceptibility to the microbiome, or a combination of host control and susceptibility. Interspecies interactions (host-microbe and microbe-microbe) thus underlie the emergent property of microbiome heritability.

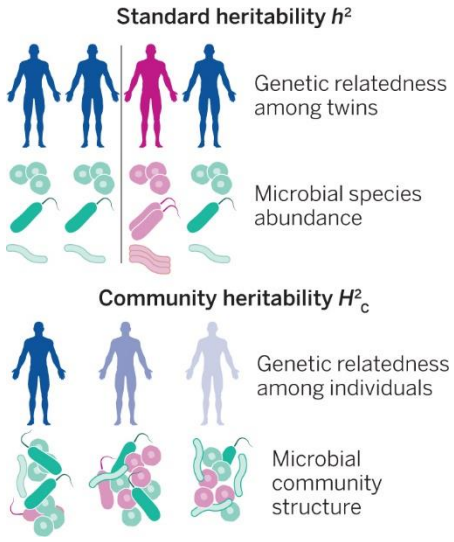

Figure C-1. Analyzing heritability. Under standard heritability (h^2) analysis, each microbe is a quantitative "trait" that is encoded by host genetics. Comparing monozygotic versus dizygotic twins allows an indirect estimate of the additive genetic factors affecting that microbe's abundance. Community heritability (H^2_C) emphasizes that the host is part of the ecosystem and measures the extent to which whole community phenotype variation is due to genetic variation in the host. It specifies that host genetic variation will have predictable effects on microbial community assembly.

Human-microbiome interactions tend to be viewed through the lens of host regulation. A key point when discussing community-wide symbiotic interactions is that heritability denotes host involvement rather than control of microbiome assembly. Thus, human genetic effects on the microbiome are most easily understood as genotype-by-genotype (i.e., hologenomic) interactions between the host and other microbial members (Bordenstein and Theis 2015). Without knowing the mechanisms underlying the heritability of a certain microbial member, we must be cautious in interpreting whether a highly heritable microbe in any symbiosis is harmful, harmless, or beneficial to the whole system.

In addition to taking a comprehensive view of microbiome heritability, it is important to understand the ecological genetics principle of broad-sense community heritability (H^2_C) (Shuster et al. 2015). H^2_C emphasizes that the host is part of an ecosystem and measures the extent to which variation in "whole-community" phenotype is due to genetic variation in the foundation (i.e., host) species of the community. It therefore specifies that host genetic variation will have predictable effects on microbial community assembly (Whitham et al. 2006), in addition to having effects on specific members of the microbiome, as measured by h^2.

The whole-community phenotype is measured by ordination methods that cluster microbial community data into single scores used to compare compositional differences (i.e., β diversity)

between the communities of various hosts. One such data clustering method is nonmetric multidimensional scaling (NMDS). Analysis of NMDS scores (by ANOVA, which tests whether there is significant variation in means among groups, among subgroups, within groups, etc.), would then identify the fraction of total variation in whole community phenotype that relates to genetic variation in the host (Whitham et al. 2006).

The utility of this approach in addition to conventional heritability measurements is that it incorporates the vast interspecies interactions that contribute to a whole community phenotype, instead of considering individual microbial members as phenotypic extensions of the host. If these interactions have a heritable component (H^2_C), then the assembly of the community is nonrandom (i.e., via ecological selection). For host-microbiome symbioses, this has been referred to as "phylosymbiosis" (Brucker and Bordenstein 2013). Given a significant H^2_C selection as an evolutionary force can potentially act on the community.

Presently, community heritability measurements have only been applied to ecological systems analyzing plant genetic influences on soil microbe, arthropod, bird, and mammal community structures (Whitham et al. 2006). Human microbiome studies could adopt H^2_C to determine whether human genetic variation across the whole genome, or certain functional categories of genes, affects microbial community assembly. Twin-based microbiome studies could derive a NMDS score for the whole microbial community or from specific taxonomic levels to test if there is a significant association with human genetic relatedness across the cohort of twins. Further, transcriptomes, metabolomes, and proteomes could potentiate identification of the candidate genes that affect microbiome heritability. Data integration from large "omics" data sets holds the potential to move the community genetics view of host and microbes from unspecified genetic effects on interacting species to precise gene-by-gene interactions.

The products of host genes work in intimate association with the products of microbial genes to enable functioning of the whole holobiont (Whitham et al. 2006). Strong degrees of microbiome heritability could therefore have profound consequences for the ecology and evolution of human and all animal and plant holobionts. A crucial outcome of this community heritability view is to underscore the deterministic and predictable interactions between hosts and microbes. Further studies also need to consider the relative roles of vertical and horizontal transmission of microbial communities in heritability assessments. Thus, genetic analysis of whole community organization is an important frontier in the life sciences, particularly for fusing the fields of ecology

and evolution and the taxonomic disciplines of zoology and botany with microbiology. The repurposing of community heritability from traditional macroecological systems (i.e., gardens) to microecological systems (i.e., human gut) will provide a more comprehensive view to studies of microbiome heritability. This view looks outwards, beyond the phenotype, to examine links at higher interspecies levels and holds the potential to unify community ecology and evolution concepts. In the words of the microbiologist Carl Woese: “Biologists now need to reformulate their view of evolution to study it in complex dynamic-systems terms.”

APPENDIX D. LIST OF PUBLICATIONS

van Opstal EJ, Bordenstein SR. Microbiome. Rethinking heritability of the microbiome. *Science*. 2015 Sep 11;349(6253):1172-3.

Shropshire JD*, **van Opstal EJ***, Bordenstein SR. An optimized approach to germ-free rearing in the jewel wasp *Nasonia*. *PeerJ*. 2016 Aug 9;4:e2316. *co-first authors

Dittmer J, **van Opstal EJ**, Shropshire JD, Bordenstein SR, Hurst GD, Brucker RM. Disentangling a holobiont – recent advances and perspectives in *Nasonia* wasps. *Frontiers in. Microbiology*. 2016 Sep 23;7:1478.

Brooks AW*, Kohl KD*, Brucker RM*, **van Opstal EJ**, Bordenstein SR. Phylosymbiosis: Relationships and functional effects of microbial communities across host evolutionary history. *PLOS Biology*. 2016 Nov 19; 14, e2000225. *co-first authors

Funkhouser-Jones LJ*, **van Opstal EJ***, Sharma A, Bordenstein SR. The maternal effect gene *Wds* controls *Wolbachia* titer in *Nasonia*. *Current Biology*. 2018 Jun 4;28(11):1692-1702. *co-first authors